UNIVERSITÀ
DI PARMA

PhD course in
"Science of Drugs, Biomolecules and Health Products"

CYCLE XXX

ENHANCING STRATEGIES TO PROMOTE MACROMOLECULES TRANSPORT ACROSS OCULAR BARRIERS

PhD coordinator:
Prof. Marco Mor

PhD supervisor:
Prof. Patrizia Santi

PhD candidate: Maria Aurora Grimaudo

Academic years 2014/2017

Index

Summary

The development of new biological drugs, for the treatment of diseases of the anterior and posterior eye segment, has posed different problems to drug delivery technologies as their unfavourable physico-chemical characteristics render these molecules poorly permeable through ocular tissues.

A brief introduction about anatomical barriers of the eye, different administration routes, limitations associated to the ophthalmic delivery of biologics and suitable delivery platforms for overcoming them are presented in **Chapter 1**.

The investigation of the influence of macromolecules related factors on their diffusion across ocular membranes is discussed in **Chapter 3**. This chapter is focused on the comparison between two model proteins (lysozyme and cytochrome c, with similar molecular weight and net charge at physiological pH) permeability and the feasibility of the application of transscleral iontophoresis for enhancing proteins transport.

Cyclosporine (1.2 kDa) delivery to the eye has been investigated by the use of polymeric micelles and ophthalmic inserts. **Chapter 4** is focused on the development and characterization of a novel micellar formulation made of poloxamer 407 and TPGS for cyclosporine targeting both the anterior and the posterior eye segment. Details about the characterization of micelles in terms of particle size, morphology, ocular irritancy, rheology and *ex vivo* penetration performance though porcine ocular tissues are provided.

Finally, preliminary results about the development of a novel ophthalmic insert of hyaluronic acid and hydroxypropyl-β-cyclodextrin for cyclosporine topical ocular delivery is presented in **Chapter 5**.

1. Introduction

During the last years, advancement in biotechnologies allowed for the production of new therapeutic biologics such as peptides, proteins, aptamers, siRNA, oligonucleotides useful also for the treatment of ocular disorders[1]. Neutralization of biomolecules, such as cytokines and growth factors, protection of photoreceptors and prevention of angiogenesis are possible roles where therapeutics macromolecules are involved[2].

The introduction of Pegaptinib in 2004 and Ranibizumab in 2006 marked the beginning of the use of biologics in the ophthalmic area[3]. Pegaptanib (Macugen®) is a RNA aptamer with anti-$VEGF_{165}$ activity approved for the treatment of wet form of macular degeneration (wet AMD)[3]. Ranibizumab (Lucentis®, 48 kDa), a monoclonal fragment of bevacizumab, was approved for the treatment of neovascular (wet) age-related macular degeneration (wet AMD) and diabetic retinopathy following retinal vein occlusion. Since the introduction of Pegaptanib, the US FDA has approved other anti-VEGF therapeutics[4]. Aflibercept (Eylea®, 97 kDa) was approved for the treatment of wet AMD, choroidal neovascularisation (CNV), diabetic macular edema (DME) and retinal vascular occlusions (RVO)[5], and demonstrated a longer intravitreal half-life and the capacity to antagonize other growth factors involved in ocular diseases[2]. It is composed by portions of the extracellular domains of human VEGF receptors 1 and 2 fused to the fragment crystallizable portion of human immunoglobulin G[6]. Another anti-VEGF antibody, currently used off label by intravitreal administration, is Bevacizumab (Avastin®), a recombinant humanized monoclonal immunoglobulin G1 antibody for the treatment of neovascular ocular diseases[7].

Moreover the use of gene therapy could be useful for its long term effects and the potential to target genetic mutations occurring in ocular diseases, such as allograft rejection, herpes simplex keratitis, corneal neovascularization and corneal dystrophies[8]. The first approach was the use of antisense oligonucleotides, single DNA strands that can block the synthesis of proteins, such as VEGF[1]; the antisense oligonucleotide Fomivirsen (Vitravene®) was the first and only approved for delaying cytomegalovirus (CMV) retinitis in patients with AIDS[9].

Despite the potentialities of the employment of biologics in the ocular therapy, their delivery to the eye is very challenging due to their complex structure prone to instability and degradation with a high MW and hydrophilic properties[10]. Thus, macromolecules are characterized by numerous delivery-related limitations, such as poor permeability across ocular tissues, low bioavailability and *in vivo* stability. Currently, many efforts by drug delivery scientists are focused on overcoming macromolecules related issues through the development of new technological platforms[1].

1.1 Anatomy of the eye

The eye is constituted by several barriers meant to keep the systemic circulation separated from ocular tissues, as this organ is part of the central nervous system[11]. The presence of these barriers places several constraints on the delivery of drugs, especially macromolecules[12].

Considering a histological classification, the eye is composed by an external layer of connective tissue, a middle vascular layer and the retina, i.e. the inner neural layer (**Figure 1**).

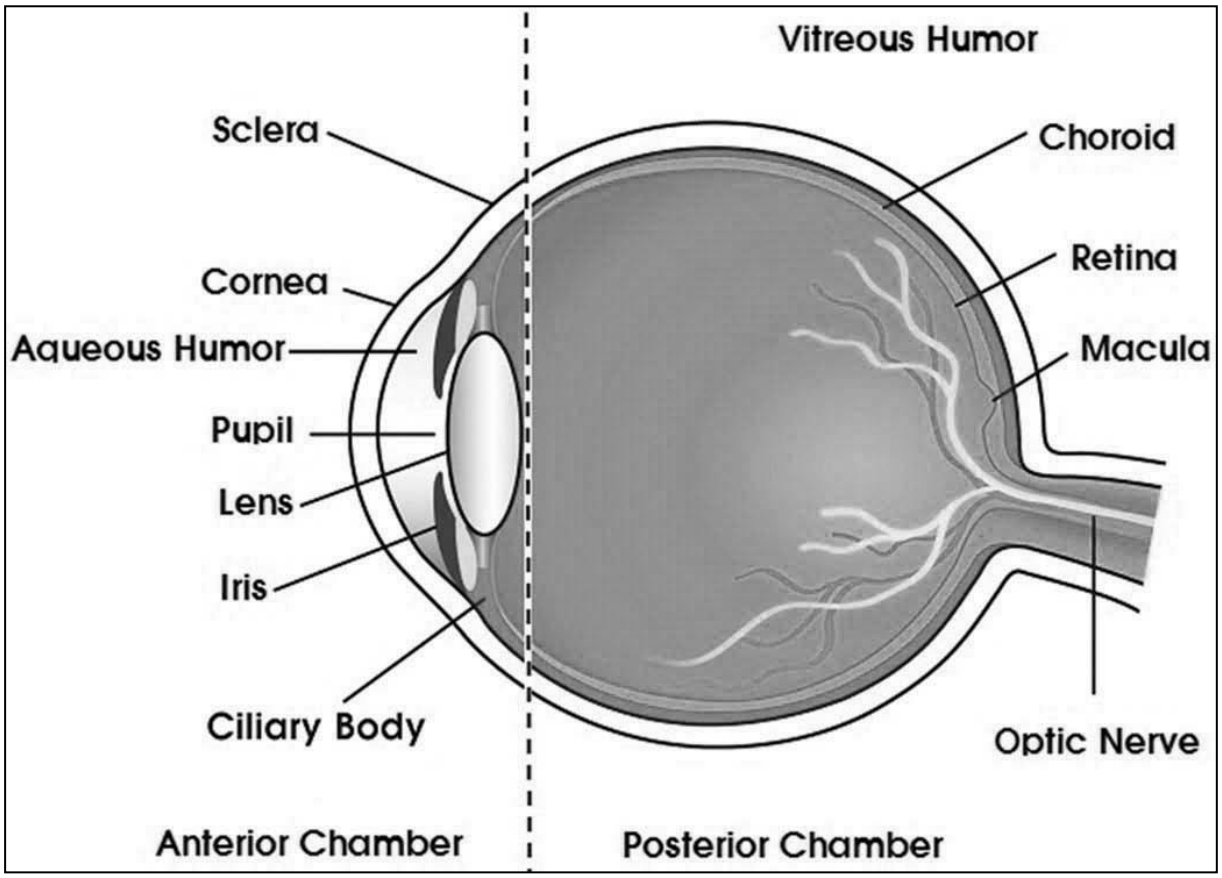

Figure 1. Anatomy of the eye (adapted from [1]).

The outer tissue, providing mechanical protection to the entire structure, is composed by the cornea and the sclera in correspondence of the anterior and posterior segment, respectively.

The cornea is covered on the external surface by the tear film and it is continuous to the sclera and conjunctiva in its periphery. Being avascular, this tissue obtains its nourishment by diffusion from the aqueous humor and from the conjunctival and

episcleral capillary network. The cornea is composed by five different layers: I) the corneal epithelium, where tight junctions provide a barrier against the entrance of exogenous substances; II) Bowman's layer, offering biomechanical rigidity to the cornea; III) the stroma, composed of collagen fibrils, keratocytes and extracellular matrix substance; IV) Descemet's membrane, the basement membrane of the endothelium; V) the endothelium, characterized by the presence of gap junctions.

On the surface of conjunctiva and cornea a mucus layer could extend up to 500 nm from the surface, playing a lubrificant and protecting role[13].

The sclera is a thick and dense connective tissue, covered by the transparent conjunctiva and composed by an irregular organization of collagen fibrils contributing to the strength and flexibility of the eye bulb[14].

The middle vascular layer, the uvea, is composed by the iris and ciliary body in the anterior segment and by the choroid in the posterior one. The iris, the most anterior structure, regulates the entrance of the light into the eye. The ciliary body is continuous to the iris and produces the components of the aqueous humor. The choroid, consisting of blood vessels, provides nutrients to the retina. The innermost layer of the choroid, Bruch's membrane, fuses with the retina, and, in particular, represents the basal membrane for the RPE (retinal pigment epithelium)[15].

In the retina, light energy is transformed into a neural signal. After passing through several retinal layers, light stimulates photoreceptors, able to convert light into neural signals and process them within the complex synaptic pathway[16].

The anterior chamber of the eye is filled by the aqueous humor, while the vitreous humor is contained in the posterior area. The aqueous humor provides nutrients to the lens (avascular and transparent structure focusing light rays on the retina) and cornea and carries waste products away, helping to maintain the intraocular pressure within the eye. The vitreous body supports physically the retina in place next to the choroid[17]; it is formed by a network of unbranched collagen fibrils with hyaluronan filling the space between them[18]. The intraocular environment is protected by the blood-aqueous barrier, composed by the endothelial cells of the uvea and non-pigmented layer of the epithelium of the ciliary body[19].

1.2 Pathologies affecting anterior and posterior eye segment

The more diffused and vision-impacting ocular diseases are:

- Dry eye syndrome (DES). This disorder is caused by decreased tear production, increased tear evaporation and/or changes in the tear composition. Photophobia, burning and stinging are the major symptoms impacting the quality of life. If untreated, DES might cause serious damage and scarring on the anterior segment of the eye, increased risk of infection and other disorders[20].
- Diabetic macular edema (DME). An over-accumulation of glucose in the ocular tissues damages tight junctions and the inner walls of blood vessels that become weak. Leakage from retinal blood vessels can cause retinal swelling and up-regulation of angiogenic growth factors[21].
- Diabetic retinopathy (DR). This is a progressive disorder where the retinal vessels become narrow, losing their function of carrying oxygen to retinal tissues and causing retinal ischemia. The retina usually tries to compensate for the reduced circulation by a process of neovascularization. These abnormal new vessels are fragile and can cause hemorrhage, scarring and retinal detachment[22].
- Age-related macular degeneration (AMD). This condition affects RPE, Bruch's membrane and choroid. Early stage AMD is characterized by retinal pigment abnormalities. The advanced stage of AMD can be either dry (non-neovascular) or wet (neovascular). The wet form presents choroidal neovascularization, epithelial proliferation and inflammation, subretinal hemorrhage and RPE detachment that can lead to vision loss[23].
- Proliferative vitreoretinopathy (PVR). It is caused by an abnormal process of migration and proliferation of cells after a break in retina or trauma. The uncontrolled wound healing path can lead to inflammation and cell over-proliferation in the periretinal area[24].
- Cytomegalovirus retinitis. It is an opportunistic infection affecting the retina, with high prevalence in patients with AIDS (up to 25% of these patients)[25].

- Uveitis. It is an inflammation of the uveal tract and can be characterised by blurred vision, eye discomfort, pain and intolerance to light. This disease can be due to accidental or surgical trauma, infections or immune disorders[26, 27].

1.3 Macromolecules administration routes and related barriers in the eye

Compared with drug delivery to other body sites, ocular delivery presents more challenges. Systemic administration necessitates high doses to penetrate the blood retinal and aqueous barriers[28]. In fact, blood-aqueous barrier prevents the entry of solutes into the aqueous humor, whereas blood-retinal barrier restricts the passage of therapeutic molecules from the blood to the posterior segment, due to the presence of tight junctions[28]. Only drugs with wide therapeutic window, such as antibiotics, can be administered systemically to treat the posterior eye segment[29].
Local ocular administration routes can be divided into topical, intraocular and periocular[28](**Figure 2**).

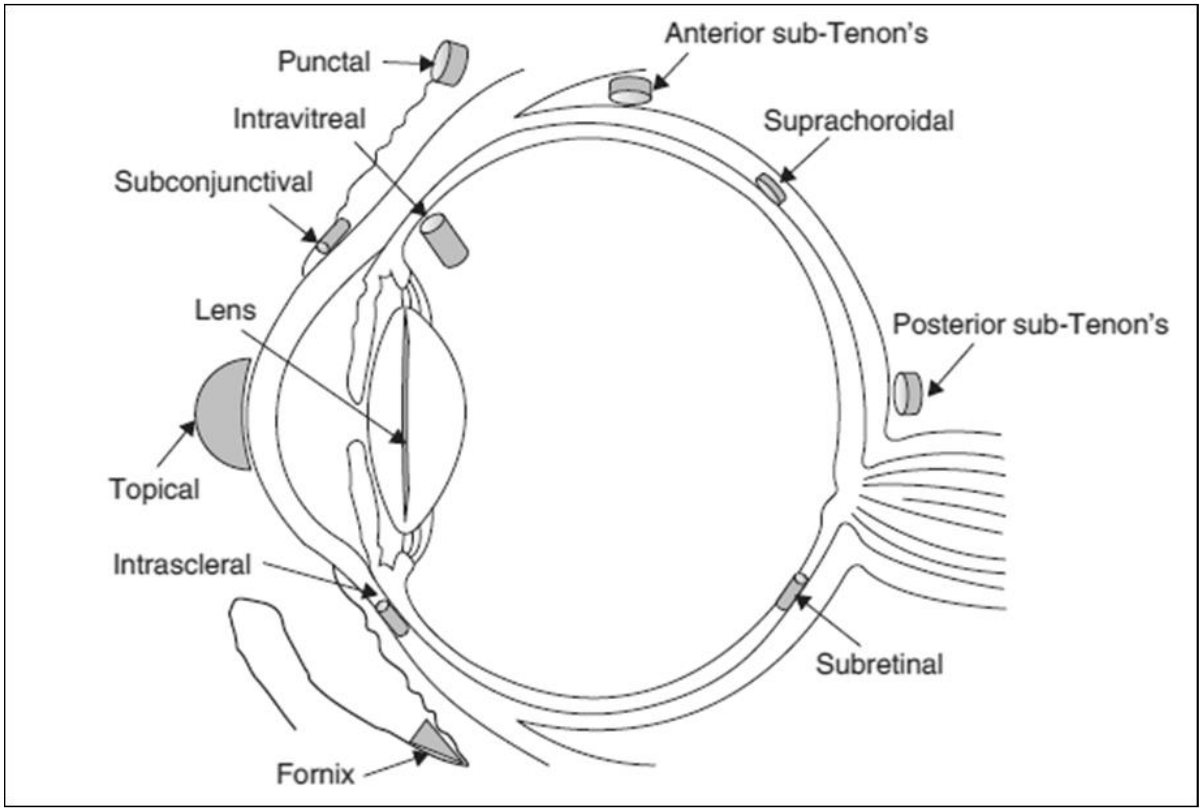

Figure 2. Ocular administration routes (adapted from [30]).

A drug applied in the conjunctival sac can permeate the cornea to reach anterior segment or cross the conjunctiva and sclera to reach the underlying tissues. The cornea represents a significant barrier for topical drug administration to the anterior segment, while the sclera is relatively permeable[31].

Intraocular delivery includes intravitreal, suprachoroidal, intrastromal, intracameral, intrascleral and subretinal routes. As the drug is directly deposited in or close to the target tissue, bioavailability is increased and side effects are reduced in comparison to systemic drug delivery[28]. However these routes are highly invasive and can produce serious side effects as cataract formation and/or retinal detachment.

Periocular routes (sub-Tenon, peribulbar, retrobulbar and subconjunctival injections) are less effective and invasive than intraocular injections, but they offer higher drug bioavailability compared to topical delivery. Additionally, larger volumes of drug solutions (500-5000 µl) can be administered compared to intravitreal delivery (50-100 µl)[32].

1.3.1 Topical delivery

Topical ocular administration using eye drops is the most common way to treat anterior segment diseases. Topically administered drugs encounter precorneal factors and anatomical barriers, negatively affecting their bioavailability. Blinking, tear film, tear turnover and induced lacrimation could be considered precorneal factors, able to lower contact time of the drug on the ocular surface up to a few minutes. The cornea represents a physical barrier for drug permeation. Tight junctions present in the external epithelium and its lipophilic properties discourage the passage of hydrophilic molecules, while hydrophilic stroma is a significant barrier to the permeation of lipophilic drugs. Moreover, stromal collagen fibers are organized into a intertwined net with narrow pore size, hindering macromolecules permeation through the tissue. Thus, drug contact time with absorptive membranes and the presence of static barriers are considered the main reason for 1-5% bioavailability for drugs[28]. This value is even lower in case of macromolecules[3]. For these reasons it is believed that macromolecules cannot be efficiently delivered in the anterior segment by simple passive diffusion mechanisms[8].

Topical application of macromolecules appears an attractive administration route also for the posterior segment; it is possible to reduce the adverse reactions typical of systemic delivery and increase patient's compliance, avoiding the need of invasive procedure[10], typical of intraocular routes. However, the topical delivery of small molecules and larger biocompounds to target vitreous, retina and choroid is very difficult[33]. In the transscleral route the drug can reach the retina after crossing several tissues, conjunctiva, sclera, choroid-Bruch's layer and RPE. The mucin layer on the

ocular surface is thought to be a barrier for macromolecules, as the gel network may limit their diffusion and reduce the permeation across the conjunctiva and sclera[34]. The conjunctiva itself often acts as a mechanical barrier to the transport of large macromolecules[29, 35], due to the presence of epithelial tight junctions. Moreover, conjunctival drug absorption is considered non productive, as the presence of blood and lymphatic vessels, causes uptake to the systemic circulation[28]. Passive diffusion through the aqueous media of the gel-like proteoglycans seems to be the primary route for drug transport through the sclera[33]. Scleral permeability has been shown to be dependent on drug molecular weight and is higher for hydrophilic and negatively-charged molecules[36].

The choroid layer containing Bruch's membrane can affect drug permeability[37]. In addition to the clearance through blood and lymphatic vessels, transporter proteins and tight junctions of the RPE are barriers in the transscleral route[36]. Transport studies demonstrated that RPE is up to 100 times less permeable to macromolecules compared to the sclera[38]. The retina itself is also a significant diffusion barrier to macromolecules, with the inner blood-retinal layer hindering the transport of macromolecules larger than 150 kDa[39] due to the presence of tight junctions[2].

In summary, topical delivery presently is limited to the treatment of external anterior segment diseases, but many efforts are focused on the development of topical formulations for targeting posterior eye segment.

1.3.2 Intraocular delivery

Intravitreal injections are used to deposit the drug in the posterior segment; they can cause serious side effects, such as eye infections, retinal vascular occlusion or retinal detachment[40]. Additionally, the drug must diffuse across the vitreous, and this has been reported to be strictly dependent on electrostatic interactions with glycosaminoglycans present in the tissue[41].

Intrascleral injections can be an alternative for drug delivery to the back of the eye, because of the possibility of obtaining a drug reservoir into the tissue and a consequent extended release[3].

Suprachoroidal space is located between the sclera and choroid. Although choriocapillaries can wash drugs away from the deposition site, suprachoroidal injections might improve efficiency in treating choroidal diseases as the drugs are delivered directly to the target tissue[42].

Subretinal administration could be used in the context of gene delivery for targeting macromolecules to retinal cells[3].

1.3.3. Periocular delivery

Periocular delivery lowers the risk of endophthalmitis or retinal detachment compared to intravitreal injection as the vitreous is not directly involved. However, drug loss from the application site can deeply reduce the efficiency of drug delivery to the posterior segment[43]. Subconjunjunctival, sub-Tenon and retrobulbar injections have been used for administering corticosteroids, local anesthetics and anti-infective compounds. The drug can permeate from the application site to the vitreous via the anterior chamber, systemic circulation or by a direct penetration pathway (sclera-choroid-Bruch's membrane-RPE)[28].

Subconjunctival injection allows drug access to the anterior eye segment; for example, subconjunctival administration of anti-VEGF antibodies suppressed corneal vascularization[44].

1.4 Biologics permeability across ocular tissues

Macromolecules permeability across the ocular tissues is influenced both by the physico-chemical properties of the drug and by the characteristics of the tissue to be crossed, as summarised below.

- Conjunctiva. The presence of tight junctions is reported to hinder the transport of protein molecules larger than 40 kDa. Enzymatic degradation and vascular drainage can affect macromolecules permeation across this tissue as well[2].
- Cornea. The presence of a physical barrier on the ocular surface constituted by the mucus layer might reduce drug penetration, as the mesh size of the gel network could limit the mobility of proteins[13]. Paracellular drug permeation is limited by the presence of tight junctions in the epithelium. Furthermore, collagen fibers of the stroma act as a sieve toward larger molecules[3]. Overall, the permeation of proteins is negligible.
- Vitreous humor. Hydrated hyaluronan acts as a molecular sieve hindering macromolecules transport[18].
- Sclera. Permeability of drugs across the sclera seems inversely proportional to their molecular radius, as glycosaminoglycans chains hinder the movement of large molecules. Additionally, some authors found that positively charged molecules exhibit lower permeability because they interact with negatively charged proteoglycans[33].
- Choroid. High choroidal blood flow can eliminate a considerable fraction of drugs before reaching the retina. The presence of melanin can also alter biologics distribution and bioavailability at the targeted site, because it can provide additional binding sites[28].
- RPE. The tight junctions of RPE are known to limit the entry of proteins. Thus, the RPE resulted approximately 10-100 times less permeable to macromolecules compared to the sclera[38]. Moreover, these cells contains melanin, able to alter ocular disposition of basic and lipophilic drugs and significantly lower their pharmacological activity[45]. Additionally, P-glycoprotein (efflux transporter) activity has been identified in RPE, potentially decreasing the amount of macromolecules reaching the neural retina[46].

- Retina. The external limiting membrane is composed of zonula adherens junctions between cells, able to form a barrier against the passage of molecules larger than 150 kDa[3].

1.5 Approaches to enhance macromolecules absorption through ocular tissues

Biopharmaceuticals ocular delivery is challenging because of their unfavourable physico-chemical properties and conventional delivery methods show low bioavailability and limited tissue targeting[3]. Controlled delivery can increase the residence time of drugs at the target site, reduce the frequency of drug administration and enhance macromolecules transport across ocular barriers[2].

1.5.1 Iontophoresis

Drugs transport to the anterior and posterior eye segment might be facilitated by the use of physical methods, such as iontophoresis[47].

Iontophoresis can be defined as the application of an electric field across a biological membrane for enhancing drug permeation. The electric field can enhance permeant transport across conjunctiva, sclera, choroid and retina[48]. Mechanisms of the iontophoretic transport include the interaction of the applied electric field with the charged drug (electrorepulsion), convective solvent flow responsible for the movement of neutral compounds (electroosmosis) and increased passive permeability. Transcorneal and transscleral iontophoresis have been studied with a variety of ophthalmic drugs, including macromolecules[47].

The *in vitro* studies on human and porcine sclera performed using dextrans up to 120 kDa indicated anodal iontophoresis (up to 2.9 mA/cm^2 for 2 h) was able to enhance dextrans permeability up to 6.5-fold compared to passive diffusion[49]. Different authors obtained higher permeability coefficients for bevacizumab across the sclera during anodal iontophoresis, in comparison to passive diffusion and cathodal iontophoresis, showing the role of the electroosmotic flow for macromolecules transport[50, 51].

siRNA and oligonucleotides, showing a high negative charge and charge to MW ratios, are good candidates for iontophoretic delivery as well[52]. For the delivery of macromolecules with a MW higher than 1 kilobase pairs, such as plasmids DNA, electric pulses can be applied after DNA periocular plasmid injection to further increase drug delivery: Blair-Parks et al. found that the amount of expressed protein was nearly 1000-fold higher in comparison with that of the DNA injection alone[53].

An experimental work focused on the application of iontophoresis technique for enhancing macromolecules transport across the sclera is presented in **Chapter 3**.

1.5.2 Soft matter nanocarriers

Nanoparticles can be defined as polymeric colloidal carriers with a diameter range from 10 to 1000 nm, further classified into nanospheres, where the drug is embedded in a polymeric matrix, and nanocapsules, characterised by an external polymeric layer that acts as a release-controlling membrane. Conversely, liposomes are phospholipid-based vesicles (diameter range from 20 nm up to several micrometers) containing one or more concentric lipid bilayers separated by aqueous compartments[54]. Several research works have been reported on the use of liposomes and nanoparticles for macromolecules ocular delivery[55].

Nanocarriers also comprise nanomicelles and dendrimers. Dendrimers are hyperbranched molecules showing host-guest entrapment properties; those made up of cationic amines have shown potential for delivering plasmid DNA, genes or siRNA to RPE and retina[56]. A detailed discussion about polymeric nanomicelles is reported in **Chapter 4**.

In general, nanocarriers have been proposed to protect the encapsulated drug from degradation, control drug release, facilitate the transport of drugs into cells and finally increase drug bioavailability[55].

1.5.3 Ophthalmic inserts

Ocular inserts allow for a more accurate dosing in comparison to classical eye drops. These systems are polymeric devices classified as hydrogels that gradually dissolve while releasing the drug. When the insert is placed in the conjunctival sac, tear fluid is responsible for hydrogel swelling and polymer chains relaxation; drug diffusion can thus occur showing different kinetics in function of polymer characteristics and matrix organization. Because of biodegradability there is no need of removal from the site of application after drug delivery. Other potential advantages are increased residence time, slow drug release rate, reduced frequency of administration, enhanced drug bioavailability. Nevertheless the initial discomfort correlated to insert application in the conjunctival sac could be considered the main related disadvantage; additionally inserts movement around the eye and occasional inadvertent loss cannot be excluded[57]. A detailed discussion about these systems is presented in **Chapter 5**.

2. General purpose

The general aim of this thesis was the evaluation of enhancing strategies to promote macromolecules and peptides absorption through different ocular membranes.

The first strategy tested was iontophoresis, which consists in the application of electric current to promote drug transport across a membrane. Two different model proteins (lysozyme and cytochrome c) were selected for their comparable molecular weight and net charge at physiological pH in order to understand the role of different molecular physico-chemical characteristics (i.e. shape, conformability, water solubility and surface charge distribution) on transscleral delivery in both passive and iontophoretic conditions.

The second strategy applied was the use of polymeric micelles, a colloidal drug delivery system able to increase ocular delivery of poorly soluble drugs. Cyclosporine, a neutral cyclic peptide of 1.2 kDa molecular weight and low water solubility, was chosen because of its critical ocular bioavailability.

Finally, cyclosporine ophthalmic inserts containing sodium hyaluronan and hydroxypropyl-β-cyclodextrin were chosen as third strategy.

3. Parameters affecting the transscleral delivery of two positively charged proteins of comparable size

3.1 Abstract

Apart from molecular weight and net surface charge, there are other macromolecule-related factors that could, in principle, influence their diffusion across biological tissues, such as shape, conformability, water solubility and surface charge distribution.

Lysozyme and cytochrome c, proteins with comparable molecular weight, isoelectric point and net surface charge in physiological conditions (approx. +7.8), are suitable model compounds for comparative studies, in particular to find out if other properties can have a role in the permeation across the sclera. The comparison between lysozyme and cytochrome c permeability was conducted by studying the permeation across the sclera and the choroid-Bruch's membrane and the diffusion across a hyaluronan gel-matrix. Melanin binding tests and the measurement of the electroosmosis flow during transscleral iontophoresis allowed for the evaluation of macromolecules affinity for the ocular tissues. Finally, anodal iontophoresis was applied to further confirm the interaction of the two proteins with the sclera.

The data here collected show that two proteins with very similar MW, pKa and charge can display very different diffusion properties across biological barriers. In particular, these differences can be attributed to a different interaction with specific components of ocular tissues: while the interaction with melanin and collagen fibers is apparently the same for the two molecules, a relevant difference was found in case of hyaluronic acid. Considering also literature evidences, the important parameters that can be responsible for this different affinity are molecular shape (spherical for cytochrome c *vs* prolate for lysozyme) and a combination of hydrophobic and electrostatic interactions that depends on the surface charge distribution. The interactions between sclera components and lysozyme are relatively strong and were not altered by the application of electric current.

3.2 Introduction

The approval of the anti-vascular endothelial growth factor aptamer pegaptanib in 2004 and of the monoclonal antibody ranibizumab in 2006 have marked the introduction on the market of ophthalmic biopharmaceuticals[3]. In the following years other pharmacological agents, including proteins and oligonucleotides, have gained FDA approval or are under investigation: bevacizumab (149 kDa) and aflibercept (115 kDa) are used (approved and off-label) for the treatment of neovascularization in both anterior and posterior segment eye diseases; ciliary neurotrophic factor (23 kDa) is in clinical trial for the treatment of retinitis pigmentosa and macular telangiectasia (Phase II); nerve growth factor (26 kDa) and glial-derived neurotrophic (17.2 kDa) are under investigation for the treatment of glaucoma[58, 59]. Because of their high molecular weight and presence of charges and owing to the limited permeability of ocular tissues, macromolecules are currently administered via intravitreal injection, with risk of retinal detachment, endophthalmitis and vitreous haemorrage[3].

For the treatment of posterior eye segment diseases, the topical administration route would be preferred, thanks to the ease of application and patient compliance; however, macromolecules diffusion during transscleral delivery is limited by the presence of barriers, such as sclera, choroid and retinal pigmented epithelium[36]. The first study on macromolecules permeability through the sclera was published in 1977 by Maurice and Polgar, who examined the diffusion of different compounds, up to the size of serum albumin, across bovine sclera[60]. The following studies were performed by Olsen et al.[61] and by Ambati who tested the permeability of molecules up to 150 kDa across human sclera[31]. The effect of molecular weight on the permeability coefficient was investigated by several authors using dextrans, proteins and oligonucleotides[33, 62-64]: the permeability through the sclera was governed by the molecular radius, more than by the molecular weight, through an inversely proportional relationship. The charge of a drug molecule also affects its transscleral permeability[28]. Negatively charged macromolecules have been found to have higher permeabilities than positively charged, across bovine and porcine sclera[37, 60]: the presence of negatively charged polymers (*i.e.* hyaluronic acid, glycosaminoglycans) in the interstitial fluids could discourage the localization of negatively charged molecules, via charge repulsion[36]. In addition to the anatomic barrier, the choroid-Bruch's membrane can hamper solute permeation, due to the presence of melanin[45, 65].

In a previous paper, cytochrome c diffusion was studied across the sclera and the choroid-Bruch's layer; the results highlighted a relatively-high permeability of this compound

(transscleral permeability coefficient: $2.5*10^{-6}$ cm/s), that was greatly increased by iontophoresis. The obtained data were discussed taking into account MW and high positive charge of cytochrome c[66]. However, apart from molecular weight and net surface charge, there are other macromolecule-related factors that could, in principle, influence their diffusion across biological tissues, such as shape, conformability, water solubility and surface charge distribution. In this paper lysozyme, a model protein of similar molecular weight, net charge and isoelectric point, was studied and compared with cytochrome c to find out if properties other than charge and molecular weight can have a role in permeation.

Cytochrome c (**Figure 3**) has a compact globular structure consisting of a single polypeptide chain (104 aminoacids) with a central heme group[67]; it has a molecular weight of 12.4 kDa and an isoelectric point of 9.59 (31.7% of aminoacids charged at physiological pH)[68]. Lysozyme (**Figure 3**) has a molecular weight of 14.3 kDa (129 aminoacids) with an isoelectric point of 9.32 (20.1% of aminoacids charged at physiological pH)[68].

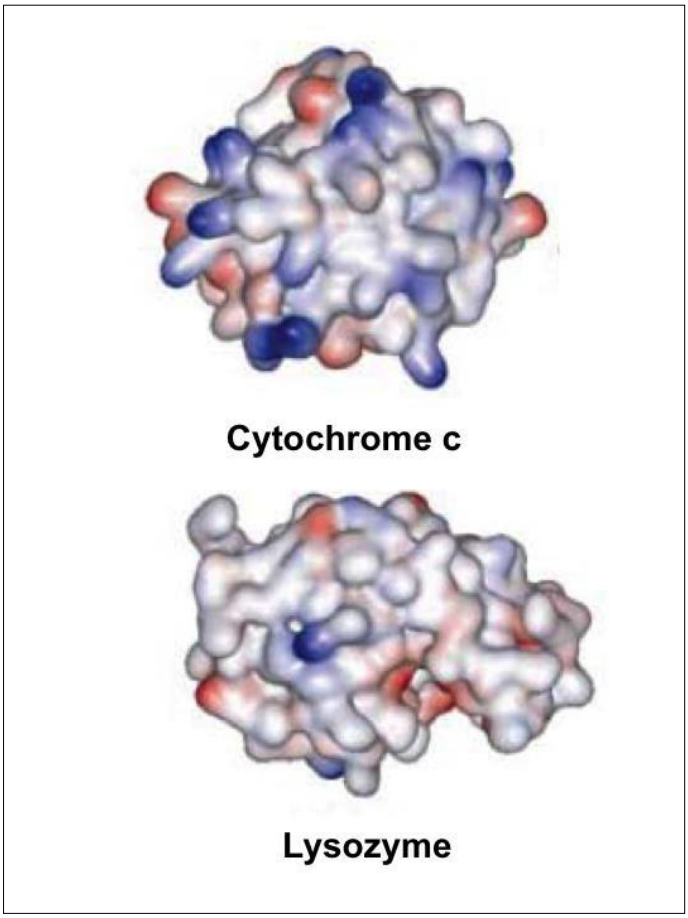

Figure 3. 3D structure of cytochrome c and lysozyme[69].

The comparison between lysozyme and cytochrome c was conducted by studying the permeation of lysozyme across the sclera and the choroid-Bruch's membrane (compared with previously collected data) and the diffusion of both proteins across a hyaluronan gel-matrix. The assessment of the two macromolecules' affinity for the ocular tissues was performed by melanin binding tests and the measurement of the electroosmosis flow during transscleral iontophoresis. Finally, anodal iontophoresis was applied in different buffers to further evaluate the interaction of the two proteins with the sclera.

3.3 Materials and methods

3.3.1 Materials

Cytochrome c from bovine hearth (MW 12.4 kDa, hydrodynamic radius 1.4–1.8 nm[70]) and lysozyme from hen white egg (MW 14.3 kDa, hydrodynamic radius 2.1–3.0 nm[70]) were purchased from Sigma (Saint-Louis, USA), as well as HEPES (4-(2-hydroxyethyl)-1-piperazineethanesulfonic acid), fluorescein isothiocyanate (FITC)-dextran (FD-150; MW 120 kDa; degree of substitution 0.006 mol FITC/mol of glucose; molecular radius 8.5 nm), melanin from *Sepia officinalis*, silver and silver chloride. Sodium hyaluronate (MW 1000 kDa) was a gift of IBSA Farmaceutici S.p.A. (Lodi, Italy). All others chemicals were of analytical or HPLC grade; Milli-Q® water was used. Buffer solutions were HEPES-buffered saline (5.96 g/l HEPES, 9.0 g/l NaCl pH 6.4 or 7.4 with NaOH, ionic strength 154 mM), phosphate-buffered saline (PBS; 0.19 g/l KH_2PO_4, 5.98 g/l $Na_2HPO_4 \cdot 12H_2O$, 8.8 g/l NaCl pH 6.4 or 7.4 with H_3PO_4, ionic strength 300 mM) and citrate buffer (0.48 g/l citric acid, 6.62 g/l sodium citrate, pH 6.4 or 7.4 with NaOH, ionic strength 25 mM).

3.3.2 Analytical methods for protein quantification

Cytochrome c was analyzed with a HPLC/UV system (Flexar, Perkin-Elmer, Norwalk, Connecticut) with a 150*4.6 mm column packed with 5 µm C_{18} silica reversed-phase particles (Phenomenex, LePecq, France) and equipped with a security guard column (Security Widepore). The mobile phase A (aqueous) was 0.1% TFA (trifluoroacetic acid) in a mixture of distilled water and CH_3CN (95:5 vol %), whereas the phase B (organic) was 0.1% TFA in CH_3CN. The flow rate was 1.6 ml/min. The LC gradient program [time (min)/% mobile phase B] was set to 0.01/25, 6/55, 9/55, 9.1/25, and 12/25. Temperature was kept at 40°C and the absorption was monitored at 214 nm. The injection volume was 100 µl. The retention time of cytochrome c was approximately 4 min. Linearity was obtained in the concentration range of 10-100 µg/ml; RSD% (relative standard deviation%) and ER% (relative error%) were lower than 15%. The LOD (limit of detection) and the LOQ (lower limit of quantification) were 5 and 10 µg/ml, respectively.

Lysozyme was quantified by an activity assay modified from[71, 72]. Briefly, a 0.18 mg/ml suspension of lyophilized bacteria (*Micrococcus lysodeikticus*) was prepared in pH 6.4 buffer solution. 165 µl of the bacterial suspension were placed in a well of a 96well plate and 85 µl of sample/standard in the same buffer were added. Absorbance at 450 nm was recorded for 4 min with a UV multiplate reader (Sunrise, Tecan, Switzerland) and

lysozyme concentration was calculated from the slope of the plot of absorbance against time. Influence of buffer and pH were evaluated.

3.3.3 Evaluation of lysozyme stability

Impact of magnetic stirring and electric current on cytochrome c stability was evaluated in a previous paper[66]. In this work, lysozyme stability was assessed in the same conditions. The influence of magnetic stirring was determined on 10 µg/ml lysozyme solutions (HEPES-buffered saline, pH 6.4, 4 ml) under constant magnetic stirring for 6 h. Hydrodynamic conditions (350 rpm) were similar to those used in the permeation experiments. Samples were collected hourly and analyzed. Experiments were performed in triplicate.

For stability studies in the presence of current, 3.5 mA was applied to 5 ml of 10 µg/ml solutions of lysozyme in HEPES buffer pH 6.4 using salt bridges to ensure connectivity between electrodes and solution. After 1 and 2 h, samples were collected and analyzed. Experiments were performed in duplicate and proteins solutions in contact to salt bridges (no current application) were used as control.

To verify the possible lysozyme aggregation, a test was performed[73]. 100 µg/ml solutions were prepared in HEPES buffer, citrate buffer or isopropanol, the last chosen as positive control. Absorbance was recorded at λ=280 nm and λ=340 nm. The aggregation index was calculated as the ratio of absorbance recorded at 340 nm to the difference between the absorbance value recorded at 280 nm and the one recorded at 340 nm. An aggregation index lower than 2 demonstrates the absence of aggregates, whereas aggregates are present when the index is higher than 5[73]. The experiment was performed in triplicate.

Cytochrome aggregation could not be evaluated because of the presence of the heme group, able to absorb at the wavelength utilized in the test.

3.3.4 Tissue preparation

Fresh porcine eyes were isolated from Landrace and Large White (age 10–11 months, weight 145–190 kg, female and male animals) supplied from a local slaughterhouse (Annoni S.p.A., Parma, Italy). The eyes were kept in PBS at +4°C until the dissection, which occurred within 2 hours from the enucleation. In the first step, muscular and connective tissues around the eye-bulb were completely removed. The anterior segment of the eye was circumferentially cut behind the limbus and removed. The obtained eyecup was then cut and everted. The neural retina was discarded and the choroid-Bruch's layer

was carefully removed from sclera with forceps, cutting with a scalpel the vessels engaged in the sclera.

3.3.5 Partition experiments

Partition experiments were performed to determine the relative affinity of lysozyme and cytochrome c to the sclera. Approximately 100 mg of sclera cut into small pieces were incubated with 0.5 ml of proteins solution in HEPES (pH 6.4 for lysozyme experiments, pH 7.4 for cytochrome c experiments) at different concentrations (5-500 µg/ml). After two hours, the solution was sampled and analysed for the determination of the final concentration in the water phase [W_f]. The peptide concentration in the sclera [S] was calculated as:

$$[S] = \frac{[\mathrm{Wi}]*\mathrm{Vw}-[Wf]*Vw}{\mathrm{Vs}} \quad \text{(eq. 1)}$$

where [W_i] is the initial concentration of protein in the aqueous phase; V_W is the volume of the aqueous phase (0.5 ml); V_S is the volume of the sclera, estimated by its weight and considering the scleral density equal to 1 g/ml. The partition coefficients were calculated as the ratio of protein concentration in the sclera to that in the buffer after 2 h. The experiments were performed in triplicate.

3.3.6 Melanin binding experiments

In vitro binding studies using melanin from *Sepia officinalis* were performed by modifying the protocols used by Potts[74]. Briefly, 1.50±0.05 mg of melanin were precisely weighted in a glass vial and then dispersed in 0.75 ml of PBS (pH 6.4 for lysozyme binding tests, pH 7.4 for cytochrome c experiments). The obtained suspension was sonicated for 20 min, then 0.75 ml of sample was added. Concentrations in contact with melanin were in the range 0.5-70 µM. Control solutions, without melanin, were also prepared. After incubation at 25°C for 1 h under magnetic stirring, the suspension was centrifuged at 12000 rpm at room temperature for 10 min. The supernatant, containing the free test compound, was separated and analyzed, together with control solutions.

3.3.7 Passive permeation experiments across sclera and choroid-Bruch's membrane

Permeation experiments were performed in Franz-type diffusion cells (Disa, Milan, Italy). The diffusion area was 0.2 and 0.6 cm^2 in case of choroid-Bruch's membrane (CH-BM) and isolated sclera, respectively. In the CH-BM experiments the pigmented tissue was applied on the diffusion cell without any kind of support, with the choroidal side facing the donor compartment containing a 0.5 mg/ml solution of lysozyme in PBS at pH 6.4 (n=3).

The receiving phase consisted of 4 ml of PBS pH 6.4, thermostated at 37°C and magnetically stirred, to avoid any boundary layer effect. For experiments on isolated sclera, the tissue was mounted with the episcleral layer facing the donor compartment. The donor contained a lysozyme solution either 10 (n=3) or 40 (n=5) mg/ml in HEPES buffered saline at pH 6.4; the receptor compartment contained 4 ml of the same buffer thermostated at 37°C and magnetically stirred.

At predetermined time intervals, to determine the amount of protein permeated, 0.3 ml of receptor solution were sampled, restoring the initial volume with fresh buffer.

Blank permeation experiments were performed across sclera and CH-BM. The receptor solution was analysed by HPLC and no interfering peak was found at lysozyme and cytochrome c retention times. The same solution was also analysed using the activity assay and revealed no enzymatic activity.

3.3.8 Diffusion experiment across hyaluronan gel

A vertical diffusion cell with a permeation area of 3.9 cm^2 was used. The donor compartment was filled with 1.75 g of the gel (1 or 2% w/w sodium hyaluronate (HA) solution) applied on a previously-hydrated regenerated cellulose membrane 0.45 µm, used as support. 100 µl of 10 mg/ml protein solution in PBS (pH 6.4 for lysozyme, pH 7.4 for cytochrome c) were poured on the top of the gel. The receiving compartment was filled with approx. 10 ml of PBS (pH 6.4 for lysozyme, pH 7.4 for cytochrome c). At predetermined time intervals, in order to determine the amount of protein permeated through the gel, 0.3 ml of receptor solution was sampled, restoring the initial volume with fresh buffer. Experiments were performed in triplicate. Possible protein absorption to the regenerated cellulose membrane was previously evaluated.

3.3.9 Iontophoretic experiments

For current-assisted experiments, only isolated sclera was used. The current (intensity 1.75 mA, density 2.9 mA/cm^2, anodal) was applied for 2 h with a continuous current generator (GS210, Yocogawa Italia srl, Cinisello Balsamo, Italy) connected with a multimeter (MK 7701 Mitek, NL Industries, Milan, Italy) to silver/silver chloride electrodes. Salt bridges (agar 2% w/w; 1 M KCl) were used to avoid the contact between the protein and the electrodes. In the case of iontophoresis (anodal), Ag electrode (anode) was put in contact with the donor compartment, while AgCl electrode (cathode) was connected to the receiving phase. The donor compartment contained 300 µl of a 40 mg/ml protein solution. The receiving compartment contained 4 ml of HEPES or citrate buffer thermostated at

37°C and magnetically stirred, to avoid any boundary layer effects. After 2 hours, the current was stopped and the experiment continued in passive conditions up to 5 or 6 hours. The donor solution contained either 40 mg/ml cytochrome c in citrate buffer at pH 6.4 (n=3) or 40 mg/ml lysozyme solution in citrate buffer pH 6.4 (n=5) or 40 mg/ml lysozyme solution in HEPES-buffered saline pH 6.4 (n=4).

3.3.10 FD-150 permeation experiments

To evaluate macromolecules interactions with sclera and their impact on electroosmosis, iontophoretic experiments across isolated sclera were performed using a high MW dextran (FD-150; donor 1 mg/ml in HEPES buffer pH 7.4) as neutral marker. FD-150 iontophoretic permeation was measured both with (n=3) and without (n=4) lysozyme or cytochrome c (both individually co-applied with dextran) in HEPES buffer at pH 7.4 at 1 or 40 mg/ml concentration. Experiments were performed using 0.6 cm^2 Franz-type diffusion cells (see paragraph 3.3.7 for details); the current (anodal, 2.9 mA/cm^2) was applied as previously detailed (paragraph 3.3.9). The amount of FD-150 permeated across the sclera was quantified using a fluorescence multilabel plate reader (Viktor^3 1420, Varian; λ_{ex} 485 nm, λ_{em} 535 nm).

3.3.11 Data processing

Permeated amount ($\mu g/cm^2$) is presented as a function of time (min). The transmembrane flux of macromolecules (J, $\mu g/cm^2$ min) is calculated from the slope of the regression line in the linear part of the curve, and the apparent permeability coefficient (P_{app}, cm/s) is calculated as:

$P_{app} = J/C_D$ (eq. 2)

where C_D (µg/ml) is the concentration of the donor solution. The time-lag (min) was determined from the intercept on the x-axis of the regression line.

3.3.12 Statistical analysis

The significance of the differences between conditions was assessed using Student's *t*-test. Differences were considered statistically significant when $p < 0.05$. All the numerical values present in the text are mean value±SD. In Figures, for sake of clarity, the experimental points are represented as mean value±standard error of the mean, as indicated in the legend, and the number of replicates is reported.

3.4 Results

3.4.1. Quantification and stability of lysozyme

Lysozyme samples were analyzed with the same HPLC/UV method used for cytochrome c[66]; a comparable linearity range was obtained (10-100 µg/ml). Lysozyme activity was evaluated using an enzymatic assay, to verify the possible inactivation in the experimental conditions used and to reduce the limit of quantification. Enzymatic assay showed that the protein is stable in the presence of magnetic stirring for 6 h (percentage of unaltered protein 96.8%±11.1%) and that lysozyme activity depends on pH and buffer composition. Since the best calibration curve and the lowest LOQ (4 µg/ml) were obtained at pH 6.4 (pH of maximum stability[75], this value was used in all experiments with lysozyme; its net charge is approx. +8 at both pH 6.4 and 7.4[76], value comparable to cytochrome c charge at pH 7.4 (+7.9,[67]). Lysozyme aggregation index in HEPES and citrate buffers was 1.8 and 0.8, respectively, showing no aggregation.

The stability of lysozyme to electric current was also checked. The enzymatic activity measured after 2 h of current application was 87±4%, whereas the control with salt bridges (without current) showed 84% of unaltered lysozyme, suggesting that protein activity is sensitive to the salt leaking from salt bridges more than to current application.

Concerning cytochrome c, previous data show that this protein is sensitive to magnetic stirring. However, limiting the experiment to 5 h, protein loss is lower than 10%. Cytochrome c resulted stable upon current application[66].

3.4.2. Passive permeation across isolated sclera

Figure 4 reports lysozyme permeation profiles compared with the data previously obtained with cytochrome c[66]. Despite the similar molecular weight and charge, the passive permeation of the two proteins differed significantly: at 10 mg/ml, permeation was detectable only for cytochrome c (after 5 h the amount permeated was 229.2±153.0 µg/cm^2); at 40 mg/ml, lysozyme was quantified in the receptor compartment, but its permeability was 9 times lower than cytochrome c. Cytochrome c permeability coefficient was approx. $2.5*10^{-6}$ cm/s[66], in agreement with literature data of molecules of comparable hydrodynamic radius[77], while lysozyme apparent permeability coefficient was almost one order of magnitude lower, i.e. $2.9*10^{-7}$±$1.18 *10^{-7}$ cm/s (calculated using the instantaneous flux between 240 and 360 min). It is worth mentioning that permeation samples were analyzed with both HPLC/UV and activity assay to be sure that the result was not simply due to a loss of activity.

The permeability difference observed could be due to a different interaction of the two proteins with the biological tissue; for this reason, further experiments were performed.

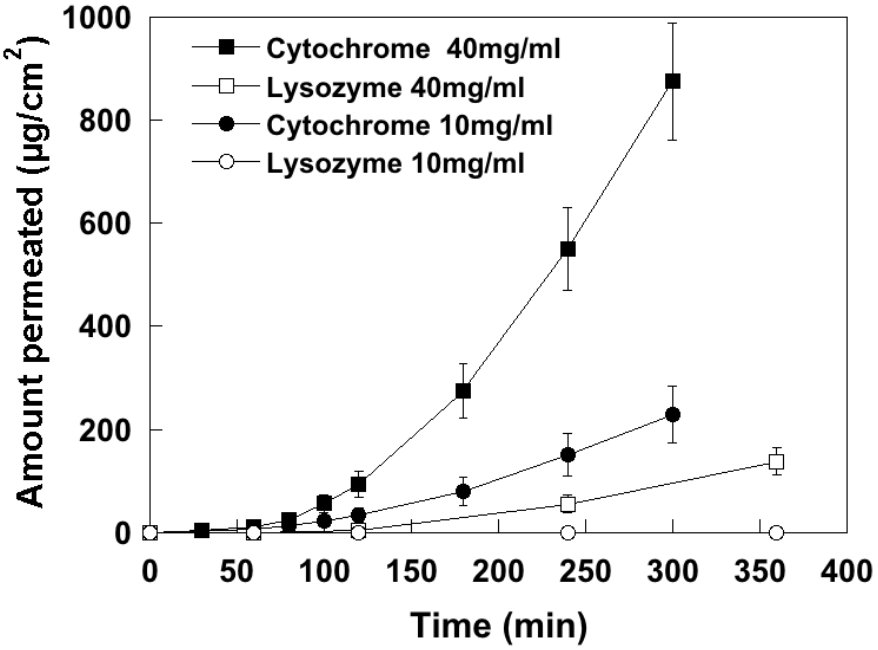

Figure 4. Lysozyme permeation profiles across isolated porcine sclera from 10 (open circle, n=3) and 40 (open square, n=5) mg/ml solutions in HEPES buffer[69]. Data are compared with cytochrome c permeation, adapted from [66] starting from 10 (full circle) and 40 (full square) mg/ml solutions in HEPES buffer. The data are represented as mean value±sem. Lysozyme permeated amounts are statistically different from cytochrome c at all time point ($p<0.05$).

3.4.3 Binding to sclera

Tissue binding can be estimated by partitioning experiments, i.e. by measuring the distribution of the molecule between the tissue and a solution. The results obtained with lysozyme and cytochrome c did not show any preferential partition/adsorption to the sclera (the value of partition coefficient resulted close to 1, with high variability). Then, an alternative indirect method based on the measurement of the electroosmotic flow (EO) during transscleral iontophoresis was used. The transscleral permeation of a neutral fluorescent marker (FD-150, MW 120 kDa) in passive and iontophoretic (anodal, 2.9 mA/cm^2) conditions was evaluated in the absence and in the presence of cytochrome c and lysozyme. FD-150 was chosen as an EO marker due to its high MW and relatively low passive permeability across the sclera[78]. The amount of FD-150 permeated after 2 h was 25 times higher for anodal iontophoresis compared to passive permeation: this enhancement is entirely due to EO, because FD-150 is a neutral molecule. Both cytochrome c and lysozyme did not hinder the transport when present at 1 mg/ml (data not

shown), while a significant reduction was present at 40 mg/ml (**Figure 5**). This behavior can be explained by protein adsorption to the scleral tissue, with consequent reduction of the negative charge of the barrier, responsible for EO[79].

In **Figure 5**, a high post-iontophoretic permeation of FD-150 is visible. Previous data demonstrated that low and high MW compounds can greatly accumulate into the sclera during current application forming a drug reservoir into the tissue. From this reservoir the drug is released also after current stop[62, 63, 78]. The release rate in this post-iontophoretic phase is governed by drug concentration in the tissue (not in the donor solution), that is proportional to the efficiency of the previous iontophoretic transport. Indeed, the post-iontophoretic flux (calculated between 180 and 300 min) resulted 1.44±0.29 μg/(cm^2·h) when FD-150 was alone in the donor solution, while it decreased to 0.59±0.09 μg/(cm^2·h) or 0.53±0.13 (μg/cm^2·h) in the presence of, respectively, cytochrome c and lysozyme. This reduction is statistically significant ($p<0.005$) and contributes to support the hypothesis of protein binding to the sclera. To support this hypothesis further experiments were carried out.

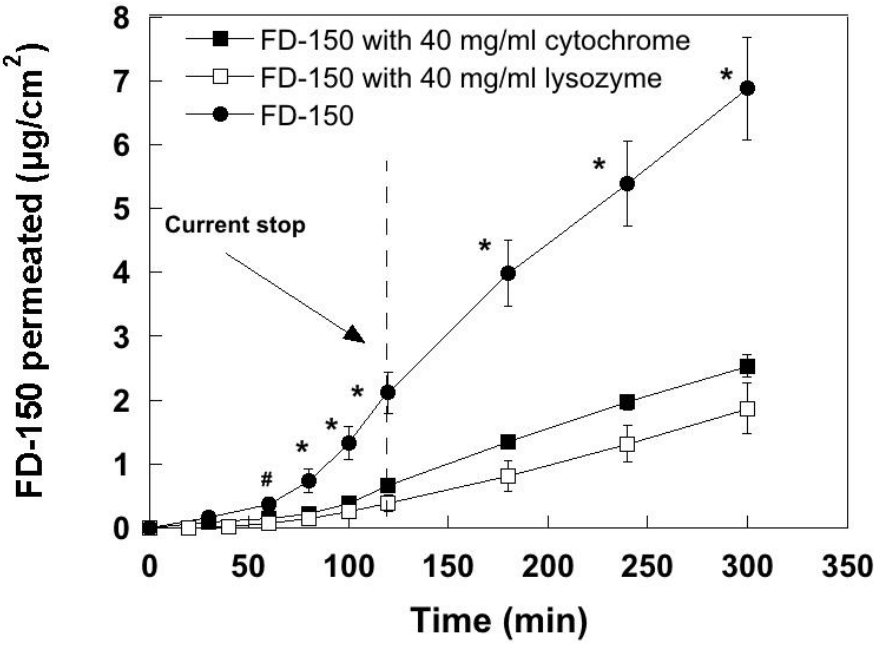

Figure 5. FD-150 (1 mg/ml, HEPES buffer, pH 7.4) permeation profiles in iontophoretic conditions (anodal, 2.9 mA/cm^2), in absence (full circle, n=4) and in the presence of 40 mg/ml lysozyme (void square, n=3) or cytochrome c (full square, n=3)[69]. The data are represented as mean value±sem. *, statistically different from both cytochrome c and lysozyme containing solutions; # statistically different from lysozyme-containing solution.

3.4.4. Diffusion across hyaluronan gel

To study the interaction of lysozyme and cytochrome c with the sclera, sodium hyaluronate, a non-sulfated glycosaminoglycan and one of the major components of ocular tissues, was selected. 100 µl of either lysozyme or cytochrome c solution (10 mg/ml in PBS) were poured on the top of a layer of 2% or 1% w/w sodium hyaluronate gel, 0.45 cm thick. To reach the receiving compartment, the proteins should permeate across the gel layer and possible interactions should be detectable.

Figure 6 shows that no diffusion is detectable across the 2% gel (protein: HA weight ratio 1:34), while, reducing to a half HA concentration (1:17 weight ratio) cytochrome c and lysozyme are recovered in the receptor solution. The two profiles show a comparable diffusion rate (lysozyme and cytochrome c flux was 0.23±0.03 and 0.28±0.09 µg/(cm^2·min), respectively), but a substantially different time-lag (lysozyme 178±53 min vs cytochrome c 79±31 min, $p<0.05$), that suggests a different interaction of the two proteins with the polymer.

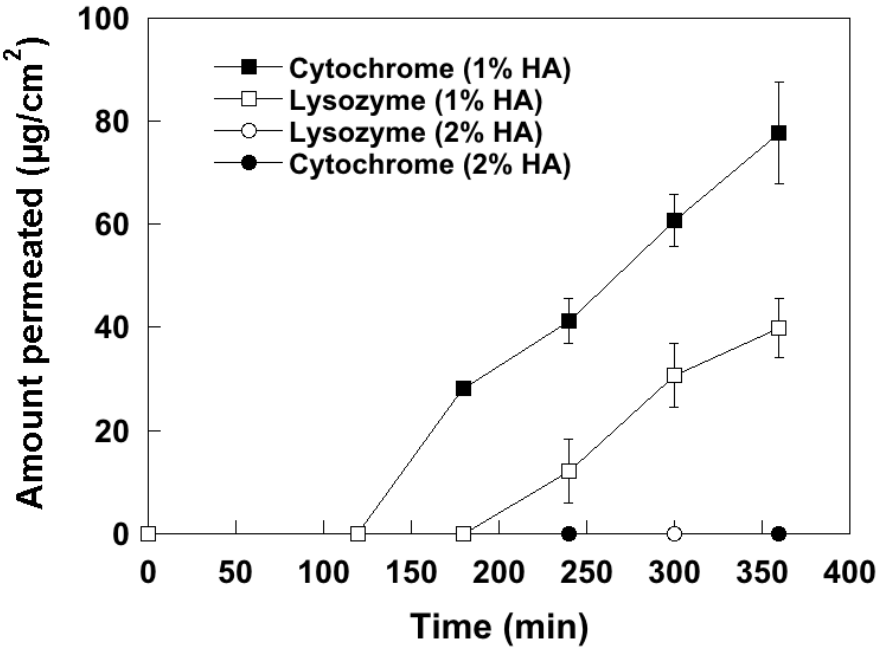

Figure 6. Cytochrome c (full symbols) and lysozyme (void symbols) permeation profiles across a layer of 1% (square) and 2% (circle) w/v hyaluronan gel, 0.45 cm thick[69]. For all conditions, n=3. The data are represented as mean value±sem. Lysozyme permeated amounts across 1% gel are statistically different from cytochrome c at all time point ($p<0.05$).

3.4.5 Binding to melanin and diffusion across the choroid-Bruch's membrane

The interaction with melanin is shown by the binding curves reported in **Figure 7**. The results obtained demonstrated a higher affinity of lysozyme for melanin in comparison with

cytochrome c, although the shape of the curves prevents the calculation of binding parameters for both proteins.

The affinity for melanin was studied also by evaluating the permeation across pigmented isolated choroid-Bruch's membrane[65]. Despite the difference in melanin binding, lysozyme permeability coefficient across choroid-Bruch's membrane resulted $1.73 \cdot 10^{-5} \pm 9.26 \cdot 10^{-7}$ cm/s, superimposable to the value obtained for cytochrome c[66].

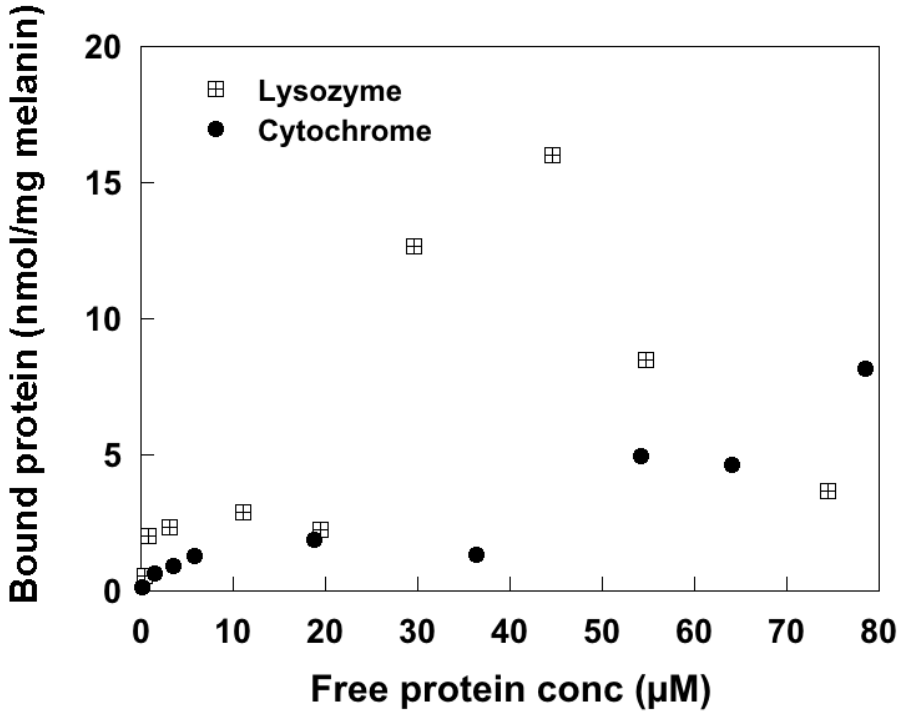

Figure 7. Binding curve of cytochrome c and lysozyme to melanin from *Sepia officinalis* in PBS (pH 7.4 for cytochrome c, pH 6.4 for lysozyme)[69]. The figure represents the amount of protein bound per mg of melanin as a function of the free protein present in solution.

3.4.6. Iontophoretic permeation across isolated sclera

Lysozyme and cytochrome c iontophoretic permeation profiles (donor concentration 40 mg/ml in citrate and HEPES buffers) are reported in **Figure 8**, and show deep differences: the amount permeated after 5 h (2 h of iontophoresis, followed by 3 h of passive diffusion, citrate buffer) were 3297±1249 and 102±116 μg/cm^2 for cytochrome c and lysozyme, respectively. Similar results were obtained in HEPES buffer; the amount permeated after 5 hours was 372±228 μg/cm^2 for lysozyme, much lower than the values previously found for cytochrome (1869±241 μg/cm^2 [66]). Thus, cytochrome c permeability resulted high and highly improved by iontophoresis while this technique does not represent an efficient method to enhance lysozyme permeation.

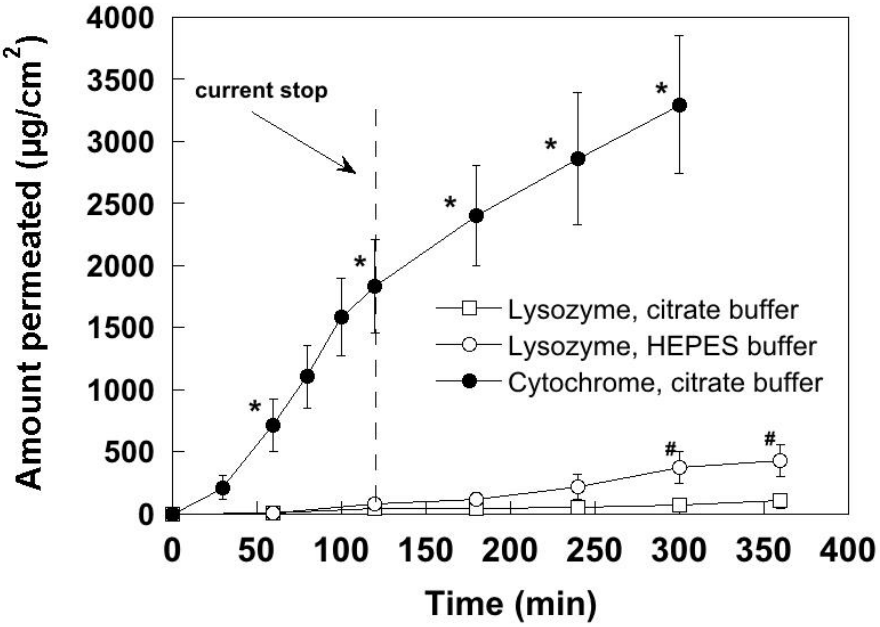

Figure 8. Iontophoretic permeation profile of cytochrome c and lysozyme at pH 6.4[69]. Lysozyme transport was evaluated from a citrate buffer (open square, n=5) and from an HEPES buffer (open circle, n=4); cytochrome c transport was evaluated from a citrate buffer (full square, n=3). The current (anodal, 2.9 mA/cm^2) was applied for 2 h. The data are represented as mean value±sem. *, statistically different from lysozyme, $^{\#}$ statistically different from citrate buffer.

3.5 Discussion

Lysozyme and cytochrome c have comparable MW (14.3 kDa and 12.4 kDa, respectively), similar aminoacid number (129 and 104), comparable pI value (9.32 and 9.59) and net surface charge at physiological conditions (approx. +7.8). These properties make these proteins suitable as model compounds for comparative studies. Indeed, cytochrome c and lysozyme have been used together as model proteins for studying macromolecules diffusion in fibrous structures[80], investigating the release properties of negatively charged nanoparticles[81] and comparing drug delivery behavior of mesoporous silicas[82].

The free diffusion coefficient of the two molecules is similar, as demonstrated by the values obtained experimentally in water[83] and calculated by molecular dynamics simulations[84]; however, the transscleral permeability of the two molecules resulted dramatically different (**Figure 4**), suggesting that properties other than MW and charge can impact on the diffusion across the sclera. The modest difference in molecular weights and radius between lysozyme and cytochrome c should not influence the permeation across this highly porous tissue[77]; additionally, the aggregation test did not highlight the presence of aggregates. Binding to sclera components may have contributed to the low lysozyme transport. This interaction was not evident when performing partition experiments with sclera, while it was indirectly demonstrated by electroosmotic flow measurement: the decrease of the electroosmotic flow in the presence of lysozyme and cytochrome c (**Figure 5**) indicates a reduction of the negative charge of the sclera, attributable to the interaction with the positively charged proteins[85-88]. The lack of preferential partitioning and the indirect evidence of binding to the sclera suggest that the two proteins interact more with water soluble compounds than with collagen fibers. Water soluble components, such as glycosaminoglicans, hyaluronic acid, dermatan sulfate and chondroitin sulphate leak out of the tissue during partitioning experiments (the sclera is minced) while are retained in the tissue during permeation experiments. Indeed, diffusion experiments across hyaluronic acid gel support this hypothesis and highlight a significant difference between the two proteins (**Figure 6**).

In the literature, evidences of lysozyme interaction with biological polymers are present and demonstrate that binding is of electrostatic nature and sensitive to ionic strength, showing optimal levels for salt concentration up to 20 mM[89, 90].

The differences in transscleral permeation and HA diffusion of the two proteins are not due to differences in MW or charge and other properties should be involved. Welsch et al. studied the interaction of lysozyme and cytochrome c with a negatively charged microgel

made of poly(N-isopropylacrylamide) and acrylic acid. They found that, even though the number of absorption sites was comparable, lysozyme binding was 10-fold stronger than cytochrome c[91]. The different affinity was attributed to a combination of both hydrophobic and electrostatic interaction, related to surface charge distribution. Other authors suggest that also the shape of the molecules can play a role[82, 92, 93]. In fact, even if the limited difference of the axial ratio between the two proteins (**Figure 3**) implies a similar friction coefficient, thus similar diffusion properties[94], the shape could influence the capability of the molecule to enter pores and/or channels of the sclera and interact with uneven tissue surfaces. Indeed, Jeong et al. studied protein loading and release from mesoporous materials and attributed the higher lysozyme loading to its prolate spheroid shape (1.9*2.5*4.5 nm^3) that allows pore entering in longitudinal direction, while cytochrome c spherical shape (2.6*3.2*3.3 nm^3) prevents its diffusion into pores[82].

Another obstacle to protein diffusion towards the deep ocular tissues is represented by melanin, an indolic polymer able to bind lipophilic and cationic molecules with high affinity, reducing their transport[37, 38, 45, 65, 95, 96]. In our case, the *in vitro* binding studies made with melanin from *Sepia officinalis* (**Figure 7**) suggest a higher affinity for lysozyme although the shape of the curves prevents the calculation of binding parameters for both proteins. This outcome could be due to different reasons, connected to each other: firstly, the particle size of melanin, which is probably different between *Sepia officinalis* and the ocular tissues, that can affect the number of binding sites on melanin surface; secondly, ionic interactions between charged macromolecules and melanin can involve different binding sites on its surface (a shift of lysozyme isoelectric point in the presence of melanin was reported[97]). Additionally, possibility of lysozyme aggregation at high concentration cannot be excluded, because the aggregation test was performed in a more diluted solution. Despite the differences observed in melanin binding, lysozyme permeability coefficient across choroid-Bruch's was superimposable to cytochrome's[66]. This discrepancy can be due to the localization of melanin that, inside the choroid, is stored in uveal melanosomes, cellular organelles included in a lipid membrane[98] that limits the access to the pigment, particularly in the case of hydrophilic and high molecular weight compounds.

Iontophoresis is a physical technique based on the principle of charges repelling each other. Electrorepulsion and electroosmosis represent the two mechanisms involved in the enhancement. Anodal iontophoresis was here selected because both proteins are positively charged and the application of anodal iontophoresis causes a convective solvent flow (electroosmosis) in the anode-to-cathode direction, thus further enhancing the

transport. In contrast with the positive results obtained with cytochrome c, lysozyme iontophoretic permeation resulted very low (**Figure 8**). This could be due to low protein mobility under current application or, again, to electrostatic interactions with tissue glycosaminoglycans. Preliminary experiments of capillary iontophoresis indicate a higher electrophoretic mobility of lysozyme compared to cytochrome c (data not shown), as also widely reported in the literature[58, 99]. For this reason, we can hypothesize that the interactions between lysozyme and the sclera are relatively strong and are not influenced by the application of an electric field. Again, ionic strength seems to play a role (**Figure 8**): it was lower in the case of citrate buffer (higher interaction, lower transport) and higher for HEPES buffer (lower interaction, higher transport). Parenthetically, lysozyme iontophoresis resulted of limited efficacy also across the skin, in comparison with cytochrome c and RNase A[68].

3.6. Conclusions

The data here collected show that two proteins, with similar MW, pKa and charge, can display very different diffusion properties across ocular barriers. The observed differences can be attributed to a different interaction with specific components of ocular tissues. While the interaction with melanin and collagen fibers is apparently the same for the two molecules, a relevant difference was found in the case of hyaluronic acid. Taking into account literature evidences, the important parameters that can be responsible for this different affinity are molecular shape (spherical for cytochrome c *vs* prolate for lysozyme) and a combination of hydrophobic and electrostatic interaction, that depend on the surface charge distribution. The interactions between sclera components and lysozyme are relatively strong and were not altered by the application of electric current.

4. Polymeric micelles suitability in macromolecules delivery to the eye

Nanocarriers have been widely investigated for overcoming poor bioavailability of drugs administered by ocular topical route[32]. Advantages of colloidal dosage forms include drug protection from degradation, increased residence time on ocular surface, sustained release of the drug at the target site, reduced frequency of administration, and, in some cases, ability to cross physiological barriers. Furthermore, these carriers can also overcome various stability-related problems, as in case of proteins and peptides[19, 55].

Among colloidal systems, polymeric nanomicelles have shown their potential to overcome limitations of traditional ocular dosage forms and provide therapeutic drug concentrations in the ocular tissues of the anterior and posterior segments[100], encouraging their use also as carriers for biologics.

Micelles are constituted of amphiphilic molecules able to self-assemble in aqueous media forming organized structures of various size and shapes, depending on the molecular weight of the hydrophilic/hydrophobic regions of the surfactant and the characteristics of the medium[101]. Micellization process in water results from a delicate balance of intermolecular forces, including hydrophobic, steric, electrostatic, hydrogen bonding and van der Waals interactions[102]. The self–assembly takes place above a certain concentration, referred as critical micellar concentration (CMC). The experimental determination of the CMC can be performed by evaluating different physical properties, such as surface tension, conductivity or osmotic pressure. When one of these properties is plotted in function of the concentration of an amphiphilic molecule, a sharp break can be observed in the curves in correspondence of the value of CMC[103].

Nanomicelles, i.e. micelles smaller than 100 nm, can be divided into three categories: polymeric, surfactant and polyionic complex nanomicelles (**Figure 9**)[101].

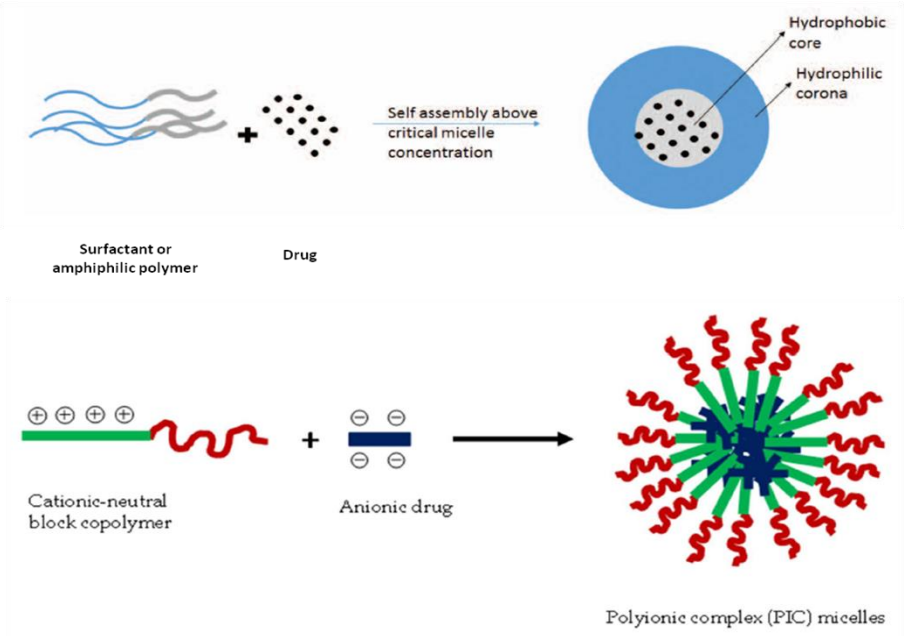

Figure 9. Schematic representation of surfactant, polymeric and polyionic complex nanomicelles, adapted from[104].

Polyionic complex nanomicelles, composed of polyion copolymers with neutral and ionic segments, have been investigated as nanocarrier systems for gene and antisense oligonucleotide ocular delivery, as electrostatic interactions between core forming blocks and oppositely charged drugs are responsible for nanomicelle formation and drug encapsulation. Surfactants nanomicelles, made from low MW surfactants, such as Tween 80 or sodium dodecyl sulphate, generally show high critical micellar concentration and thus physical instability. To overcome these limitations, polymeric micelles, i.e. micelles made of amphiphilic polymers, can be employed, being able to exhibit lower CMC and better stability against dilution. Polymeric non ionic surfactants are the major type of surface active polymers used in ophthalmic delivery systems since their advantages with respect to compatibility, stability and toxicity are significant compared to the cationic, anionic, or amphoteric polymers. In fact they are generally less toxic, less haemolytic, less irritating to the ocular surface and maintain near physiological pH values in solution[105].

Amphiphilic polymers are made by distinct core-forming hydrophobic segments and corona-forming hydrophilic segments[104, 106]. The corona-forming blocks make nanomicelles soluble in aqueous media, while the hydrophobic core can host hydrophobic drugs, increasing their solubility in water.

Drug can be encapsulated in the nanomicelle during or after nanomicelle formation depending on the preparation method and physicochemical properties of the drug. The

most commonly used methods of nanomicelle preparation are direct dissolution, solvent evaporation, film hydration and dialysis method.

There are different sites of solubilisation in nanomicelles as physical properties (microviscosity, polarity or hydration degree, for example) are not uniform along the system[106, 107]. Hydrophilic drugs can thus be adsorbed on the surface of the nanomicelle, drugs with intermediate hydrophobicity may be located in intermediate positions within the nanomicelle, and completely insoluble hydrophobic drugs may be located in the inner core of the nanomicelle. The core compartment should demonstrate high loading capacity and controlled release of the drug in order to prevent drug burst release before reaching the target site[108].

The corona is responsible for nanomicelles interactions with the biological environment. It determines nanomicelles charge and provides steric protection, in dependence of surface density of hydrophilic blocks. Additionally, the corona can present reactive groups suitable for further nanomicelle derivatization. Specific ligands can be attached in order to optimize the controlled release and specificity of pharmacological effect[106].

Small size is one of the most interesting features of polymeric nanomicelles, as it permits also simple sterilization process by filtration[109, 110] and promotes cellular entry processes[104]. Micellar size depends on several factors including copolymer molecular weight and relative proportion of hydrophilic and hydrophobic chains[104]; incorporation of drugs into nanomicelles affects dimensions[104], as well as the presence of others excipients such as cosolvents in the formulation[111].

Polymers utilized to prepare nanomicelles should be biocompatible and biodegradable; the degradation products should not be toxic or inflammatory to the ocular tissues[104]. The most widely studied core-forming polymers are poly(lactide), poly(propylene oxide) (PPO), poly(glycolide), poly(lactide-co-glycolide), and poly(ε-caprolactone) (PCL). Poly(ethylene glycol) (PEG) (MW 1-15 kDa) is the most used as hydrophilic corona-forming blocks; this polymer is inexpensive, has a low toxicity and can serve as an efficient steric protector of various biologically active macromolecules[112]. Among possible alternatives to PEG, poly(N-vinyl-2-pyrrolidone) is frequently considered as a primary substitute[113].

The physical stability of polymeric nanomicelles includes their thermodynamic and kinetic stability. Thermodynamic stability describes the formation of micelles and equilibrium between unimers and organised structures. Polymeric nanomicelles exhibit high thermodynamic stability related to low critical micellar concentration values, making them less prone to disassembly at low concentrations than standard

surfactants[114]. Polymeric nanomicelles also possess good kinetic stability, meaning that the dissociation of nanomicelles into unimers is a slow process, even when the system is subjected to dilution below CMC. Thermodynamic and kinetic stability of nanomicelles have a strong impact on drug release from the nanomicellar systems to the targeted tissue[110], as well as the biodegradation rate of copolymers.

4.1 Potential use of polymeric micelles in ophthalmology

The application of nanomicelles encapsulating hydrophobic drugs for treating ocular diseases could be advantageous because these nanocarriers can be dispersed in an aqueous solution and applied as eye drops in the conjunctival sac. This feature avoids sticky feeling and blurred vision commonly associated to the use of ointments. Additionally, lipidic excipients can cause ocular burning, conjunctival hyperemia, discharge, epiphora, eye pain, foreign body sensation, pruritus and stinging[115], with these adverse effects more or less pronounced depending on the lipidic excipient used[116]. Additionally, amphiphilic excipients used in nanomicelles favour the spreading of the formulation on the ocular surface.

Once applied in the conjunctival sac, nanomicelles are diluted, because of tear turnover (physiological tear fluid rate 3 µl/min[117]) and induced lacrimation[28]. For these reasons, nanomicelles should show a good thermodynamic and kinetic stability.

Another important property is the capability to be retained in the conjunctival sac or on the ocular surface; this could be obtained either increasing the viscosity or through mucoadhesion. The use of thermoreversible polymers permits the administration of nanomicelles in a liquid form, while after the contact with biological tissues at the physiological temperature a sol-gel transition can be achieved, making the formulation more viscous and thus more difficult to be eliminated by tear fluid. This is the case of micelles prepared using poloxamers for which the corneal contact time increases proportionally to the viscosity of the formulation, with this value that has to be superior to the minimum value required for eye drops (10 mPa·s)[118].

Another strategy involves the use of mucoadhesive polymers that permit the adhesion of nanomicelles to the pre-corneal or conjunctival mucus layer by non-covalent bonds, remaining on the ocular surface longer[119]. The same effect can be obtained also with nanomicelles bearing a positive charge able to interact with the negatively charged ocular surface.

When the constituting polymer is not mucoadhesive, nanomicelles can be superficially coated with mucoadhesive polymers such as chitosan or hyaluronate[120]. In particular chitosan, the cationic polysaccharide derived from chitin, has been widely used in biomedical and pharmaceutical applications[121, 122] and investigated for the development of novel nanomicellar formulations for corneal delivery of drugs[123-125]. Chemical modification of polymers with specific functional groups (for example –SH) potentially able to interact with ocular mucins has also been investigated[126, 127].

If topical administration is performed to target the cornea and the anterior eye segment the drug should be taken up by cornea cells and permeate across this tissue. Several authors suggested that nanomicelles, if sufficiently stable, could be internalized by epithelial cells[126, 128-130]. However, this hypothesis has not yet been confirmed since it is not possible to understand if the drug accumulated in the tissue is free or incapsulated in nanomicelles. Another hypothesis is that the drug is released from nanomicelles on the ocular surface and then taken up by corneal cells. The capability of polymeric surfactants to interact with cell membrane, acting as permeability enhancers, could explain the better performance obtained with micelles with respect to other vehicles[131-134].

Topically applied drug-loaded polymeric micelles have the potential to reach the posterior segment of the eye by the transscleral route, through the conjunctiva, the sclera and the choroid to reach the retina. In fact, polymeric micelles because of their small size and hydrophilic surface can probably travel through the hydrophilic pores of the sclera, which range from about 30 to 300 nm in size[110]. Cholkar et al. demonstrated the feasibility of cyclosporine[135] and rapamycin[136] delivery to the posterior eye segment: nanomicelles seems to be transported through a conjunctival-scleral pathway and accumulate in the sclera, which can further act as a reservoir. The use of amphiphilic polymers able to block P-gp efflux transport in the RPE could also permit drug access to the retina.

4.2 Ophthalmic applications of polymeric micelles

Polymeric micelles have largely being investigated as carriers for the delivery of different classes of drugs, as anti-inflammatory agents[123, 126, 128, 129, 131, 132, 137, 138], antiglaucoma drugs[124, 139, 140], antioxidants[133, 141-143], antifungal compounds[134, 144] and genes[145, 146]. Wide attention was also dedicated to cyclosporine A[119, 130, 147, 148].

4.2.1 Cyclosporine A

Dry eye disease (DED), one of the most frequent ocular illness, can be caused by insufficient tear production and/or evaporative loss resulting in ocular burning, stinging, foreign body sensation, visual disturbance, inflammation and potential damage to ocular surface[149]. Cyclosporine is a potent immunosuppressive agent able to improve DED by reducing lymphocyte activation, production of inflammatory substances and by increasing the number of globet cells, which are responsible for the secretion of lubricious mucins[150]. Cyclosporine has shown to avoid the problems generated by long-term corticosteroid local therapies (delayed wound healing, ocular surface complications, risk for infections, high intraocular pressure, and cataract formation). The low water solubility of this drug (0.012 mg/ml at 25°C[151]) and high octanol-water partition coefficient (logP=3[152]) make necessary the use of oily phases in topical eye drop, decreasing the ocular tolerance and patient compliance. Thus, the use of nanomicelles has been investigated as alternatives for ophthalmic application[119, 130, 147, 148].

Prosperi-Porta et al.[119] developed mucoadhesive block copolymer micelles based on phenylboronic acid (PBA), a synthetic molecule able to form high-affinity complexes with 1,2-cis-diols of sialic acid residues of the corneal mucins and previously investigated for the development of cyclosporine-loaded functionalized nanoparticles[153, 154]. Single-angle surface plasmon resonance confirmed excellent *in vitro* mucoadhesion of PBA-containing micelles (36-50 nm) compared to chitosan, which supports their potential to improve bioavailability of topically applied ophthalmic drugs. PBA-contained micelles encapsulated 15% w/w cyclosporine; although drug release in simulated tear fluid using cellulose dialysis tubes (50 kDa MWCO) was not controlled, the mucoadhesive properties encourage the use of this system for further studies.

Di Tommaso et al.[130] investigated *in vivo* in rats the benefits of the employment of a novel cyclosporine (0.5% w/w) topical aqueous formulation based on methoxy poly(ethylene) glycol-hexylsubstituted poly(lactides) copolymers. The micelle size was

54±1 nm with a polydispersity index of 0.229±0.008. The cyclosporine concentration was significantly higher in the corneas of healthy rats treated with the micelle formulation (6470±1730 ng_{drug}/g_{tissue}) in comparison with an oil solution (0.5% w/w, 580±110 ng_{drug}/g_{tissue}), suggesting micelles capability to overcome corneal barriers. Also in the case of the iris-ciliary body, micelles determined an higher accumulation (890±610 ng_{drug}/g_{tissue}) compared to oil solution, for which the cyclosporine concentrations were below the limit of quantification of the analytical method.

Guo et al.[147] examined the use of polyvinyl caprolactam-polyvinyl acetate-polyethylene glycol graft copolymer (PVCL-PVA-PEG, Soluplus®). The mean diameter, the polydispersity index, and the zeta potential of the cyclosporine (0.5 mg/ml) nanomicelles were 73.14±24.42 nm, 0.067 and -6.7 mV, respectively. *In vivo* studies performed on rabbits showed that 0.5 mg/ml cyclosporine-loaded nanomicelles delivered higher levels of drug into the cornea, when compared to the oil-based 10 mg/ml cyclosporine ophthalmic solution. In fact, after single instillation (50 µl) and four times regimen instillations (200 µl) the amount of drug found inside the cornea was 168% and 343% higher than cyclosporine amount obtained after the application of the oil-based solution, respectively.

Luschmann et al.[148] developed a self-assembling micellar system to deliver cyclosporine A to the cornea based on poly(ethylene glycol)-fatty alcohol ether type (Sympatens AS and Sympatens ACS). A homogeneous distribution of the colloidal structures with a size of 9.2±1.2 nm and neutral zeta potential was observed. *Ex vivo* penetration studies using excised porcine corneas showed that the average drug concentration for the 0.05% w/v cyclosporine micellar solution was 1557±407 ng_{drug}/g_{cornea}. It was significantly higher than using Restasis® (545±137 ng_{drug}/g_{cornea}) or a 2% w/v cyclosporine oily solution (452±142 ng_{drug}/g_{cornea}).

4.3 Poloxamer 407/TPGS mixed micelles as promising carriers for an efficient cyclosporine penetration in ocular tissues (submitted research work)

4.3.1 Abstract

Cyclosporine is an immunosuppressant agent approved for the treatment of dry eye disease and used off-label for other ocular pathologies. Its formulation and ocular bioavailability is a real challenge due to the large molecular weight (1.2 kDa), high lipophilicity and low water solubility. The aim of the work was to develop an aqueous micellar formulation for an efficient cyclosporine delivery to the ocular tissues, using a water soluble derivative of vitamin E (TPGS: d-alpha tocopheryl polyethylene glycol 1000 succinate) and a poloxamer (poloxamer 407) as excipients. The mixed micelles were characterized in terms of particle size, zeta potential, rheology, stability upon dilution and freeze drying. Additionally, the enzymatic-triggered release of vitamin E and vitamin E succinate from TPGS was investigated *in vitro* in the presence of esterase. Compared to the commercially available ophthalmic formulation, the poloxamer 407:TPGS 1:1 molar ratio micellar formulation significantly improved cyclosporine solubility, which increased proportionally to surfactants concentration reaching 0.4% (w/v) for 20 mM surfactants total concentration. Cyclosporine-loaded mixed micelles efficiently retained the drug once diluted in simulated lachrymal fluid and, in the presence of a 20 mM surfactants concentration, were stable upon freeze-drying. The drug-loaded mixed micelles were applied *ex vivo* on porcine cornea and compared to Ikervis®. Drug accumulation in the cornea resulted proportional to drug concentration (6.4±1.9, 17.6±5.4 and 26.9±7.4 $\mu g_{drug}/g_{cornea}$, after 3 h for 1, 2.5 and 4 mg/ml cyclosporine concentration respectively). The formulation containing cyclosporine 4 mg/ml (20 mM surfactant) was also evaluated on the sclera, with a view to targeting the posterior segment. The results demonstrated the capability of mixed micelles to diffuse into the sclera and sustain cyclosporine delivery (28±7, 38±10, 57±9, 145±27 $\mu g/cm^2$ cyclosporine accumulated after 3, 6, 24 and 48 h respectively). Reservoir effect experiments demonstrated that the drug accumulated in the sclera can be slowly released into the underlying tissues. Finally, all the formulations developed in this work successfully passed the HET-CAM assay for the evaluation of ocular irritability.

4.3.2 Introduction

Cyclosporine (**Figure 10**) is a neutral cyclic peptide with immunosuppressive activity which can be isolated from several species of fungi[20]. Its pharmacological effects are mediated by binding two cytoplasmic proteins, called cyclophilin A and cyclophilin D, within T cells. Cyclosporine binding to cyclophilin A ultimately causes inhibition of T-lymphocyte activation[155, 156], while drug binding to cyclophilin D is thought to be primarily responsible for apoptosis inhibition[157]. Given its mechanism of action, cyclosporine is used for the treatment of immune-mediated ocular surface disorders[158]. In particular, this drug has been approved for the treatment of severe dry eye syndrome (DES) being able to suppress pathological processes on the eye surface, simultaneously increasing tear production[159].

The first cyclosporine formulation for ocular use (Restasis®) was marketed in 2003 in the USA and is still the only formulation approved in that country. It is an anionic emulsion of castor oil in water to be applied twice a day, containing 0.5 mg/ml cyclosporine. The most recently approved formulation, Ikervis®, was marketed in 2015 in Europe; it is a nanoemulsion containing cyclosporine 1 mg/ml. Ikervis® is the only approved “once a day” formulation[160], thanks to the presence of cetalkonium chloride, which imparts a positive charge to the nanodroplets thus prolonging the contact time with the epithelial layers of the eye[161]. These few available options and the need of improving the therapeutic levels explain the strong research efforts carried out on ocular cyclosporine formulations in the last decade[160, 162]. Together with the progress that has yet to be achieved in DES treatment, other diseases could benefit from advances in this field, since cyclosporine is also used off-label to treat posterior blepharitis[163], ocular rosacea[164], vernal keratoconjunctivitis[165], atopic keratoconjunctivitis[166], and acute corneal graft rejection[167]. Finally, it is worth mentioning that, systemically administered, cyclosporine represents a relevant therapy for the treatment of uveitis[168]. Since systemic administration can lead to severe side effects[155], the availability of topical formulations capable of delivering significant amount of drug across the sclera to the uvea can be of help in the management of this condition.

Cyclosporine formulation and bioavailability is a real challenge due to the unfavourable physico-chemical characteristics of this drug, having high molecular weight (1.2 kDa) and high lipophilicity (logP around 3[152]). Its very low water solubility (<0.1 mg/ml[168]) makes necessary the use of lipidic excipients, often associated to adverse effects, such as ocular burning, conjunctival hyperaemia, discharge, epiphora, eye pain, foreign body sensation,

pruritus, stinging, and visual disturbance[169] with more or less severity and symptoms depending on the lipidic excipients used[170].

Several studies have focused on colloidal systems such as solid lipid nanoparticles[171, 172], nanostructured lipid carriers[173], nanoparticles[174-176], liposomes[177] , nanosuspensions[178] and micelles[119, 130, 135, 147, 148, 179]. Micelles may be particularly useful for cyclosporine ocular delivery being able to increase water solubility of poorly soluble drugs without the need for an oily phase, and to enhance permeability across the physiological barriers[100, 101, 106]. Guo et al.[147] demonstrated a significantly more efficient *in vivo* penetration into rabbit cornea when cyclosporine (0.5 mg/ml) was encapsulated in polyvinyl caprolactam-polyvinyl acetate-polyethylene glycol graft copolymer micelles compared to a cyclosporine oil-based solution of much higher concentration (10 mg/ml). Di Tommaso et al.[130] detected higher cyclosporine amounts in the corneas of rats treated with methoxy poly(ethylene) glycol-hexylsubstituted poly(lactides) micelles (5 mg/ml cyclosporine) (6470±1730 ng_{drug}/g_{tissue}) in comparison with an oily solution of the drug at the same concentration (580±110 ng_{drug}/g_{tissue}). Luschmann et al.[148] observed *in vitro* a more efficient cyclosporine penetration into porcine cornea for drug (1 mg/ml) encapsulated in poly(ethyleneglycol)-fatty alcohol ether type based micelles (1557±407 ng_{drug}/g_{cornea}) compared to Restasis® (545±137 ng_{drug}/g_{cornea}). More recently, Prosperi-Porta et al.[119] developed poly(L-lactide)-b-poly(methacrylic acid-co-3-acrylamidophenylboronic acid) block copolymer micelles as mucoadhesive cyclosporine delivery system, while Bonferoni et al.[179] demonstrated the enhancing effect of palmitoyl glycol chitosan micelles to promote *ex vivo* drug penetration in pig cornea.

The aim of this work was to design a cyclosporine-loaded micellar formulation for the treatment of ocular diseases. For the preparation, a temperature-responsive poloxamer (poloxamer 407) and a water soluble derivative of vitamin E (TPGS, D-α-Tocopheryl polyethylene glycol 1000 succinate) were selected (**Figure 10**). This micellar formulation, together with the possibility of drug solubilization, may combine the temperature-dependent self-assembly of the poloxamer (able to increase formulation viscosity and ocular retention) and the potential antioxidant properties of TPGS. These excipients may also increase drug permeability through diverse mechanisms[105, 180-182]. Additionally, most polyoxyethylated nonionic surfactants are P-glycoproteins efflux pump inhibitors[183], and thus they may increase ocular penetration, as P-glycoproteins have been identified in human and rabbit corneas and RPE[46].

First, cyclosporine solubility studies were performed to select the proper poloxamer 407:TPGS ratio and concentration, and set the preparation method of cyclosporine-loaded

formulations. Selected formulations were characterised in terms of particle size, zeta potential, morphology, rheology, stability upon dilution and freeze drying. Cyclosporine-loaded formulations were evaluated for irritation using HET-CAM assay. E*x vivo* tests were performed on porcine eye bulbs to evaluate cyclosporine accumulation into the cornea, using the commercially available formulation Ikervis®[160, 170] as reference. Finally, since cyclosporine can be useful for the treatment of posterior segment diseases such as uveitis, the penetration of the drug across the sclera and its accumulation inside the tissue was evaluated as a function of time.

Cyclosporine A

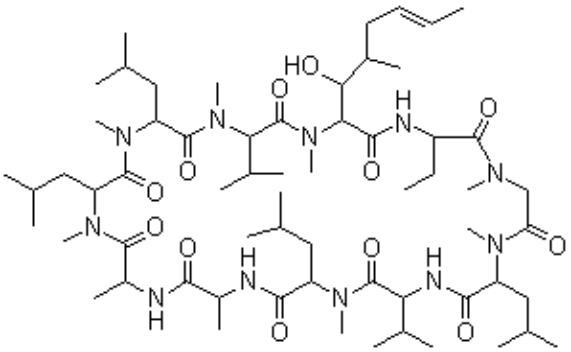

Poloxamer 407
(a= 100, b=65)

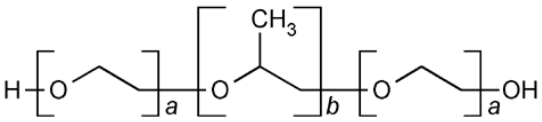

Vitamin E TPGS
(n≈23)

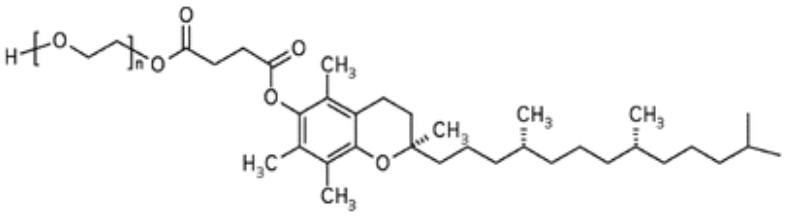

Figure 10. Chemical structure of cyclosporine A, poloxamer 407 (Pluronic® F127) and D-α-Tocopheryl polyethylene glycol 1000 succinate (Kolliphor® TPGS).

4.3.3 Materials and methods

4.3.3.1 Materials

Cyclosporine ($C_{62}H_{111}N_{11}O_{12}$, MW 1202.61 g/mol, crystalline solid) was from ThermoFisher Scientific (Karlsruhe, Germany), D-α-Tocopheryl polyethylene glycol 1000 succinate (Kolliphor® TPGS, MW 1513 g/mol) and poloxamer 407 (Pluronic® F127, MW 12.6 kDa) were a kind gift from BASF (Ludwigshafen, Germany). Kolliphor® TPGS is a mixture containing mainly monoester, a certain amount of diester and residual free PEG 1000. Trifluoroacetic acid (TFA, MW 114.02 g/mol), acetone (MW 58.08 g/mol), pyrene (MW 202.26 g/mol), vitamin E (D-alpha tocopherol, MW 430 g/mol), vitamin E succinate (D-alpha tocopherol succinate, MW 530.78 g/mol) and esterase from porcine liver (4992 IU/ml) were purchased from Sigma Aldrich (St. Louis, MO, USA). Ikervis® (Santen, Tampere, Finland) was used as reference (cationic nanoemulsion, cyclosporine 1 mg/ml). Milli-Q water (Purelab® Pulse, Elga Veolia, UK) was used; all other chemicals were of analytical or HPLC grade. Buffered solutions were phosphate-buffered saline (PBS; 0.19 g/l KH_2PO_4, 5.98 g/l Na_2HPO_4▪$12H_2O$, 8.8 g/l NaCl, pH 7.4) and simulated lachrymal fluid (SLF; $CaCl_2$ 0.06 mg/ml, $NaHCO_3$ 2.18 mg/ml, NaCl 6.7 mg/ml, pH 7.4).

4.3.3.2 Cyclosporine quantification method

Cyclosporine was analyzed using an HPLC-UV system (Infinity 1260, Agilent Technologies, Santa Clara, CA, USA), with a reverse-phase Nova-Pack C_{18} cartridge (150*3.9 mm, 4 µm) (Waters, Milford, Massachussets, USA) and a C_{18} guard column (3.2*0.8 mm, Security Guard™ Cartridge, Phenomenex, Torrance, USA) thermostated at 65°C. The mobile phase was a mixture CH_3CN: water with TFA 0.1% in 65:35 (v/v) ratio pumped at 1.6 ml/min. The injection volume was 100 µl, and absorbance was monitored at 230 nm. Cyclosporine retention time was ca. 5 min. Two calibration curves were built in the concentration ranges 0.25-5 and 2.5-50 µg/ml. The RSD% and RE% were lower than 2 and 6% respectively, for all the concentration tested. The LLOQ (lower limit of quantification) was 0.25 µg/ml (RSD% 1.72; RE% 12) and the LOD (limit of detection) was 0.125 µg/ml.

4.3.3.3 Cyclosporine solubility studies

Cyclosporine was added in excess to surfactants aqueous solutions. After stirring overnight, suspensions were centrifuged at 12000 rpm for 10 min (Scilogex D3014 High Speed Micro-Centrifuge, Rocky Hill, Connecticut, USA), the supernatant was filtered (0.45

µm, regenerate cellulose, Phenomenex, Torrance, USA), diluted with CH_3CN to a final surfactants concentration of 1 mM and analysed with HPLC-UV system. Experiments were carried out varying: a) poloxamer 407:TPGS molar ratio, b) surfactants total concentration (from 0.5 to 20 mM) and c) cyclosporine mode of addition into aqueous surfactants mixture (either as powder or ethanolic solution).

4.3.3.4 CMC determination

500 µl of pyrene solution in acetone (2 mg/ml) were added into vials and then organic solvent was evaporated[184]. Solutions (5 ml) containing either poloxamer 407 or TPGS or poloxamer 407:TPGS 1:1 molar ratio were poured into the vials at a concentration ranging from 0.0025 to 1 mM. In case of poloxamer 407: TPGS 1:1 molar ratio mixture, the same experiment was also performed with the addition of 0.5 ml of ethanol to the surfactant solutions evaporated overnight (see 4.3.3.6). The systems were kept under magnetic stirring (200 rpm, room temperature) for 48 h, then pyrene suspensions were filtered through 0.50 µm hydrophilic PTFE filters (Dismic®, Toyo Roshi Kaisha, Japan). Pyrene fluorescence emission spectrum (range 360-460 nm) was recorded with a FluoroMax-2 spectrofluorimeter (Horiba Scientific, Edison, New Jersey, USA) using an excitation wavelength of 335 nm. The ratio of the first to the third vibronic peak (I_1/I_3) was used as an index of micelles formation.

4.3.3.5 Enzymatic release of vitamin E succinate and vitamin E from blank micelles

The *in vitro* sensitivity to enzymatic hydrolysis was carried out using esterase from porcine liver. Blank micelles (B20, see 4.3.3.6) were diluted 1:4 with an esterase solution in PBS at pH 7.4 to give a final TPGS concentration of 2.5 mM and a final esterase concentration of 50 IU/ml (volume 1 ml). The resulting solution was incubated at 37°C for 48 hours. At pre-determined time intervals, 100 µl of the reaction mixture were withdrawn and diluted 1:10 with methanol causing esterase precipitation. Samples were centrifuged at 10000 rpm for 15 minutes, and the concentrations of vitamin E and vitamin E succinate in the supernatant were measured by HPLC. By performing the same experiment on 10 mM TPGS micelles, obtained with the same protocol as B20, the impact of the presence of poloxamer 407 on TPGS degradation was evaluated. Additionally, TPGS hydrolysis was also studied on a 10 mM TPGS solution and a 20 mM poloxamer 407:TPGS 1:1 molar ratio mixture. Each condition was tested in triplicate. Control samples obtained in the same conditions but without esterase were analysed as well.

A specific HPLC-UV method, modified from[185], was developed in order to simultaneously determine vitamin E and vitamin E succinate. With this method, it was also possible to separate two peaks of TPGS, that could be attributed to the mono- and di-D-α-tocopherol polyethylene glycol 1000 succinate. In details, analysis was made using an Infinity 1260 apparatus (Agilent Technologies, Santa Clara, CA, USA), equipped with a reversed phase column (Waters, Simmetry 300 C_{18} 5 µm 4.6*250 mm) thermostated at 40°C and a mixture acetate buffer: methanol in 3:97 (v/v) ratio, pumped at 2 ml/min as mobile phase. Acetate buffer was obtained by mixing 0.1 M acetic acid and 0.1 M sodium acetate solutions in 82:18 (v/v) ratio; the pH was adjusted to 4.8 using 0.1 M NaOH. The detection wavelength was 215 nm and injection volume was 10 µl. Under these conditions, vitamin E and vitamin E succinate had a retention time of 4.8 and 3.3 minutes, respectively. Linearity was evaluated in the interval 1.3-52 µg/ml for vitamin E and 4-64 µg/ml for vitamin E succinate. The method was validated for precision (RSD%< 5% for both compounds) and accuracy (RE%< 10% for both compounds).

4.3.3.6 Preparation of cyclosporine-loaded micelles

Poloxamer 407 and TPGS 1:1 molar ratio were dispersed in water to obtain final total concentration of 5, 10 and 20 mM. Cyclosporine was added as ethanolic solution; namely, 100 µl of 10, 25 or 40 mg/ml cyclosporine solutions were added to 1 ml of 5, 10 or 20 mM surfactants solutions respectively, to obtain formulations coded as F5, F10 and F20. Formulations were stirred (200 rpm) at room temperature for 2 h and the organic solvent was left to evaporate overnight (14-16 h) at room temperature (19±1°C). Formulations were then filtered through 0.2 µm acetate cellulose filters (SFCA-PF, 26 mm in diameter, Corning® Incorporated, Germany). Drug loading was checked before and after sterilising filtration and no difference was found. Blank micelles (B5, B10 and B20) were also prepared following the same procedure but without cyclosporine. The determination of the residual ethanol content was performed using an enzymatic commercial kit (Megazyme, Bray, Ireland) and resulted approximately 50 µl/ml.

4.3.3.7 Light scattering and TEM analysis

Micelle size and zeta potential were measured at room temperature in a Zetasizer® 3000HS (Malvern Instruments, UK). Analysed samples were cyclosporine-loaded formulations (F5, F10 and F20) and blank micelles (B5, B10 and B20). Micelle size was measured after diluting formulations in Milli-Q water up to 2 mM final surfactants

concentration. Zeta potential was measured by diluting 1:1 the samples used for light scattering with KCl 1 mM.

For TEM analysis, micelle formulations (5 µl) were placed on carbon coated grids; the excess was carefully removed with a filter paper. 5 µl of 2% w/v phosphotungstic acid were added and left for 60 s; then, 5 µl of Milli-Q water were added for 60 s and the excess was carefully removed with a filter paper. Samples were dried and observed using a high resolution transmission electron microscope (JEOL-JEM 2010, JEOL USA Inc., Peabody, MA, USA). Diameter of the micelles/aggregates was measured using a calibrated scale.

For comparison, also poloxamer 407:TPGS 1:1 molar ratio surfactant mixtures were analysed.

4.3.3.8 Micelle stability upon dilution

Stability of cyclosporine-loaded micelles against dilution was tested according to [143]. Aliquots (200 µl of F5, 100 µl of F10, 50 µl of F20) were placed into quartz cells containing SLF (total volume 1000 µl) maintained at 35°C by means of a recirculation system. Absorbance was registered at 233 nm for F5 and at 240 nm for F10-F20 every 30 s for 30 minutes (UV/VIS spectrophotometer Agilent 8453, Germany). Experiments were performed in triplicate.

4.3.3.9 Micelle stability during freeze-drying

Formulations B10, B20, F10 and F20 were frozen at -20°C overnight and then freeze-dried (Telstar Lyoquest Plus 85°C/ECO; Telstar Spain) obtaining a dried powder. Reconstitution was performed by adding Milli-Q water (the same volume as initially in the vial) and magnetically stirring (200 rpm, room temperature) for 60 minutes. The reconstituted formulations were characterized in terms of size, zeta potential, drug loading and stability upon dilution, as previously described.

4.3.3.10 Rheological characterization

Rheological analysis of surfactant mixtures, B10, B20, F10 and F20 were performed using a Rheolyst AR-1000N rheometer equipped with an AR2500 data analyzer, a Peltier Plate and a cone geometry (6 cm diameter, 2.1°) (TA Instruments, Newcastle, UK). Angular frequency sweeps (0.1 to 50 rad/s) were recorded at 35°C (to mimic ocular surface temperature) and then viscosity was evaluated under shear rate controlled conditions.

4.3.3.11 Tissue preparation

Fresh porcine eyes were isolated from Landrace and Large White (age 10–11 months, weight 145–190 kg), female and male animals supplied from a local slaughterhouse (Annoni S.p.A., Parma, Italy). The eyes were kept in PBS at 4°C until the dissection, which occurred within 2 h from the enucleation. Firstly, muscular and connective tissues around the eye-bulb were completely removed. Only bulbs with macroscopically intact corneas were used, whereas eyes showing opaque corneas were discarded. To get isolated sclera, the anterior segment of the eye was circumferentially cut behind the limbus and removed. The obtained eyecup was then cut and everted. The neural retina and the choroid-Bruch's layer were discarded and the obtained sclera was frozen at -80°C. Detailed procedures were described in a previous work[77].

4.3.3.12 Cornea penetration studies

Cyclosporine penetration test was performed on whole eye bulbs using a commercially available applicator (Iontofor-CXL®, area 0.6 cm^2, SOOFT Italia S.p.A, Montegiorgio, Italy) secured on the corneal surface thanks a weak suction vacuum system (**Figure 11A**). Cyclosporine-loaded F5 (n=3), F10 (n=4) and F20 (n=6) formulations (volume 200 µl) and Ikervis® (n=4, volume 100 µl) were applied on the cornea for 3 h. The corneal surface was then washed with NaCl 0.9% solution, the applicator was removed and the ocular surface was carefully dried. Then, cornea was excised and the drug was extracted with 3 ml of a mixture CH_3CN:1% CH_3COOH (87:13) overnight at room temperature. Extraction solutions were filtered (0.45 µm, regenerated cellulose, Phenomenex, Torrance, USA) before HPLC analysis. When needed, the extraction solution was concentrated under N_2 flux down to a volume of 1 ml. The extraction procedure was validated; the recovery efficiency was 93.6±5.2% (n=6) and the limit of quantification 0.33 $\mu g_{drug}/cm^2_{tissue}$ (corresponding to approximately 2.6 $\mu g_{drug}/g_{tissue}$; average cornea weight 128±8 mg/cm^2).

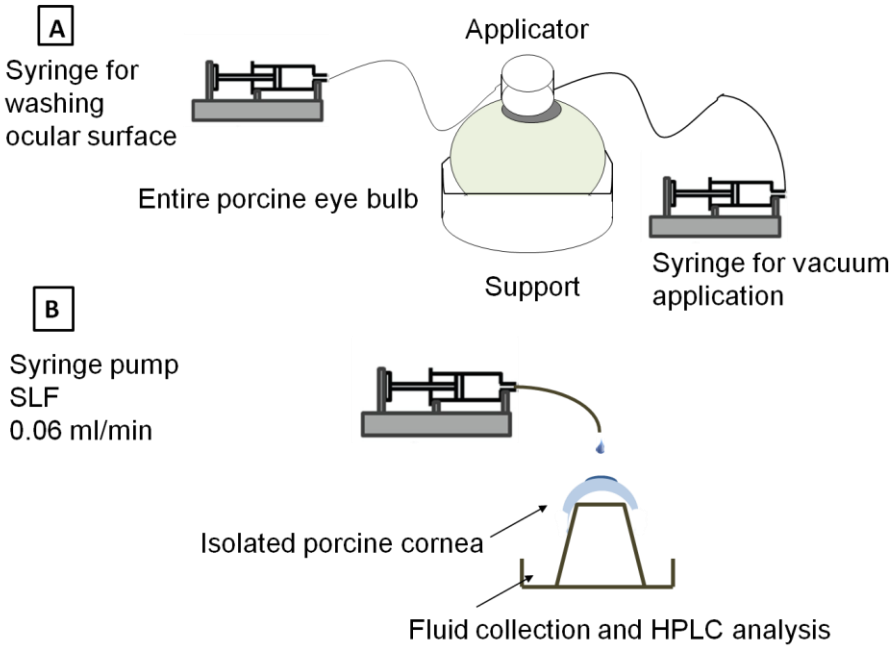

Figure 11. Experimental set-up of (A) cornea penetration studies on intact eye bulb and (B) cornea adhesion experiments.

4.3.3.13 Adhesion experiments

Adhesion tests of the formulations on the corneal surface were performed at room temperature (**Figure 11B**). Freshly isolated corneas were placed on a support, and 20 µl of cyclosporine-loaded formulation or Ikervis® were applied. After 5 min of equilibration, SLF was flushed on the cornea at 60 µl/min using a syringe pump (Harvard Apparatus, Holliston, USA). Samples were collected at predetermined times and analysed with HPLC-UV system.

4.3.3.14 Sclera penetration studies

Experiments were performed using Franz-type diffusion cells (area 0.6 cm^2). The scleral tissue was mounted with the choroidal side facing the receptor compartment. The receptor medium consisted of 4 ml of NaCl 0.9% solution thermostated at 37°C and magnetically stirred, to avoid any boundary layer effects (cyclosporine solubility: 0.035 mg/ml). The donor compartment was filled with 0.2 ml of formulation F20. After 3 (n=6), 6 (n=6), 24 (n=3), or 48 (n=4) hours, the receptor fluid was sampled, the formulation was removed, the sclera was carefully washed and contact area was isolated. Cyclosporine was extracted by adding 1 ml of mixture CH_3CN:1% CH_3COOH (87:13) and keeping in contact for 2 hours at room temperature (recovery: 94%). Extraction solutions were filtered (0.45 µm regenerated cellulose filters, Phenomenex, Torrance, USA) before HPLC analysis.

Further experiments were performed to evaluate the reservoir effect. F20 was applied to the sclera for 3, 6 or 24 hours (n=3); then, the formulation was carefully removed, the sclera surface was dried with a cotton bud and permeation experiment was continued up to 48 h. After this time, cyclosporine was extracted from the sclera and quantified in the receptor phase, as previously described.

4.3.3.15 HET-CAM test

Fertilized hen's eggs (50-60 g; Coren, Spain) were used for performing irritation test on the chorio-allantoic membrane (HET-CAM)[186]. Eggs were incubated in a climatic chamber (Ineltec, model CC SR 0150, Barcelona, Spain) at 37 °C and 60% relative humidity for 9 days. Eggs were turned 3 times per day, and the last day they were placed with the wider extreme upward. On the ninth day, the eggshell was partially removed (1 cm in diameter) on the air chamber with a rotary saw (Dremel 300, Breda, The Netherlands). The inner membrane was wet with 0.9% NaCl (30 min) and then carefully removed to expose the CAM. A predetermined volume (300 µl) of formulations (F5, F10, F20) and blank (B5, B10 and B20) micelles were poured on the CAM of different eggs. 0.9% NaCl and 0.1 M NaOH solutions were used as negative and positive controls, respectively. The vessels of CAM were observed during 5 min, recording the times at which hemorrhage (Th, vessels bleeding), vascular lysis (Tl, vessels disintegration), or coagulation (Tc, denaturalization of intra- and extra- vascular proteins) occurred. The irritation score (IS) was calculated with the following equation:

$$IS=5x\frac{301-Th}{300}+7x\frac{301-Tl}{300}+9x\frac{301-Tc}{300} \quad \text{(eq. 3)}$$

Formulations effects on CAM vessels were analyzed from photographs recorded 5 min after the beginning of the assay.

4.3.3.16 Statistical analysis

Differences between conditions were assessed using Student' *t*-test. Differences were considered statistically significant when $p<0.05$. In the text, all data are reported as mean value±sd.

4.3.4 Results and discussion

For micelles preparation, a temperature-responsive poloxamer (poloxamer 407) and TPGS, a water soluble derivative of vitamin E (**Figure 10**) were used. Required properties for the micellar formulation are cyclosporine solubilisation capability, small size, viscosity suitable to prolong the retention time on ocular surface, stability upon dilution and, possibly, the stability upon freeze-drying. The release of Vitamin E from TPGS could be as well a positive feature considering the antioxidant properties of this compound.

4.3.4.1 Cyclosporine solubility

Poloxamer 407:TPGS molar ratio was selected on the basis of drug solubilisation capacity. Drug solubility results as a function of poloxamer and TPGS molar fraction (**Figure 12a**) revealed that the two components have a comparable capacity to solubilise cyclosporine ($p>0.05$). Thus, the 1:1 molar ratio was selected in order to set a good balance on other features (mucoadhesion, thermoreversibility, P-gp inhibition, antioxidant activity) each component can provide to the formulation.

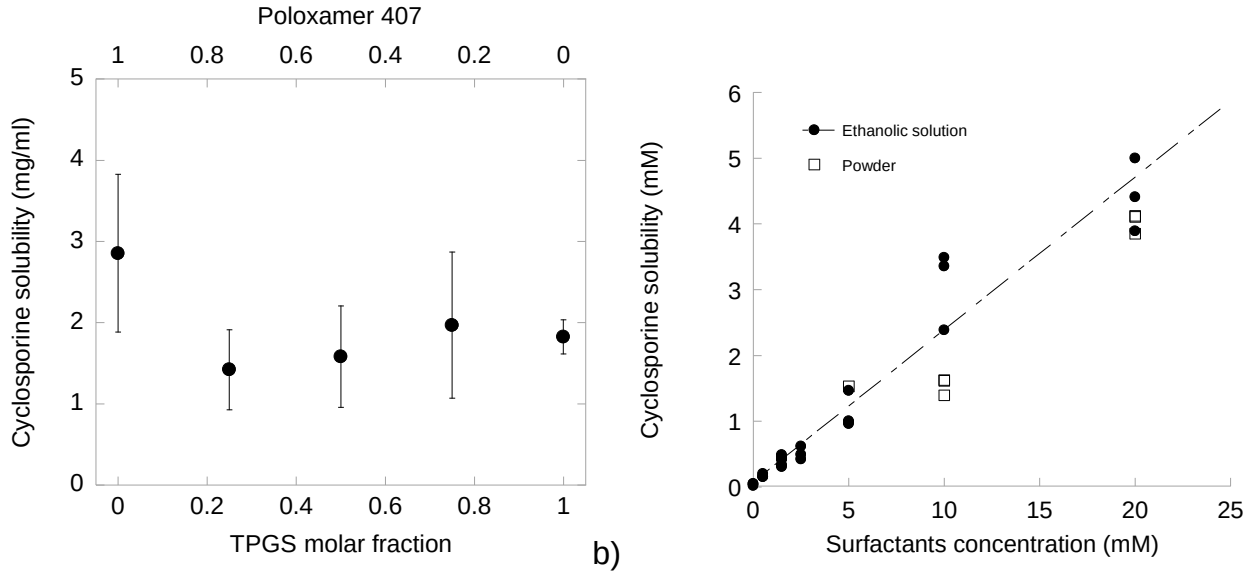

Figure 12. Panel a) Cyclosporine solubility as a function of TPGS and poloxamer molar fraction. The total surfactants concentration is 5 mM in aqueous medium (mean±sd, n=5 for 0.5 TPGS molar fraction, n=3 for all the other evaluated molar ratios). Panel b) Cyclosporine solubility as a function of surfactants (poloxamer 407:TPGS 1:1 molar ratio) concentration; the drug was added either as powder or as ethanolic solution.

The data obtained highlight the relevant ability of these polymers to dramatically increase cyclosporine aqueous solubility (0.047±0.017 mg/ml). Indeed, the formulation prepared

with 20 mM surfactants concentration enhanced nearly 100-fold cyclosporine apparent solubility.

All the tested mixtures, ranging from 0.5 to 20 mM, were above the CMC of mixed micelles (see 4.3.4.2), thus, as expected, cyclosporine solubility was linearly correlated to the surfactants concentration. As shown in **Figure 12b**, the method of drug incorporation (powder *versus* ethanolic solution) did not impact on drug solubility. Given the high cyclosporine solubility in ethanol, this result suggests that the residual ethanol (about 50 µl/ml) did not play a relevant role in drug solubilisation in the presence of the mixed micelles.

4.3.4.2 CMC determination.

CMC of the poloxamer 407:TPGS 1:1 molar ratio mixture was determined using pyrene as probe[184]; for comparison, the CMC of each surfactant separately was also determined. **Figure 13** reports the ratio of the first (I_1) to the third (I_3) vibronic peak of pyrene as a function of surfactants concentration. Two different linear regions can be identified in each profile; since I_1/I_3 indicates the polarity of the medium in which pyrene is dissolved, the two regions correspond to pre-micelles and post-micelles formation. CMC can thus be estimated from the crossover concentration. CMC of poloxamer 407 and TPGS resulted 0.456 mM and 0.091 mM respectively, which is in agreement with the data reported in literature (0.45 mM[184] and 0.13 mM[187], respectively). Theoretically, the poloxamer 407:TPGS 1:1 molar ratio solution could be treated as an ideal mixture of its pure components, showing a CMC intermediate between the values for the pure components[140]. The CMC values for the surfactants mixture can thus be calculated using the following equation[188]:

$$\frac{1}{CMC(mixed\ micelles)} = \frac{X(Pluronic)}{CMC(Pluronic)} + \frac{X(TPGS)}{CMC(TPGS)} \quad \text{(eq. 4)}$$

where $CMC_{(mixed\ micelles)}$ is the theoretical CMC of mixed micelles, $X_{(Pluronic)}$ and $X_{(TPGS)}$ are the molar fractions of poloxamer 407 and TPGS, and $CMC_{(Pluronic)}$ and $CMC_{(TPGS)}$ are the experimental CMC of poloxamer 407 and TPGS, respectively. The theoretical CMC of mixed micelles resulted to be 0.151 mM, while the experimental CMC value was 0.110 mM. The CMC in the presence of ethanol (added in a 1:10 ratio and then evaporated overnight as described in 4.3.3.6) was also evaluated since this solvent was used for the preparation of drug-loaded micelles. In this case, the experimental CMC value (0.138 mM) was slightly higher. The small shifts from the theoretical CMC of mixed micelles towards

lower CMC values suggest favourable interactions between both surfactants and therefore true co-micellization[140].

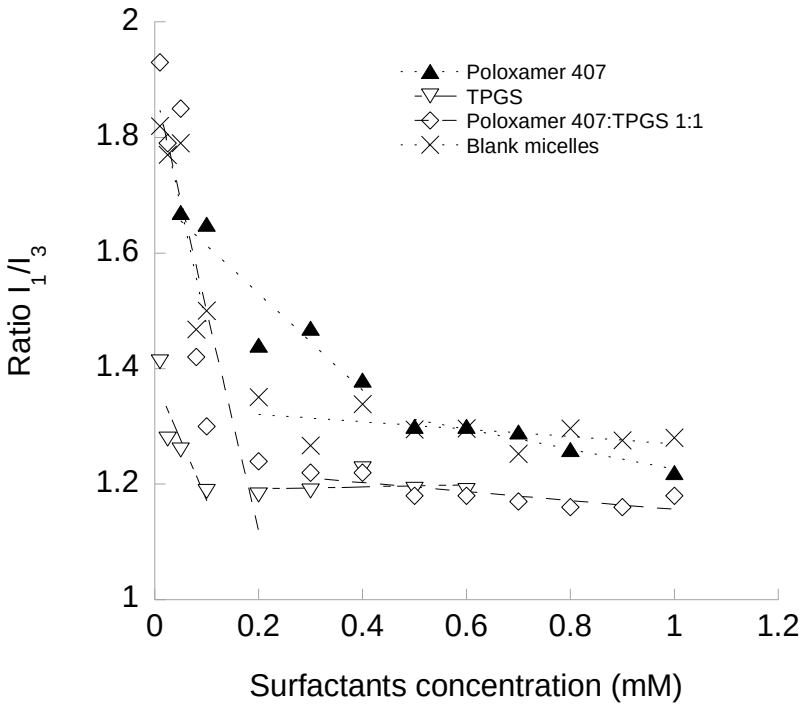

Figure 13. CMC determination test results expressed as the ratio of the first to the third vibronic peak of pyrene as a function of the concentration of the surfactants.

4.3.4.3 Characterization of poloxamer 407:TPGS 1:1 molar ratio micelles

Poloxamer 407:TPGS 1:1 molar ratio formulations were further characterized. In particular, cyclosporine loaded micelles (F5, F10, F20) and blank micelles (B5, B10 and B20), prepared in the same way but without drug, were studied.

4.3.4.3.1 DLS analysis and TEM images

The zeta potential of all formulations evaluated (**Table 1**) was very close to zero, in agreement with the non-ionic nature of the surfactants used. This characteristic can highly impact on the possibility of micelles interaction. Indeed, the analysis of undiluted formulation gave in all cases high polydispersity index (data not shown). For this reason, the samples were analysed after dilution to a final surfactant concentration of 2 mM. The results obtained with blank and cyclosporine-loaded micelles are presented in **Table 1**; for comparison, data obtained with surfactant mixtures are also reported. Blank micelles differ from surfactant mixtures for the presence of small amounts (approx. 50 µl/ml) of residual ethanol**.**

Diluted polymeric mixtures were characterized either by the presence of aggregates bigger than 1 µm or by large and very disperse particles. On the contrary, diluted blank micelles (B5, B10 and B20), are characterized by a smaller size (**Table 1**) although large (about 220 nm in size) aggregates were still present in B5.

Table 1. Size and zeta potential of poloxamer 407:TPGS 1:1 mixtures, blank micelles (B5, B10 and B20) and cyclosporine (CyA)-loaded micelles (F5, F10, F20). Micelle size was measured after diluting formulations in Milli-Q water up to 2 mM final surfactants concentration. Zeta potential was measured by diluting sample used for light scattering 1:1 with KCl 1 mM (mean±sd of different batches, §n=2, *n=3, #n=4).

Sample	Particle size (nm)	Polydispersity index	Zeta potential (mV)
5mM mixture	Presence of aggregates#		-0.079±0.366*
10mM mixture	307.6±124.8#	0.350±0.121#	-0.081±0.196*
20mM mixture	Presence of aggregates #		-0.018±0.200
B5	223.6±115.5*	0.283±0.107*	-4.040±3.804*
B10	30.3±9.1*	0.229±0.059*	-1.944±1.655*
B20	60.0±34.4*	0.170±0.050*	0.015±0.102*
F5 (CyA 1 mg/ml)	Presence of aggregates#		-0.057±0.120*
F10 (CyA 2.5 mg/ml)	202.7±65.1*	0.284±0.130*	0.155±0.300§
F20 (CyA 4 mg/ml)	200.1±125.6#	0.270±0.065#	-9.621±4.729*

The decrease in the size of poloxamer micelles in the presence of ethanol has been previously explained by a decrease in interfacial tension between the hydrophobic PPO chains and the solvent, which alters the self-assembly process, making the formation of smaller micelles more energetically favorable[111]. Since all the formulations were diluted to 2 mM, differences in size between B5 and B10-20 can be due to a different ethanol/surfactant interaction in the original formulation. Despite ethanol content is comparable in the three formulations (approximately 50 µl/ml), it was probably more strongly associated to the polymers in case of B20. Indeed, following the freeze drying process, only the 20 mM formulation was able to re-form micelles with a comparable size

(see 4.3.4.3.5). The loading of cyclosporine into the micelles determined an increase in the average size giving approximately 200 nm micelles for F10 and F20 and bigger aggregates for F5 (**Table 1**).

Undiluted formulations were also analysed by TEM. Formulations containing 5mM surfactants were characterized in all cases by undefined structures (**Figure 14**, first row), in reasonable agreement with DLS data. In case of 10 and 20 mM formulations, more defined rounded-shape structures are present. It is also possible to appreciate the size reduction due to the ethanol treatment. It is, however, worth mentioning that micelles are dynamic in nature, thus the determination of the size is always complicated; in particular, sample preparation required for TEM analysis may lead to artefacts[189].

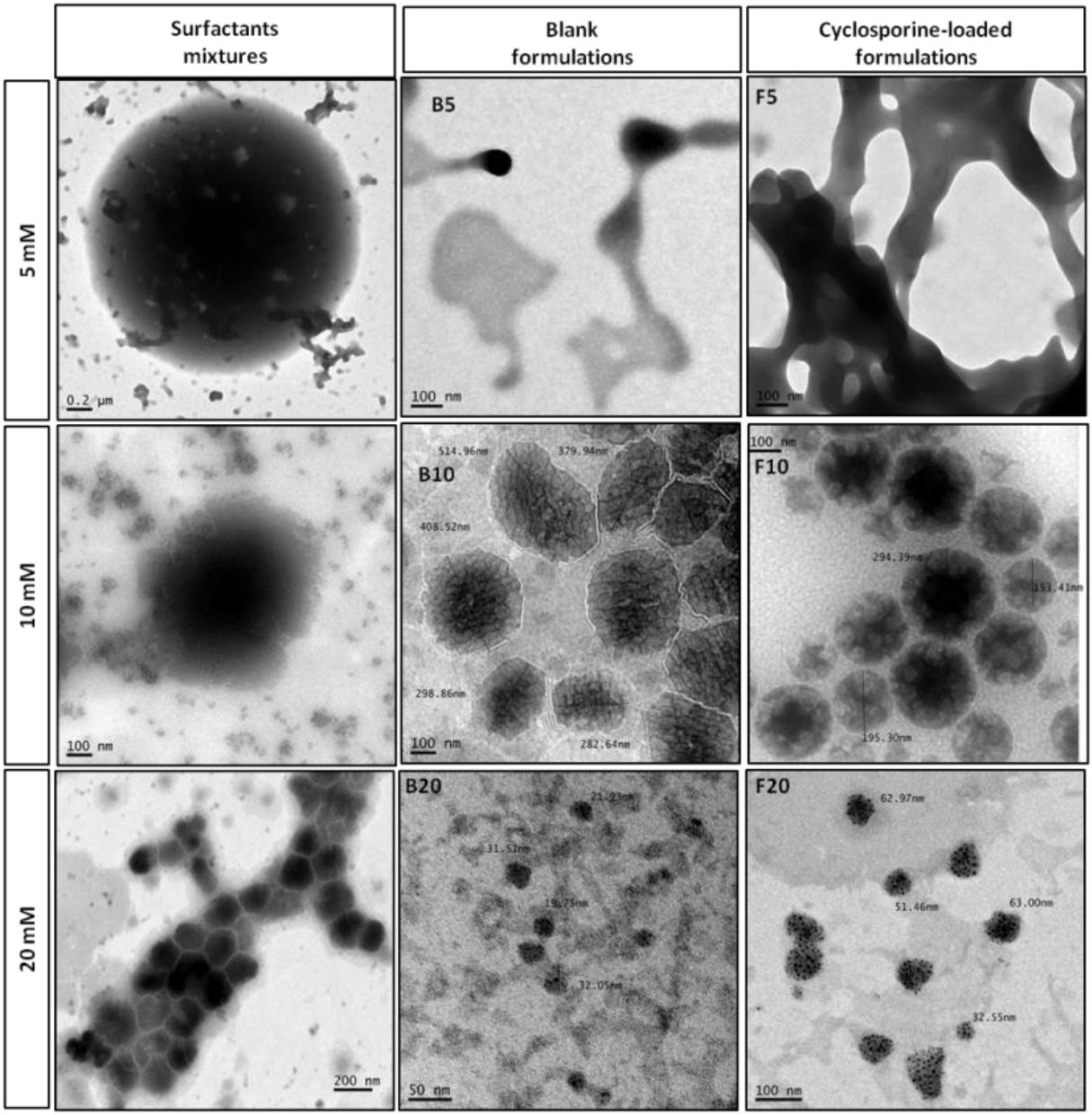

Figure 14. TEM images of surfactant mixtures, blank (B5, B10, B20) and cyclosporine–loaded (F5, F10, F20) micelles.

4.3.4.3.2 Rheology

Rheological analysis of 10 mM and 20 mM formulations, both blank and cyclosporine-loaded, were performed (**Figure 15**). Both 10 mM and 20 mM formulations exhibited a pseudoplastic-like behaviour with viscosity values decaying from 15 to 4 mPa·s and from 70 to 20 mPa·s, respectively, when the shear rate increased from 1 to 10 s^{-1}. Human tears also exhibit shear thinning behaviour with viscosity values in the range of 1.05 to 5.97 mPa·s in the 1 to 10 s^{-1} shear rate range[190]. It has been previously reported that the minimum shear viscosity of eye drops required for precorneal residence in human beings

is 10 mPa·s and that the corneal contact time of the formulations increases proportionally to the viscosity up to 20 mPa·s[118]. Thus, the rheological features of the developed mixed micelles formulations seem to be adequate for prolonged residence on the ocular surface.

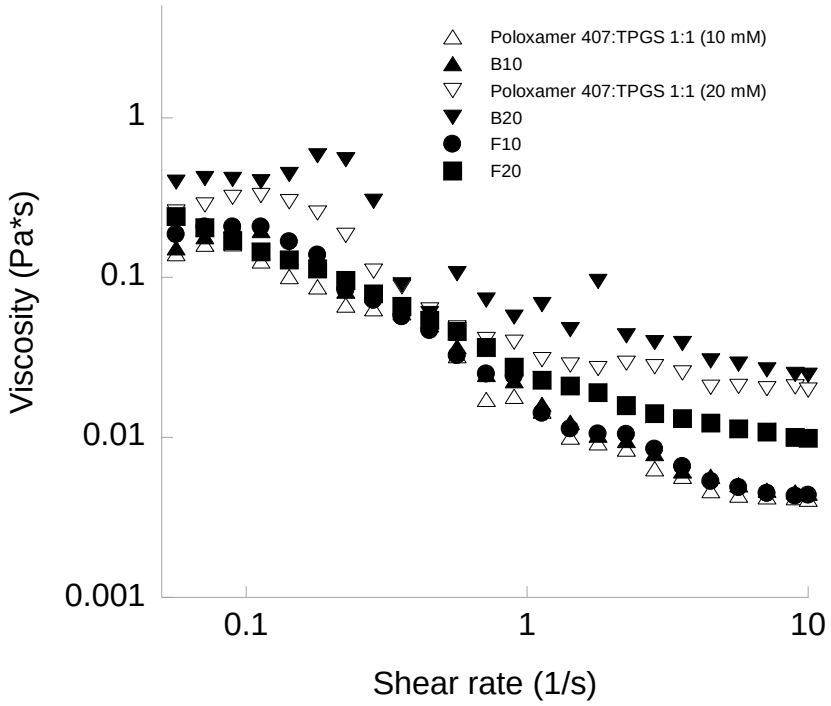

Figure 15. Rheological behaviour of 10-20 mM poloxamer 407:TPGS 1:1 molar ratio formulations (poloxamer 407:TPGS 1:1 molar ratio solutions, blank and cyclosporine-loaded micelles) as a function of shear rate at 35°C.

4.3.4.3.3 Release of vitamin E and vitamin E succinate

Vitamin E TPGS can be used as an efficient source of natural vitamin E and vitamin E succinate, both compounds with well known antioxidant properties. In fact TPGS, which is stable in solution between pH 4.5 and 7.5, can be a substrate for esterases, enzymes ubiquitously present in human body and also in ocular tissues[191, 192]. In our case, TPGS hydrolysis could lead to a reduction or even loss of the self-assembling properties promoting drug release in contact with (or inside) the ocular tissues. Additionally, the release of antioxidant compounds could be beneficial in the treatment of different ocular diseases, although there are controversies on their efficacy[193-196].

The kinetics of formation of vitamin E and vitamin E succinate from the TPGS participating in the poloxamer 407:TPGS 1:1 mixed micelles (B20) was compared to that of simple TPGS micelles treated in the same way (**Figure 16a)**. The presence of poloxamer 407 significantly ($p<0.05$) reduced vitamin E formation at all time points, while it did not alter

vitamin E succinate formation. TPGS hydrolysis is much slower compared to the one reported in the literature for low MW vitamin E esters[197] suggesting that the presence of the PEG1000 chain significantly hinders enzyme access to the esters bonds.

In **Figure 16b** the amount of vitamin E and vitamin E succinate found after 48 h is reported for all the 4 conditions investigated. The result also suggests that ethanol affects esterase activity causing a minor but statistically significant ($p<0.05$) decrease in TPGS metabolism. This finding may be related to the impact of ethanol on micelles size and compactness and thus on esterase accessibility to TPGS. An alternative hypothesis could be linked to a direct inhibitory effect of ethanol (present at approximately 50 µl/ml concentration) on enzyme activity even if literature data indicate that the presence of 10% organic solvent (methanol) did not have any effect on esterase activity[198]. Finally, the stability of vitamin E in the aqueous solution at 37°C for 48 h was not evaluated and could, at least in principle, affect the release profiles reported in **Figure 16**. Nevertheless, the presence of polymeric surfactants should contribute to increase its stability.

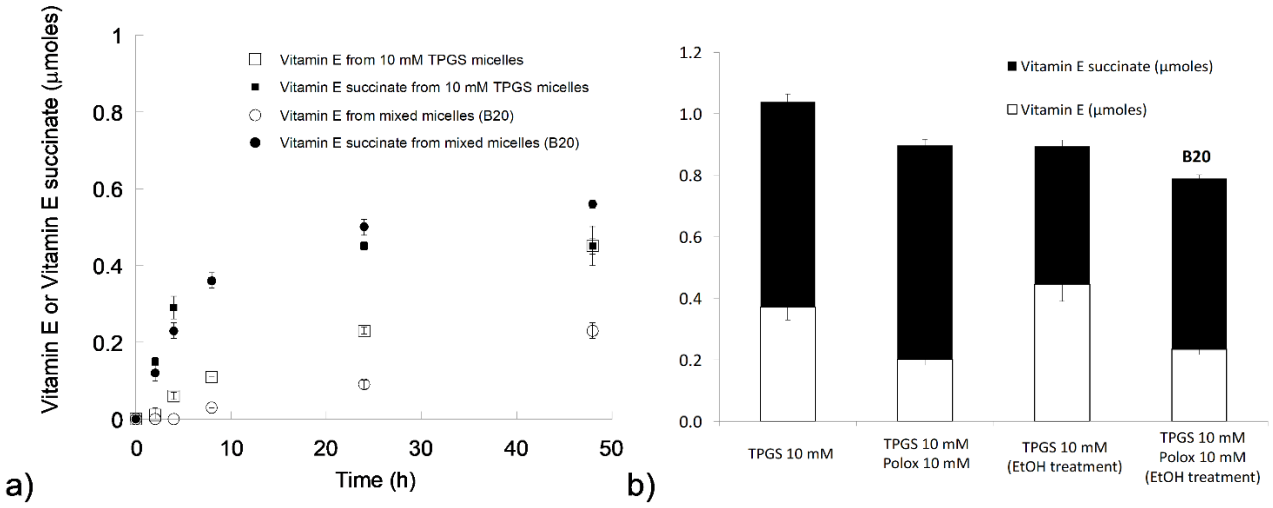

Figure 16. Panel a) Amount of vitamin E (void symbols) and vitamin E succinate (full symbols) formed in the presence of esterase as a function of time from TPGS micelles (squares) and from poloxamer 407:TPGS 1:1 mixed micelles B20 (circles). Panel b) Amount of vitamin E (white bar) and vitamin E succinate (black bar) recovered after 48 h in the different conditions tested. All the data are presented as mean±sd (n=3).

4.3.4.3.4 Stability upon dilution

Stability against dilution tests were carried out to gain an insight into the capability of F5, F10 and F20 to retain the drug once diluted in SLF at 35°C, trying to mimic physiological conditions. Absorbance was recorded immediately after dilution of the formulations and

monitored for 30 min. The absorbance (**Figure 17**) showed an initial increase in the first few seconds followed by a complete and stable recovery, which indicated that cyclosporine remained encapsulated inside micelles[143].

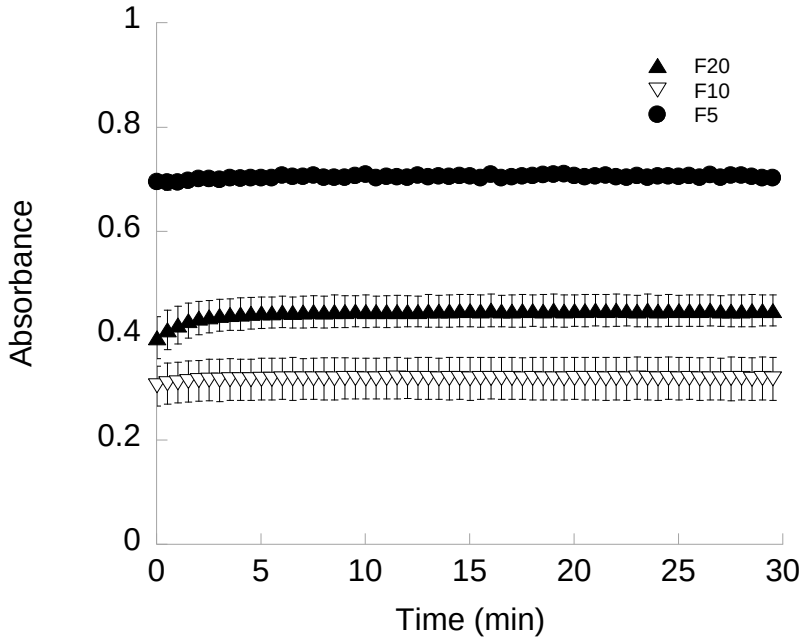

Figure 17. Monitoring of the absorbance of F5 (full circles), F10 (void triangles) and F20 (full triangles) after 5-, 10- and 20- fold dilution, respectively, in SLF (mean±sd, n=3).

4.3.4.3.5 Stability against freeze-drying and reconstitution of freeze-dried micelles

Stability after freeze-drying without the use of any cryoprotectant was preliminarily checked by measuring micelles size by DLS and evaluating the stability upon dilution. Formulations prepared with 10 mM total surfactants concentration were not stable. Differently, reconstituted B20 and F20 recovered initial particle size and zeta potential (see **Table 2**), drug loading (drug loss lower than 10%) and stability upon dilution (data not shown). Ethanol was still present in the formulation, but at a 10-fold lower concentration (approximately 5 µl/ml). This result suggests a strong interaction with micelles core (PPO blocks) that could support the role of ethanol in micelles size.

Table 2. Size of poloxamer 407:TPGS 1:1 molar ratio micelles after freeze-drying (mean±sd, n=3) and related increase factors obtained by dividing size and PDI after freeze-drying to the mean size and PDI obtained after filtration through 0.2 µm membrane.

Sample	Particle size after freeze-drying (nm, d_f)	PDI after freeze-frying	d_f/d_i	PDI_f/PDI_i	Zeta potential after freeze-drying (mV)
10 mM solution	Aggregates(>1 µm)		-	-	-2.970±5.184
B10	Aggregates(>1 µm)		-	-	-2.740±4.832
F10	Aggregates(>1 µm)		-	-	-13.683±3.889
20 mM solution	Aggregates(>1 µm)		-	-	0.062±0.070
B20	39.79±13.7	0.179±0.056	0.66±0.23	1.05±0.33	-4.059±0.967
F20	142.90±12.09	0.194±0.028	0.71±0.06	0.72±0.11	-0.023±0.137

4.3.4.4 Ex vivo permeation and accumulation of cyclosporine-loaded formulations into and across ocular tissues

The pH of cyclosporine-loaded mixed micelle formulations was between 6.8 and 7.1, values compatible with ocular administration and comparable to Ikervis® (pH=5.5-7[161]) and Restasis® (pH 6.5-8[199]).

After micelles characterization, the formulations were tested on ocular tissues, to figure out their potential for cyclosporine delivery. As previously explained, cyclosporine is useful for the treatment of anterior segment diseases (dry eye syndrome, blepharitis, ocular rosacea, vernal keratoconjunctivitis, atopic keratoconjunctivitis), but could also be used for the treatment of inflammatory diseases affecting the posterior segment. For this reason, cyclosporine accumulation and permeation were evaluated on both cornea (anterior segment targeting) and sclera (posterior segment targeting). In any case, an essential pre-requisite is the absence of ocular irritation, which was evaluated using the HET-CAM assay.

4.3.4.4.1 HET-CAM test

Poloxamer 407:TPGS (1:1 molar ratio) based formulations were tested in terms of ocular biocompatibility using the HET-CAM test, which is a common preliminary organotypic method, often in agreement with the *in vivo* Draize test, for the evaluation of ocular

irritancy[186]. F5, F10 and F20 formulations were investigated to elucidate the effect of different drug concentrations, while corresponding blank formulations were used to confirm the tolerability of the surfactants. None formulation was irritating: no hemorrhage, lysis, coagulation or any inflammatory reactions in the CAM occurred during the 5 min of the test (data not shown). These events were observed only in the case of the positive control (NaOH 0.1 M, IS equal to 21.04). Results obtained were in line with the data reported in literature. Fathalla et al.[200] tested *in situ* gels of poloxamer 407 (18.4 mM) by using HET-CAM test, demonstrating no irritation. Indeed, poloxamer 407 has already been approved for ophthalmic application by FDA, namely it is present in 4 different multipurpose solutions available on the US market. Regarding the ophthalmic use of TPGS, even if few direct evidences have been reported on its ocular tolerability, this excipient is contained in medical devices present in the EU market (e.g. COQUN®, Visudrop™) and has been used without toxicity problems in clinical studies[201].

4.3.4.4.2 Cornea penetration and adhesion experiments

Cyclosporine loaded formulations (F5, F10 and F20) were evaluated in infinite dose conditions on porcine cornea, previously shown suitable for mimicking human cornea in *ex vivo* experiments[202]. **Figure 18a** reports on the amount accumulated in the cornea after 3 h of contact, in comparison with Ikervis®. The same drug accumulation was obtained for F5 and Ikervis®, characterised by equivalent nominal cyclosporine concentration (1 mg/ml); the different volume applied (200 *vs* 100 µl) was not relevant, given the infinite dose conditions used (in fact, the accumulated cyclosporine amount in the cornea was 100-fold lower than the applied doses in both cases). The obtained result is promising considering that Ikervis® is an effective formulation, with low administration frequency (once a day) and that the comparable F5 performance has been obtained without using oil phase nor cetalkonium chloride[203, 204]. The efficacy of Ikervis® is attributed to the presence of nanometric positively charged dispersed drops that can interact with the ocular structures and enhance cyclosporine uptake[161]. In case of F5, the enhancing effect could be due to the role of surfactants, able to interact with the membrane of the epithelial cells[105, 187].

Using poloxamer 407/TPGS micelles it is possible to increase drug loading up to 4 mg/ml obtaining a concentration-dependent drug accumulation (**Figure 18a**). This is very interesting, considering the numerous diseases affecting the anterior eye segment that could be efficiently treated with cyclosporine[165-167]. The data reported also demonstrated that the size of the cyclosporine-loaded micelles did not influence drug uptake, suggesting

that probably these micelles did not enter the cells as such, as reported by other authors[205, 206], but rather delivered their payload when in contact with the apical cells of the corneal epithelium. Indeed, given the results presented in 4.3.4.3.3, drug release and uptake could also be linked to TPGS hydrolysis.

The residence time of the formulation on the ocular surface is another important parameter affecting ocular bioavalability[28]. Mucoadhesive properties have been reported for Ikervis®[161] and are well known for poloxamers. In this paper we evaluated the retention of cyclosporine on the top of the cornea where the apical cells are characterized by the presence of membrane-associated-mucins[207]. The results, obtained upon flushing the surface with SLF (set up in **Figure 11B**), reported a similar behaviour for all the formulations tested although F10 formulation showed somehow longer permanence (**Figure 18b**).

a)

	Cyclosporine content (mg/ml)	Cyclosporine accumulated ($\mu g_{DRUG}/g_{CORNEA}$)	Cyclosporine accumulated ($\mu g_{DRUG}/cm^2$)
Ikervis®	1.0	4.71 ± 1.11	0.60 ± 0.14
F5	1.0	6.39 ± 1.90	0.82 ± 0.24
F10	2.5	17.52* ± 7.72	2.24* ± 0.99
F20	4.0	26.56* ± 18.45	3.40* ± 2.36

* Statistically different from Ikervis (p<0.05)

b)

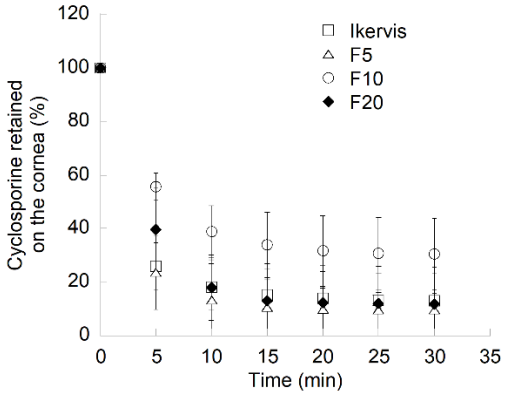

Figure 18. Panel a) The table reports cyclosporine accumulation into porcine cornea (mean±sd, contact time 3 h) from Ikervis®, F5, F10 and F20, obtained using the setup presented in Figure 2A. Panel b) Percentage (%) of cyclosporine retained on the cornea upon flushing the surface with simulated tear fluid at 0.06 ml/min as presented in Figure 11B (mean±sd, n=4).

4.3.4.4.3 Sclera penetration and permeation experiments

Topical administration of cyclosporine-loaded micelles could be advantageous to administer therapeutic drug doses to the uvea. In this case, F20 was chosen owing to the high drug concentration and the small size of the micelles (**Table 1** and **Figure 14**). Micelles size could allow their permeation into the scleral pores and channels[104] and then diffuse to the underlying tissue, achieving the uvea[136]. The formulation was applied for 3, 6, 24 and 48 hours and the drug was quantified both in the sclera and in the receptor compartment.

The results (**Figure 19a**) highlight that micelles diffused into scleral pores and, as expected, drug retention into the sclera was roughly proportional to the application time. Several hours (nearly one day) were needed for the transfer of cyclosporine to the receptor compartment and the amounts recovered were not linked to the application time, being the same for formulations applied for 24 and 48 hours. This result suggests that the sclera could act as a reservoir with, apparently, a limited capacity to release the drug into the receptor phase (where sink conditions were present). To check this hypothesis, further experiments were performed as follows: F20 was applied to the sclera for 3, 6 or 24 hours, then the formulation was carefully removed and the experiment was continued up to 48 hours, when cyclosporine quantification in the tissue and in the receptor solution was made. The results obtained are reported in **Figure 19b**. Indeed, the experiments demonstrated that the drug accumulated in the tissue could be released in the receptor phase even if with a very slow rate.

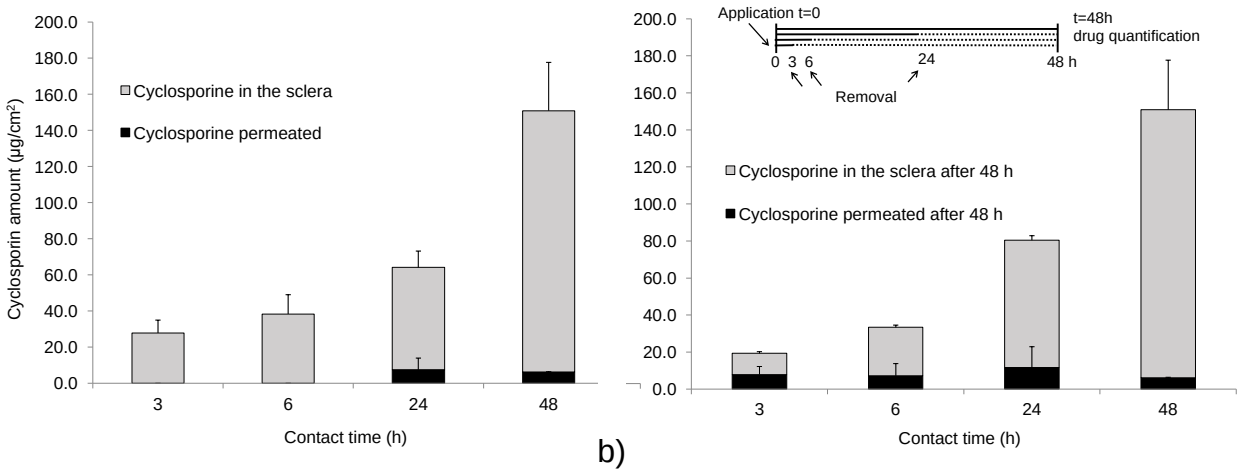

a) b)

Figure 19. Panel a) Amount of cyclosporine retained into or permeated through the sclera following the application of 200 µl of F20 for different times (3 h n=6, 6 h n=6, 24 h n=3, or 48 h n=4, mean±sd). Panel b) Evaluation of reservoir effect (n=3, mean±sd). At different times (3-6-24 h), F20 was removed and the tissue was left on diffusion cells up to 48 h from the beginning of the test. At the end of experiment, cyclosporine was quantified in the sclera and in the receptor compartment.

The low amount of drug permeated in all cases could be explained considering: 1) the difficulty of micelles penetration across the deeper sclera, where a diverse fibre organization (thinner and regularly arranged collagen fibres, compact structure) compared with the outer one (large collagen fibres, organized in rather irregular bundles) is

present[208, 209], and 2) the high stability of micelles, as demonstrated with the stability upon dilution test. However, *in vivo* enzymatic systems located in the sclera and in the choroid[191, 210, 211] can hydrolyze TPGS, impacting on micelles structure and possibly favouring cyclosporine release. In fact, as previously demonstrated (**Figure 16**) TPGS can be metabolized into vitamin E and vitamin E succinate, loosing or reducing its surfactant properties.

An additional consideration can be made comparing the nanomicelles accumulation in the sclera (28±7 µg/cm^2) and in the cornea (3.40±2.36 µg/cm^2, **Figure 18a**) after 3 hours of contact. In similar conditions, the 8-fold higher drug accumulation obtained in the sclera reflects the high porosity of this tissue and the possibility of diffusion of intact micelles.

4.3.5 Conclusions

Poloxamer 407/TPGS mixed micelles increased cyclosporine solubility without the need for an oil phase, avoiding irritant effects for the ocular tissues as demonstrated with the HET-CAM tests. Cyclosporine-loaded micelles exhibited proper size for ocular administration, sufficient stability against dilution, can be sterilized by filtration and freeze dried without the need for a cryoprotectant. Formulations prepared with 10 and 20 mM total surfactants concentration also showed adequate rheological properties at 35°C. Promising results were obtained with *ex vivo* experiments on porcine ocular tissues; in fact, therapeutically significant cyclosporine amounts were detected in cornea. Additionally, micelles accumulated inside the scleral tissue, giving rise to a relevant reservoir effect and suggesting the possibility of a controlled release of cyclosporine to the underlying tissues, also mediated by TPGS hydrolysis. Finally, vitamin E and vitamin E succinate release from TPGS could, at least in principle, support and complement the therapeutic activity of the drug. Further investigations are needed to evaluate long term stability and *in vivo* tolerability.

5. Hydrogels in ophthalmology

Drug delivery scientists are focusing their research toward the design of novel ocular delivery systems easy to administer, with low administration frequency and sustained drug release in order to increase therapeutic efficacy and patient compliance. Nowadays, great progresses in the development of ophthalmic formulations have been performed by investigation on hydrogels. These structures are composed by crosslinked hydrophilic polymers able to absorb large quantities of water, demonstrating high versatility because of their transparency, high water content, good biocompatibility and mechanical properties. Consequently, hydrogels could be employed in ophthalmology as ocular inserts, soft contact lenses, foldable intraocular lenses, *in situ* gelling vehicles, adhesives for corneal wound repair, vitreous substitutes and intravitreal drug delivery systems (**Figure 20**)[212].

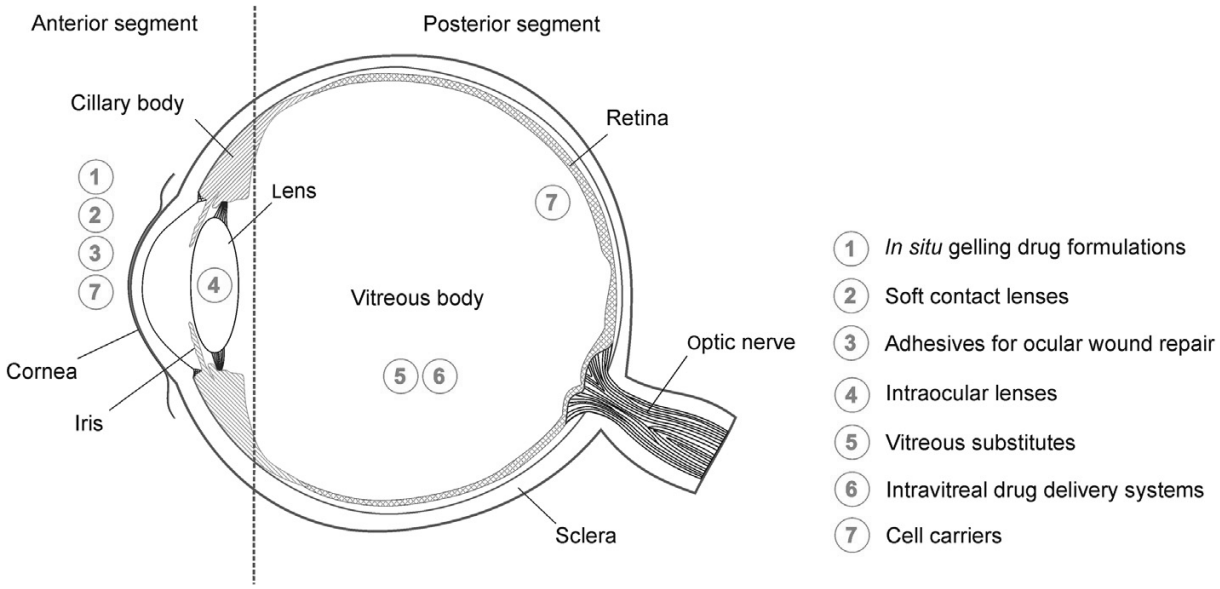

Figure 20. Application of hydrogels in ophthalmology, from [212].

Independently from the specific application, hydrogels should deliver the right dose with the appropriate kinetic; this feature depends on the physico-chemical characteristics of the drug, polymer type and concentration, cross-linking entity and method of drug loading.

5.1 Hydrogels as ocular inserts

Hydrogels as ocular inserts are solid or semi-solid polymeric devices that gradually dissolve while releasing the drug[57]. When the insert is placed in the conjunctival sac, tear fluid begins to penetrate into the matrix, leading to swelling and polymer chains relaxation; by this way, drug diffusion takes place and can show different kinetics in function of

polymer characteristics and matrix organization[57]. Because of biodegradability there is no need of removal from the site of application after drug delivery. Other potential advantages are increased residence time, slow drug release rate, reduced frequency of administration, enhanced drug bioavailability. Moreover, ocular inserts allow for a more accurate dosing in comparison to classical eye drops. However, the initial discomfort correlated to insert application could be considered the main related disadvantage; additionally inserts movement around the eye and occasional inadvertent loss cannot be excluded[57].

The use of mucoadhesive polymers in the design of ocular inserts can be advantageous. In fact these inserts can further facilitate drug absorption prolonging residence time at the application site and leading to a potential increased bioavailability. The majority of inserts showing mucoadhesive properties is hydrophilic and originates chain interactions with the mucins after swelling. Among the most used polymers in drug delivery field, the better mucoadhesion characteristics are shown by chitosan, hyaluronan, cellulose derivatives, polyacrylate and alginate[213].

5.1.1 Hydrogel loading and characterization

The easiest method to load drugs into hydrogels is performed by incubating cross-linked gels in concentrated drug solutions. An alternative method is the loading of the drug while polymer crosslinking is carried out. The first method permits to preserve drug stability but not to reach a good control of drug loading. On the other hand, the second method may cause undesired reactions between the drug and polymeric network, leading to a decrease in drug stability. Concerning drug release, the swelling rate and water adsorption capacity of hydrogels are considered the key parameters in controlling drug release from the polymeric network, as well as the possibility of interactions of host molecules with polymeric backbone of the hydrogel[212, 214].

The successful design of an ocular insert involve the study of several characteristics, listed below[213, 215].

- Thickness. An appropriate thickness, evaluated by a Dial calliper, is required for minimizing the foreign body sensation by patients after administration.
- Mechanical properties. Texture analyzer is commonly used for characterising mechanical strength of inserts; the tensile strength can be calculated by elongation at break or Young's modulus. A good balance between softness and stiffness should be achieved.
- Swelling behaviour. Swelling of the polymers is fundamental for bioadhesion and its degree can regulate drug release from the matrix. The swelling properties of the

inserts, i.e. water absorption capacities, are evaluated by measuring the percentage of hydration that can be achieved after immersion of inserts in buffer at different time points.

- Surface morphology. Surface texture and/or drug distribution can be observed using scanning electron microscopy (SEM), transmission electron microscopy (TEM) and relating imaging techniques. The morphology of the insert should be homogeneous and ensure an uniform drug distribution.
- Drug content and release. The uniformity of the drug in the insert should be evaluated, as well as drug release profiles. Release kinetics depend on the physic-chemical characteristics of the materials used as well as the morphology of the insert. *In vitro* tests are commonly carried out using dialysis membranes or Franz-type diffusion cells.
- Biocompatibility. Biocompatibility should be assessed by performing cytotoxicity tests on model cell lines or HET-CAM test, an alternative method for ocular irritancy evaluation[186].

5.1.2 Macromolecules delivery using ocular inserts

Ocular inserts have been investigated for the delivery of anti-glaucoma drugs[216, 217], anti-inflammatory compounds[218, 219] and anti-virals[220], while few reports are present in literature regarding macromolecules inclusion.

Peptides and proteins require specific attention during the development and manufacturing of ophthalmic inserts, avoiding heating and the occurrence of denaturation reactions. Everaert and coworkers[221] studied a manufacturing technique for lysozyme incorporation in ocular devices made of hydroxypropyl methylcellulose, without the use of heat or shear forces. Authors succeeded in their goal minimising contact with air, employing temperature between 2 and 8 °C and applying minimal shear forces.

Hermans et al.[222] developed ocular chitosan fims in order to prolong cyclosporine delivery to the eye surface; hydroxypropyl-β-cyclodextrin was added to the formulations in order to potentially enhance cyclosporine absorption in ocular tissues.

Koelwel et coworkers[223] tested ocular inserts of different alginates with hydroxyethylcellulose cointaining epidermal growth factor (EGF) for the treatment of keratoconjunctivitis.

5.2 Cyclosporine-loaded crosslinked inserts of sodium hyaluronan and hydroxypropyl-β-cyclodextrin for ocular administration

(Experimental work carried out at the Departamento de Farmacología, Farmacia y Tecnología Farmacéutica, R+DPharma Group (GI-1645), Facultad de Farmacia and Health Research Institute of Santiago de Compostela (IDIS), Universidade de Santiago de Compostela, 15872 Santiago de Compostela, Spain)

5.2.1 Aim of the work

Cyclosporine is one of the most used pharmacological agents for the treatment of several immune-mediated ocular surface disorders[158]. The design of a novel formulation employing a hydrogel as ocular insert could be advantageous in order to obtain a sustained drug release, to reduce the frequency of administration and achieve appropriate cyclosporine levels in the target tissues.

Hyaluronan is a widely used excipient for ophthalmic applications because of its physicochemical properties, e.g. high water binding capacity, pseudoplastic behaviour and optical transparency[224]. It is also used as mucoadhesive excipient for increasing ocular residence time as it contains acidic groups able to interact with the sialic parts of ocular mucins as mucus glycoproteoglycans do[225]. Although poor biomechanical properties and fast dissolution in water might discourage the use of this polymer for sustained release formulations[224], hyaluronan can readily undergo crosslinking reactions that help tuning physical erosion and bioadhesion[216].

Cyclodextrins are also commonly explored to increase the apparent aqueous solubility of hydrophobic drugs in the lachrymal fluid, which in turn creates greater concentration gradient and facilitates cornea penetration[226, 227]. Cyclodextrins can also reduce drug irritation and increase chemical stability[226]. Cross-linked networks of cyclodextrins or the grafting of cyclodextrins to preformed medical devices, such as contact lenses, demonstrated to be useful to exploit the host capability of cyclodextrins. Cyclodextrins confined in the network can develop cooperative binding with guest molecules, increasing the uptake and also slowing the release once in contact with the aqueous medium[228, 229] .

Thus, the aim of this work was to develop a cyclosporine loaded ocular insert by using sodium hyaluronan (HA) and hydroxypropyl β-cyclodextrin (HPβCD) as safe ophthalmic excipients (**Figure 21**). Crosslinking reaction was carried out by using poly(ethylene glycol) diglycidyl ether (PEGDE, **Figure 21**). Sodium hyaluronan was used for its biocompatibility and mucoadhesiveness, as previously discussed. HPβCD was selected for controlling cyclosporine dissolution rate from the crosslinked inserts in the tear film, leading to a

potential increased ocular bioavailability. Four different crosslinked networks were characterised in terms of microstructure, water uptake and mechanical properties. *In vitro* cytotoxicity assay on fibroblasts and HET-CAM test were performed to assess compatibility of blank crosslinked inserts and the presence of toxic residual products of the crosslinking reaction. At the end, crosslinked inserts were loaded with cyclosporine and *in vitro* release in simulated lachrymal fluid was studied.

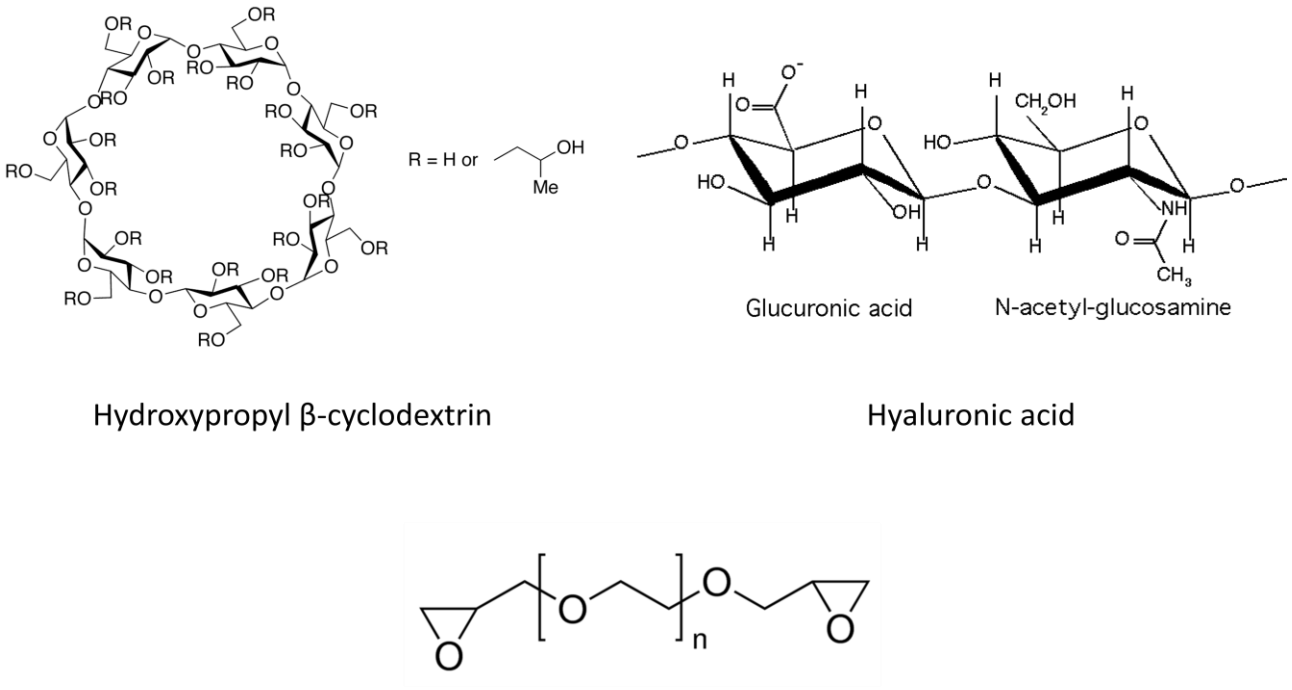

Figure 21. Chemical structure of hyaluronic acid, hydroxypropyl β-cyclodextrin and poly(ethylene glycol) diglycidyl ether.

5.2.2 Material and methods

5.2.2.1 Materials

Cyclosporine ($C_{62}H_{111}N_{11}O_{12}$, MW 1202.61 Da, crystalline solid) was from ThermoFisher Scientific (Karlsruhe, Germany). Sodium hyaluronate (HA, MW 1000 kDa) was purchased from Guinama (La Pobla de Valbona, Spain). Hydroxypropyl β-cyclodextrin (HPβCD, Kleptose® HP oral grade, MW 1399 g/mol) was from Roquette (Lestrem, France). Ethanol absolute AnalaR Normapur® (Reagent Ph Eur, Reagent USP) was from VWR Chemicals (Milano, Italia). Poly(ethylene glycol) diglycidyl ether (PEGDE, MW 526 g/mol, density 1.14 g/ml) was purchased from Sigma Aldrich® (Saint Louis, MO, USA). Potassium hydroxide (MW 56.10 g/mol) was from Honeywell Fluka™ Chemika (Morris Plains, NJ, USA). Water was purified using reverse osmosis (resistivity>18MΩ·cm, MilliQ, Millipore®, Spain). Buffered solution was simulated lachrymal fluid (SLF; $CaCl_2$ 0.06 mg/ml, $NaHCO_3$ 2.18 mg/ml, NaCl 6.7 mg/ml, pH 7.4 adjusted with HCl 1 N).

5.2.2.2 Cyclosporine quantification method

Cyclosporine was analyzed using an HPLC/UV system (Infinity 1260, Agilent Technologies, Santa Clara, CA, USA), with a reverse-phase Nova-Pack C_{18} cartridge (150x3.9 mm, 4 µm) (Waters, Milford, Massachussets, USA) and a C_{18} guard column (3.2x0.8 mm, Security Guard™ Cartridge, Phenomenex, Torrance, USA) thermostated at 65°C. The mobile phase was a mixture CH_3CN:Milli-Q water with TFA 0.1% in 65:35 (v/v) ratio pumped at 1.6 ml/min. The injection volume was 100 µl, and absorbance was monitored at 230 nm. In these conditions, cyclosporine retention time was ca. 5 min. Two calibration curves were built in the concentration ranges 0.25-5 and 2.5-50 µg/ml. The RSD% and RE% were lower than 2 and 6% respectively for all the concentration tested. The LLOQ (lower limit of quantification) was 0.25 µg/ml (RSD% 1.72; RE% 12) and the LOD (limit of detection) was 0.125 µg/ml.

5.2.2.3 Preparation of blank crosslinked inserts

HA-HPβCD crosslinked inserts were prepared by solvent casting evaporation technique. HA (4.3% w/v) and HPβCD solutions (22.7-113-227-454 mg/ml) were both prepared in KOH 2 mM and mixed in order to obtain a final HA concentration of 4% w/v (10 ml final volume). Different HPβCD concentrations were tested to assess the role of cyclodextrins concentration on insert characteristics (final HPβCD 0.15-0.75-1.5-3% w/v). PEGDE (0.1 ml) was then added as crosslinker to HA-HPβCD dispersions (1 ml). After a 12 h reaction

time in the oven at 25°C, gels were cast on a Petri disc (φ=5 cm) and dried for 48 h at 37°C. Inserts (coded B1-B2-B3-B4, see **Table 3**) were then cut as 9 mm discs and immersed in 1 ml of absolute ethanol overnight in order to remove the crosslinker in excess (37°C, 150 osc/min, VWR® Incubating Mini Shaker, Spain), finally kept for 20 min at room temperature to allow for ethanol evaporation.

5.2.2.4 Preliminary characterization of blank crosslinked inserts

5.2.2.4.1 Inserts thickness and weight

Once dried, three circles (0.9 cm in diameter) were characterised for weight and thickness (Caliper Digital Electronic, Fowler™, Newton, MA, USA).

5.2.2.4.2 Swelling behaviour

Blank crosslinked inserts (0.9 cm discs) were weighed (Wd) and then immersed in 1 ml of SLF pH 7.4 at room temperature. The weight increase of the swollen film (Ws) was determined every 30 min for 4 h. The experiment was performed in triplicate for each formulation. The swelling ratio (SR) was calculated as follows:

$SR = \frac{(Ws - Wd)}{Wd}$ (eq. 5)

5.2.2.4.3 Mechanical properties

Puncture strength (PS) was estimated using a TA-TX Plus Texture Analyzer (Stable Micro Systems, Surrey, UK). Blank inserts (0.9 cm in diameter) were fixed into the support rig with a hole of 1 cm of diameter with an upper plate to avoid the slippage. A 5 mm of diameter stainless steel spherical ball probe (P/5S) descended with a rate of 1 mm/s. The PS was estimated by normalizing the maximum force recorded before rupture by the mean thickness of the films.

5.2.2.4.4 Microstructure

Scanning electronic microscopy images of blank inserts were obtained using a field emission scanning electron microscopy (FESEM; FESEM Ultra Plus, Zeiss, Oberkochen, Germany). Inserts were placed onto metal plates and 10 nm thick iridium film was sputter-coated (model Q150T-S, Quorum Technologies, Lewes, UK) on the samples before viewing.

5.2.2.4.5 Cytotoxicity test

In vitro cytotoxicity of blank crosslinked inserts was evaluated by using murine fibroblasts (CCL-163, ATCC, USA). Cells were seeded in a 12-well plate ($1.5 \cdot 10^5$ cells/plate) and grown for 24 h at 37°C/5% CO_2. Fibroblasts were cultured in 2 ml DMEM medium (Dulbecco's modified Eagle's Medium, 10% fetal bovine serum, 1% penicillin-streptomycin). After 24 h, 9-mm inserts were cut into two halves, sterilised under UV lamp for 20 min each side and placed in contact with cells for 48 h at 37°C/5% CO_2. Negative controls included cells without treatment. At the end of the culturing period, cell medium and formulations residues were removed, cell viability was determined by Cell Proliferation Reagent WST-1 (Sigma-Aldrich®, Saint Louis, MO, USA). Briefly, 50 µl of reagent and 1 ml of DMEM without serum were added to each well. After 20 min final solutions were read at 450 nm (UV Bio-Rad Model 680 microplate reader, USA). Cell viability was calculated as a percentage of alive cells with regard to control cells. As cellular mitochondrial succinate-tetrazolium-reductase system cleaves tetrazolium salts of WST-1 reagent to formazan (**Figure 22**), the amount of formazan dye formed resulted directly correlated to the number of metabolically active cells in the medium[230]. Each formulation was characterised in terms of cell viability in triplicate.

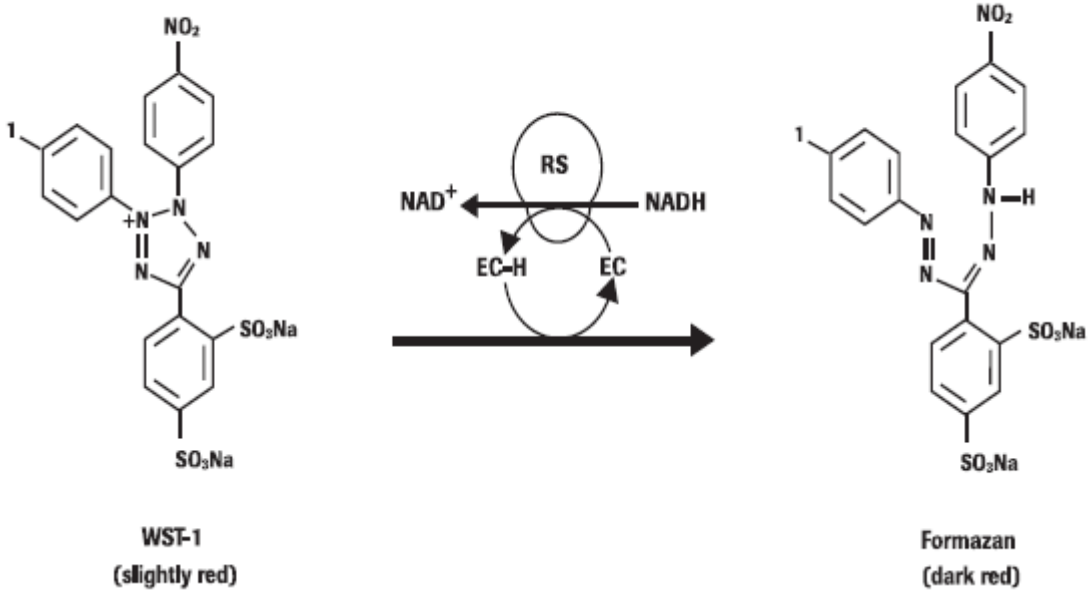

Figure 22. Cleavage of the tetrazolium salt WST-1 (4-[3-(4-Iodophenyl)-2-(4-nitrophenyl)-2H-5-tetrazolio]-1.3-benzene disulfonate) to formazan (EC=electron coupling reagent; RS=mitochondrial succinate tetrazoilum-reductase system).

5.2.2.4.6 HET-CAM test

Fertilized hen's eggs (50-60 g; Coren, Spain) were used for performing irritation test on the Chorio-Allantoic Membrane (HET-CAM)[231]. Eggs were incubated in a climatic chamber (Ineltec, model CC SR 0150, Barcelona) at 37°C and 60% relative humidity for 9 days. Eggs were turned 3 times per day, while the last day were placed with the wider extreme upward. On the ninth day, the eggshell was partially removed (2 cm in diameter) on the air chamber with a rotary saw (Dremel 300, Breda, Netherlands). The inner membrane was wet with 0.9% NaCl (for 30 min in the climatic chamber) and then carefully removed to expose the CAM. Formulations (9-mm discs, blank inserts) were placed on the CAM of different eggs. 0.9% NaCl and 5 M NaOH solutions were used as negative and positive controls, respectively. The vessels of CAM were observed during 5 min, recording the times at which hemorrhage (Th), vascular lysis (Tl), or coagulation (Tc) occurred. The irritation score (IS) was calculated with the following formula:

$$IS = 5 \times \frac{301-Th}{300} + 7 \times \frac{301-Tl}{300} + 9 \times \frac{301-Tc}{300} \quad \text{(eq. 3)}$$

Formulations effects on CAM vessels were analyzed 5 min after the beginning of the assay by photographs taken with a digital camera (Canon SX 260HS, without zoom) and downloaded in the computer in JPEG format. GIMP® software was used to delete zones without good luminosity, obtaining a representative zone of the membrane with the tested formulations.

5.2.2.5 Cyclosporine loading into crosslinked inserts and *in vitro* release studies

For obtaining cyclosporine-loaded inserts, blank formulations (0.9 cm in diameter discs) were immersed into 1 ml of 5 mg/ml cyclosporine 75:25 EtOH:H_20 solution overnight and then dried for 2 hours at 40°C (formulations coded as F1-F2-F3-F4, as listed in **Table 4**). After insert soaking and drying, drug-loaded discs were inserted in a tube containing 5 ml SLF at 37°C under magnetic stirring. The solution was sampled at predetermined time points by taking 0.3 ml of solution, immediately replaced with the same volume of fresh SLF. Experiments carried out up to 4 h. Solutions was then kept under magnetic stirring overnight at room temperature for ensuring complete dissolution of the inserts and sampled. Collected samples were analysed as described in section 5.2.2.2.

5.2.2.6 Statistical analysis

Differences between conditions were assessed using Student's t-test. Differences were considered statistically significant when $p<0.05$. In the text, all data are reported as mean value±sd.

5.2.3 Preliminary results

The characteristics of the blank inserts in terms of composition, thickness and weight are listed in **Table 3**. No substantially different results were obtained in terms of weight and thickness as a function of HPβCD concentration. Additionally, the weight of the prepared film was approximately 50% of the theoretical amount, calculated considering the volume and the concentrations of the casted solutions and the diameter of the Petri disc. This suggests a loss of material during the overnight washing step.

Table 3. Characteristics of blank crosslinked inserts (n=4).

Insert	Theoretical HA content (% w/w)	Theoretical HPβCD (% w/v)	Thickness (μm)	Weight (mg/cm^2)
B1	96.4	3.6	275±66	12.54±2.64
B2	84.2	15.8	295±30	12.85±1.77
B3	72.7	27.3	283±78	13.84±1.42
B4	57.1	42.9	320±80	19.18±1.90

Another source of variability is the different HA % in the final insert. In fact, given the high hygroscopicity of this compound, a different content can translate in a different percentage of water in the dry insert. All blank crosslinked inserts presented a high capability of absorbing water (**Figure 23**). The high degree of swelling can be advantageous to ensure a rapid adhesion of the inserts on the ocular mucosa and the permanence of the dosage form. Crosslinked inserts rapidly reach high levels of swelling and becoming fragile, breaking the swollen structure. Although the results obtained in terms of swelling ratio are not statistically different, the different time needed for entirely destroy crosslinked inserts structures could be justified by the different structure. In fact B1 and B2, containing a theoretical HPβCD concentration of 3.6 and 15.8 % w/v, broke down after 2 h, while B3 and B4 structures were intact up to 4 h. This result supports the role of HPβCD on the hydrogel crosslinking, probably acting as grafting element on the polymeric network. This hypothesis is suggested as poly(ethylene glycol) diglycidyl ether, used as crosslinker

compound because the epoxy groups are known to react with hydroxyl groups[232], could favour the formation of bounds between hyaluronic acid backbone and cyclodextrin, both presenting reactive groups (**Figure 21**)

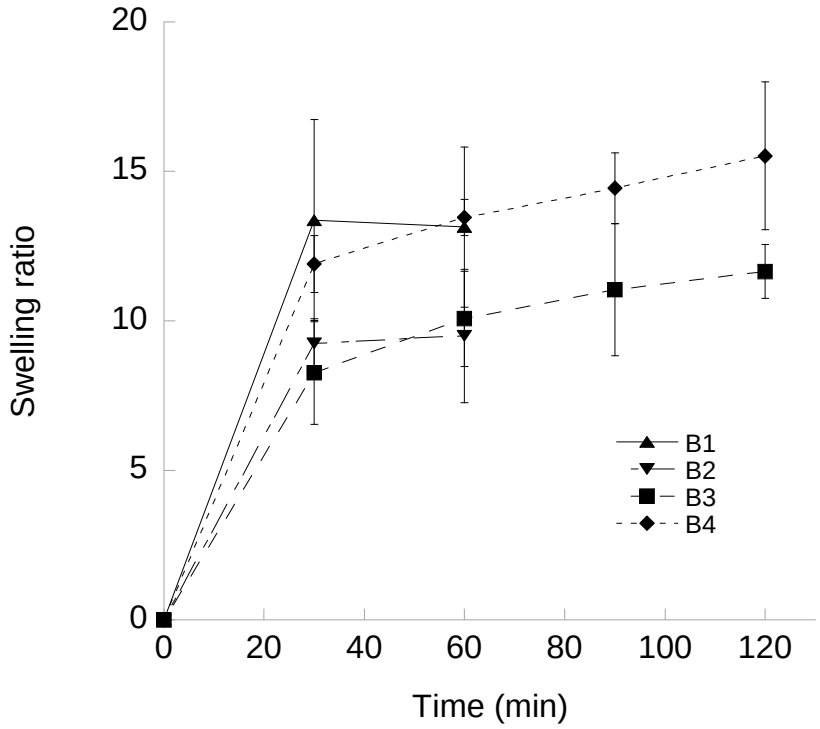

Figure 23. Swelling behaviour in SLF at room temperature of blank crosslinked inserts (mean±sd, n=3)

SEM images of blank crosslinked inserts (**Figure 24**) showed very porous structures, that justify the high degree of swelling achieved by these formulations. B3 and in particular B4 inserts showed particles on the surface which may be due to HPβCD in excess that was not incorporated in the hydrogel during the crosslinking reaction[219].

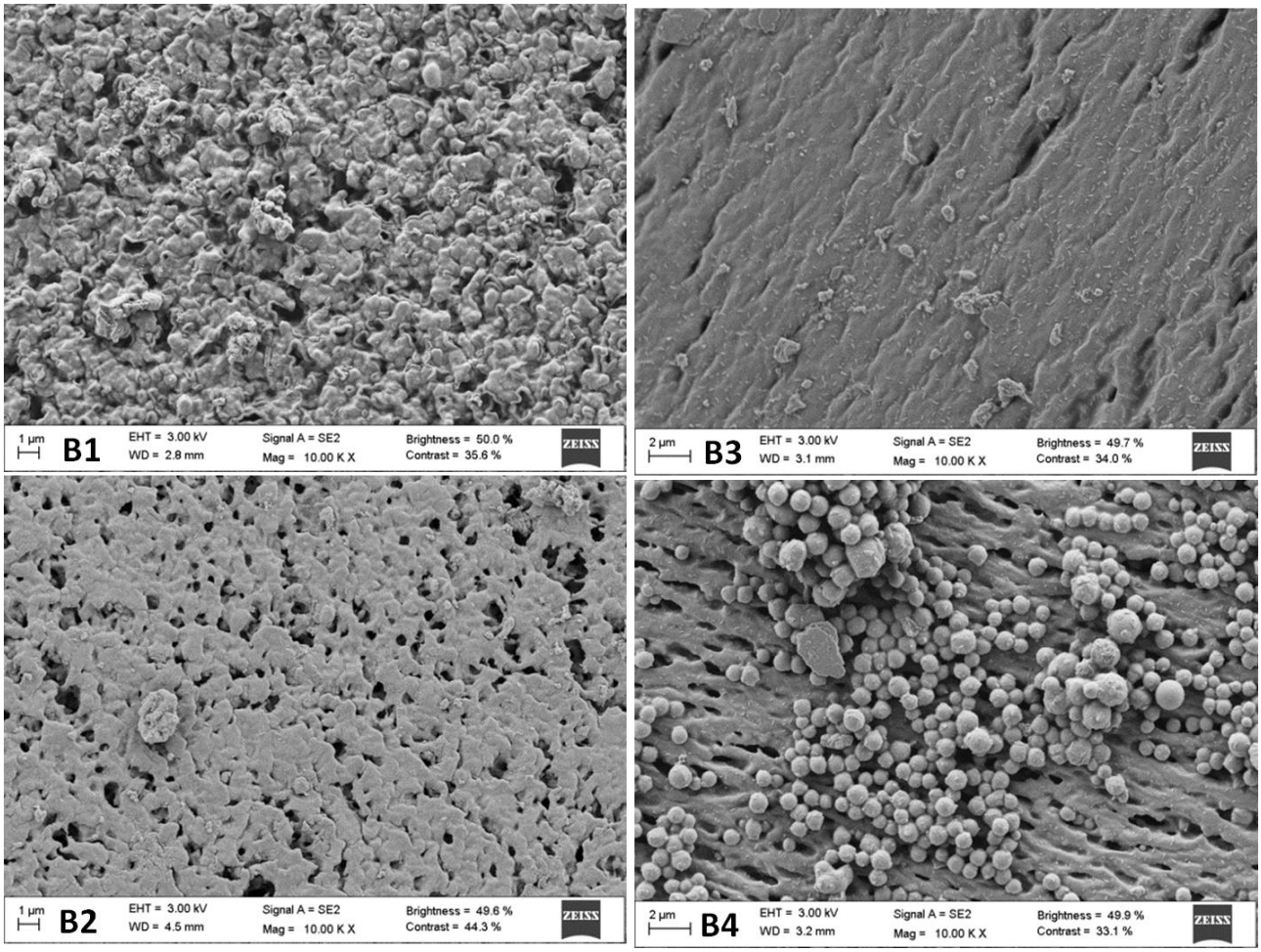

Figure 24. SEM micrographs of surface of blank crosslinked inserts.

Puncture strength (PS) at break for blank dry inserts was evaluated to figure out the influence of HPβCD content on mechanical properties (**Figure 25**): no statistically different results were obtained in terms of PS varying HPβCD concentration. Moreover, results obtained for all the formulations demonstrated that dry inserts are brittle and prone to break easily[233].

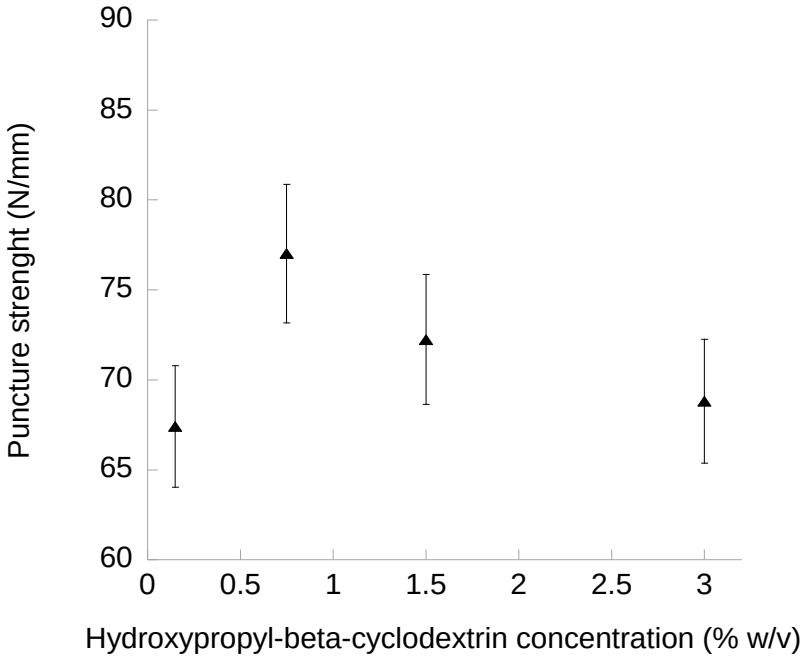

Figure 25. Puncture strength values in function of HPβCD concentration before inserts rupture (mean±5%).

Blank crosslinked inserts were then evaluated in terms of cytocompatibility towards murine fibroblasts to ensure no residual toxic secondary subproducts of the crosslinking reaction and/or crosslinker excess were present. As shown in **Figure 26a**, cell viability reduction was lower than 20% after contact with murine fibroblasts for 48 h, showing thus a good biocompatibility of the formulations. Blank inserts were also tested in terms of irritancy using HET-CAM test (**Figure 26b**): none of the formulation caused hemorrhage, vessels lysis or coagulation, as in case of saline solution. These events occurred only in case of the positive control (NaOH 5 M, IS equal to 20), resulting in a rosette-like coagulation.

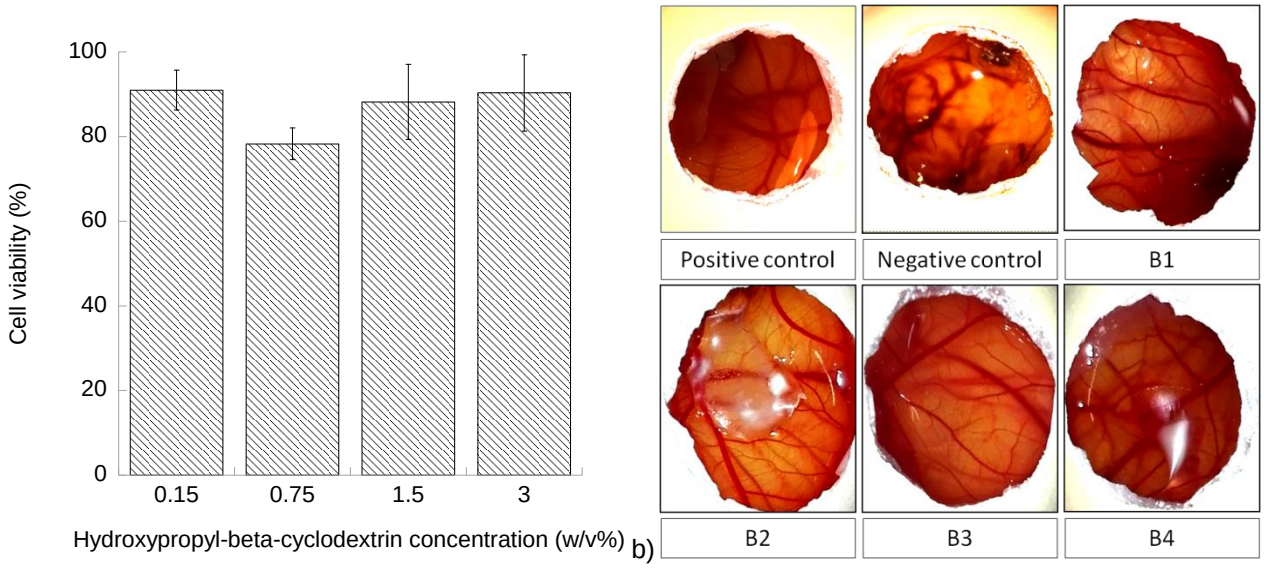

Figure 26. Panel a: murine fibroblasts viability after blank crosslinked inserts for 48 h (mean±sd, n=3). Panel b: HET-CAM photographs of blank inserts after 5 min form the beginning of the test, negative and positive control were 0.9% NaCl and 5 M NaOH, respectively.

After preliminary tests on blank inserts, cyclosporine was loaded in the formulations; cyclosporine-loaded inserts details are listed in **Table 4**.

Table 4. Characteristics of cyclosporine-loaded inserts (n=3).

Insert	Theoretical HA (% w/v)	Theoretical HPβCD (% w/v)	Weight (mg/cm^2)	Cyclosporine content (mg_{drug}/cm^2)	Cyclosporine content (% w/w)
F1	96.4	3.6	31.92±12.94	0.29±0.12	0.92±0.12
F2	84.2	15.8	30.53±3.37	0.20±0.04	0.67±0.17
F3	72.7	27.3	22.18±1.53	0.25±0.07	1.14±0.23
F4	57.1	42.9	24.39±6.31	0.21±0.03	0.87±0.15

Surprisingly, the amount of drug loaded was not related to the theoretical amount of HPβCD. This result suggests that probably the drug is not included in the cyclodextrin cavity, rather it is dispersed in the hydrogel matrix. The increment in weight of the inserts observed after drug loading could be due to the incorporation of water during the overnight soaking. Cyclosporine release profiles from crosslinked inserts are shown in **Figure 27**. Drug release from F1 and F2 resulted controlled only in the first 40 minutes, while a fast and almost quantitative release occurred between 70 and 90 min in agreement with the

results obtained in terms of swelling behaviour (**Figure 23**). Conversely, F3 and F4 were able to control drug release at least to 4 h, with a nearly zero order profile during the first hour (13.4 and 9.7 ng/(mg_{insert}·min) for F3 and F4, respectively).

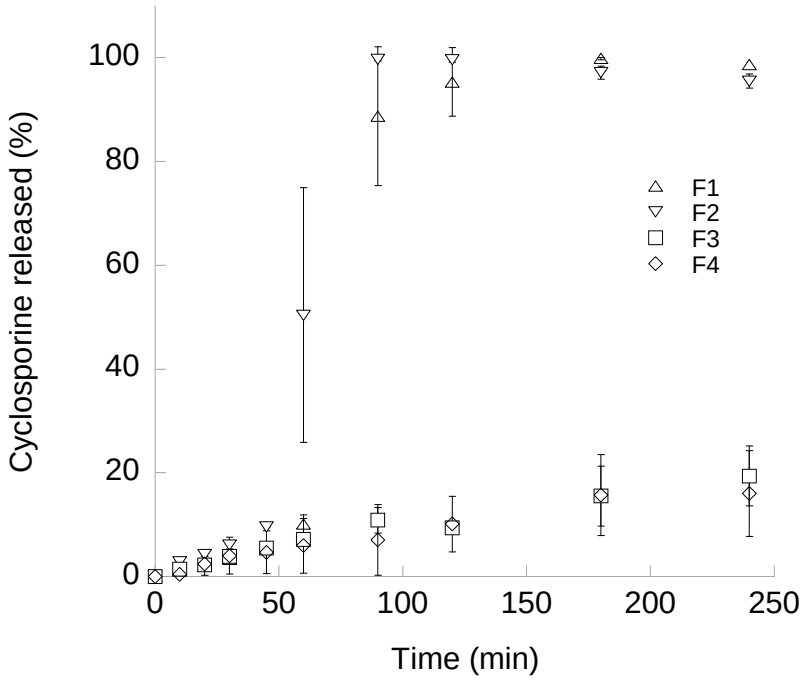

Figure 27. Cyclosporine release profiles from crosslinked inserts in SLF at 37°C (F1 and F2 n=2, F3 and F4 n=3).

5.2.4 Future perspectives

Further studies will be performed to characterize cyclosporine-loaded crosslinked inserts. DSC analysis will be carried out to evaluate the interactions between inserts components and the formation of inclusion complexes between cyclosporine and HPβCD. F3 and F4 release profiles will be studied up to 24 h, to exploit the potentiality of these formulations in sustaining drug release. Accumulation and permeation studies through porcine tissues (conjunctiva, sclera, choroid-Bruch's membrane) will be assessed for the evaluation of drug targeting and thus for the employment of the formulation for treating posterior and anterior eye segment diseases.

6. General conclusions

Ocular iontophoresis is confirmed to be a promising method to enhance proteins transport across the ocular tissues. Nevertheless the results obtained in this work highlight that many factors can impact on the efficiency of this technique, such as molecular shape and surface charge distribution.

Other novel approaches can be used to enhance macromolecules and peptides absorption to the eye. The results obtained show the suitability of polymeric micelles made of TPGS and poloxamer 407 for obtaining improved cyclosporine penetration into ocular tissues in comparison to the commercial Ikervis®; cyclosporine-loaded polymeric micelles seem promising for targeting both the anterior and the posterior eye segment.

Preliminary results obtained with cyclosporine-loaded ocular inserts of sodium hyaluronan and hydroxypropyl-β-cyclodextrin demonstrated their convenient use for obtaining a controlled and sustained drug release, encouraging a further characterization of the systems by *in vitro* and *ex vivo* tests.

7. Presentation of the results

7.1 Publications

- Grimaudo, M.A., Tratta E., Pescina S., Padula C., Santi P., Nicoli S. *Parameters affecting the transscleral delivery of two positively charged proteins of comparable size.* International Journal of Pharmaceutics, 2017. **521**(1-2):214-221. ISSN 0378-5173
  10.1016/j.ijpharm.2017.02.044
- Submitted paper: Grimaudo, M.A, Pescina S., Padula C., Santi P., Concheiro A., Alvarez-Lorenzo C., Nicoli S. *Poloxamer 407/TPGS mixed micelles as promising carriers for an efficient cyclosporine penetration in ocular tissues.*

7.2 Presentation of the results in conferences and doctoral school

- M.A. Grimaudo, Tratta E., S. Pescina, C. Padula, P. Santi, S. Nicoli "Trans-scleral delivery of Cytochrome C and Lysozyme: iontophoresis as an enhancing strategy" (9th AItUN Annual meeting, Milano, 25-27 May 2015)
- M.A. Grimaudo, S. Pescina, C. Padula, P. Santi and S. Nicoli "Passive and iontophoretic delivery of a model protein across the sclera" (ULLA Summer School, Chateney-Malabry, Université de Paris Sud, 04-11 July 2015)
- M.A. Grimaudo, S. Pescina, C. Padula, P. Santi, S. Nicoli "Permeazione di due proteine modello attraverso sclera porcina isolata" XV (Scuola estiva di formazione in discipline tecnologico-farmaceutiche, Fisciano, Università degli Studi di Salerno, 09-11 September 2015)
- M.A. Grimaudo, S. Pescina, C. Padula, P. Santi, S. Nicoli "Impact of some molecular properties on macromolecules transport across ocular tissues" (10th AItUN Annual meeting, Parma, 05-06 May 2016)
- M.A. Grimaudo, S. Pescina, C. Padula, P. Santi and S. Nicoli "Cyclosporine A loaded nanomicelles for the treatment of the dry eye syndrome" (AAPS Paris Summer School, Paris, 27-28 August 2016)
- M.A. Grimaudo, S. Pescina, C. Padula, P. Santi, A. Concheiro, C. Alvarez-Lorenzo, S. Nicoli "Pluronic®F127/TPGS micelles as promising carriers for cyclosporine ocular delivery" (Advanced school in Nanomedicine, Pula, Cagliari, 25-28 September 2017)

8. References

1. Joseph, M.; Trinh, H.M.; Cholkar, K.; Pal, D.;Mitra, A.K., *Recent perspectives on the delivery of biologics to back of the eye.* Expert Opin Drug Deliv, 2017. **14**(5): p. 631-645.
2. Radhakrishnan, K.; Sonali, N.; Moreno, M.; Nirmal, J.; Fernandez, A.A.; Venkatraman, S.;Agrawal, R., *Protein delivery to the back of the eye: barriers, carriers and stability of anti-VEGF proteins.* Drug Discov Today, 2017. **22**(2): p. 416-423.
3. Kim, Y.C.; Chiang, B.; Wu, X.;Prausnitz, M.R., *Ocular delivery of macromolecules.* Journal of Controlled Release, 2014. **190**(0): p. 172-181.
4. Kang-Mieler, J.J.; Osswald, C.R.;Mieler, W.F., *Advances in ocular drug delivery: emphasis on the posterior segment.* Expert Opin Drug Deliv, 2014. **11**(10): p. 1647-60.
5. Jain, G.K.; Warsi, M.H.; Nirmal, J.; Garg, V.; Pathan, S.A.; Ahmad, F.J.;Khar, R.K., *Therapeutic stratagems for vascular degenerative disorders of the posterior eye.* Drug Discov Today, 2012. **17**(13-14): p. 748-59.
6. Heier, J.S.; Brown, D.M.; Chong, V.; Korobelnik, J.F.; Kaiser, P.K.; Nguyen, Q.D.; Kirchhof, B.; Ho, A.; Ogura, Y.; Yancopoulos, G.D.; Stahl, N.; Vitti, R.; Berliner, A.J.; Soo, Y.; Anderesi, M.; Groetzbach, G.; Sommerauer, B.; Sandbrink, R.; Simader, C.;Schmidt-Erfurth, U., *Intravitreal aflibercept (VEGF trap-eye) in wet age-related macular degeneration.* Ophthalmology, 2012. **119**(12): p. 2537-48.
7. Lynch, S.S.;Cheng, C.M., *Bevacizumab for neovascular ocular diseases.* Ann Pharmacother, 2007. **41**(4): p. 614-25.
8. Hao, J.; Li, S.K.; Kao, W.W.Y.;Liu, C.-Y., *Gene delivery to cornea.* Brain research bulletin, 2010. **81**(2-3): p. 256-261.
9. Geary, R.S.; Henry, S.P.;Grillone, L.R., *Fomivirsen: clinical pharmacology and potential drug interactions.* Clin Pharmacokinet, 2002. **41**(4): p. 255-60.
10. Witting, M.; Obst, K.; Friess, W.;Hedtrich, S., *Recent advances in topical delivery of proteins and peptides mediated by soft matter nanocarriers.* Biotechnol Adv, 2015. **33**(6 Pt 3): p. 1355-69.
11. Benhar, I.; London, A.;Schwartz, M., *The privileged immunity of immune privileged organs: the case of the eye.* Front Immunol, 2012. **3**: p. 296.

12. Remington, L.A., *Chapter 1 - Visual System*, in *Clinical Anatomy and Physiology of the Visual System (Third Edition)*. 2012, Butterworth-Heinemann: Saint Louis. p. 1-9.
13. Ruponen, M.;Urtti, A., *Undefined role of mucus as a barrier in ocular drug delivery.* Eur J Pharm Biopharm, 2015. **96**: p. 442-6.
14. Remington, L.A., *Chapter 2 - Cornea and Sclera*, in *Clinical Anatomy and Physiology of the Visual System (Third Edition)*. 2012, Butterworth-Heinemann: Saint Louis. p. 10-39.
15. Remington, L.A., *Chapter 3 - Uvea*, in *Clinical Anatomy and Physiology of the Visual System (Third Edition)*. 2012, Butterworth-Heinemann: Saint Louis. p. 40-60.
16. Remington, L.A., *Chapter 4 - Retina*, in *Clinical Anatomy and Physiology of the Visual System (Third Edition)*. 2012, Butterworth-Heinemann: Saint Louis. p. 61-92.
17. Remington, L.A., *Chapter 6 - Aqueous and Vitreous Humors*, in *Clinical Anatomy and Physiology of the Visual System (Third Edition)*. 2012, Butterworth-Heinemann: Saint Louis. p. 109-122.
18. Bishop, P.N., *Structural macromolecules and supramolecular organisation of the vitreous gel.* Prog Retin Eye Res, 2000. **19**(3): p. 323-44.
19. Gaudana, R.; Ananthula, H.K.; Parenky, A.;Mitra, A.K., *Ocular drug delivery.* The AAPS Journal, 2010. **12**(3): p. 348-60.
20. Yavuz, B.; Bozdag Pehlivan, S.;Unlu, N., *An overview on dry eye treatment: approaches for cyclosporin a delivery.* ScientificWorldJournal, 2012. **2012**: p. 194848.
21. Ciulla, T.A.; Amador, A.G.;Zinman, B., *Diabetic retinopathy and diabetic macular edema: pathophysiology, screening, and novel therapies.* Diabetes Care, 2003. **26**(9): p. 2653-64.
22. Crawford, T.N.; Alfaro, D.V., 3rd; Kerrison, J.B.;Jablon, E.P., *Diabetic retinopathy and angiogenesis.* Curr Diabetes Rev, 2009. **5**(1): p. 8-13.
23. Nowak, J.Z., *Age-related macular degeneration (AMD): pathogenesis and therapy.* Pharmacol Rep, 2006. **58**(3): p. 353-63.
24. Sadaka, A.;Giuliari, G.P., *Proliferative vitreoretinopathy: current and emerging treatments.* Clin Ophthalmol, 2012. **6**: p. 1325-33.
25. Jabs, D.A., *Ocular manifestations of HIV infection.* Trans Am Ophthalmol Soc, 1995. **93**: p. 623-83.
26. Airody, A.; Heath, G.; Lightman, S.;Gale, R., *Non-Infectious Uveitis: Optimising the Therapeutic Response.* Drugs, 2016. **76**(1): p. 27-39.

27. Majumder, P.D.; Ghosh, A.;Biswas, J., *Infectious uveitis: An enigma.* Middle East African Journal of Ophthalmology, 2017. **24**(1): p. 2-10.
28. Gaudana, R.; Ananthula, H.; Parenky, A.;Mitra, A., *Ocular Drug Delivery.* The AAPS Journal, 2010. **12**(3): p. 348-360.
29. Urtti, A., *Challenges and obstacles of ocular pharmacokinetics and drug delivery.* Adv Drug Deliv Rev, 2006. **58**(11): p. 1131-5.
30. Weiner, A.L., *CHAPTER 2 - Drug Delivery Systems in Ophthalmic Applications A2 - Yorio, Thomas*, in *Ocular Therapeutics*, A.F. Clark and M.B. Wax, Editors. 2008, Academic Press: London. p. 7-43.
31. Ambati, J.; Canakis, C.S.; Miller, J.W.; Gragoudas, E.S.; Edwards, A.l.; Weissgold, D.J.; Kim, I.; Delori, F.o.C.;Adamis, A.P., *Diffusion of High Molecular Weight Compounds through Sclera.* Investigative ophthalmology & visual science, 2000. **41**(5): p. 1181-1185.
32. Gaudana, R.; Jwala, J.; Boddu, S.H.;Mitra, A.K., *Recent perspectives in ocular drug delivery.* Pharmaceutical Research, 2009. **26**(5): p. 1197-216.
33. Geroski, D.H.;Edelhauser, H.F., *Transscleral drug delivery for posterior segment disease.* Adv Drug Deliv Rev, 2001. **52**(1): p. 37-48.
34. Argueso, P.; Guzman-Aranguez, A.; Mantelli, F.; Cao, Z.; Ricciuto, J.;Panjwani, N., *Association of cell surface mucins with galectin-3 contributes to the ocular surface epithelial barrier.* J Biol Chem, 2009. **284**(34): p. 23037-45.
35. Barar, J.; Javadzadeh, A.R.;Omidi, Y., *Ocular novel drug delivery: impacts of membranes and barriers.* Expert Opin Drug Deliv, 2008. **5**(5): p. 567-81.
36. Kim, S.H.; Lutz, R.J.; Wang, N.S.;Robinson, M.R., *Transport barriers in transscleral drug delivery for retinal diseases.* Ophthalmic Res, 2007. **39**(5): p. 244-54.
37. Cheruvu, N.P.S.;Kompella, U.B., *Bovine and Porcine Transscleral Solute Transport: Influence of Lipophilicity and the Choroid–Bruch's Layer.* Investigative ophthalmology & visual science, 2006. **47**(10): p. 4513-4522.
38. Pitkanen, L.; Ranta, V.P.; Moilanen, H.;Urtti, A., *Permeability of retinal pigment epithelium: effects of permeant molecular weight and lipophilicity.* Invest Ophthalmol Vis Sci, 2005. **46**(2): p. 641-6.
39. Jackson, T.L.; Antcliff, R.J.; Hillenkamp, J.;Marshall, J., *Human retinal molecular weight exclusion limit and estimate of species variation.* Invest Ophthalmol Vis Sci, 2003. **44**(5): p. 2141-6.
40. Rowe-Rendleman, C.L.; Durazo, S.A.; Kompella, U.B.; Rittenhouse, K.D.; Di Polo, A.; Weiner, A.L.; Grossniklaus, H.E.; Naash, M.I.; Lewin, A.S.; Horsager,

A.;Edelhauser, H.F., *Drug and gene delivery to the back of the eye: from bench to bedside.* Invest Ophthalmol Vis Sci, 2014. **55**(4): p. 2714-30.

41. Käsdorf, Benjamin T.; Arends, F.;Lieleg, O., *Diffusion Regulation in the Vitreous Humor.* Biophysical Journal, 2015. **109**(10): p. 2171-2181.
42. Yamada, N.;Olsen, T.W., *Routes for Drug Delivery to the Retina: Topical, Transscleral, Suprachoroidal and Intravitreal Gas Phase Delivery.* Dev Ophthalmol, 2016. **55**: p. 71-83.
43. Mac Gabhann, F.; Demetriades, A.M.; Deering, T.; Packer, J.D.; Shah, S.M.; Duh, E.; Campochiaro, P.A.;Popel, A.S., *Protein transport to choroid and retina following periocular injection: theoretical and experimental study.* Ann Biomed Eng, 2007. **35**(4): p. 615-30.
44. Al-Debasi, T.; Al-Bekairy, A.; Al-Katheri, A.; Al Harbi, S.;Mansour, M., *Topical versus subconjunctival anti-vascular endothelial growth factor therapy (Bevacizumab, Ranibizumab and Aflibercept) for treatment of corneal neovascularization.* Saudi J Ophthalmol, 2017. **31**(2): p. 99-105.
45. Pitkanen, L.; Ranta, V.P.; Moilanen, H.;Urtti, A., *Binding of betaxolol, metoprolol and oligonucleotides to synthetic and bovine ocular melanin, and prediction of drug binding to melanin in human choroid-retinal pigment epithelium.* Pharmaceutical Research, 2007. **24**(11): p. 2063-70.
46. Dey, S.;Mitra, A.K., *Transporters and receptors in ocular drug delivery: opportunities and challenges.* Expert Opin Drug Deliv, 2005. **2**(2): p. 201-4.
47. Short, B.G., *Safety evaluation of ocular drug delivery formulations: techniques and practical considerations.* Toxicol Pathol, 2008. **36**(1): p. 49-62.
48. Li, S.K.; Zhu, H.;Higuchi, W.I., *Enhanced transscleral Iontophoretic transport with ion-exchange membrane.* Pharmaceutical Research, 2006. **23**(8): p. 1857-67.
49. Nicoli, S.; Ferrari, G.; Quarta, M.; Macaluso, C.;Santi, P., *In vitro transscleral iontophoresis of high molecular weight neutral compounds.* Eur J Pharm Sci, 2009. **36**(4-5): p. 486-92.
50. Chopra, P.; Hao, J.;Li, S.K., *Iontophoretic transport of charged macromolecules across human sclera.* International Journal of Pharmaceutics, 2010. **388**(1–2): p. 107-113.
51. Pescina, S.; Ferrari, G.; Govoni, P.; Macaluso, C.; Padula, C.; Santi, P.;Nicoli, S., *In-vitro permeation of bevacizumab through human sclera: effect of iontophoresis application.* Journal of Pharmacy and Pharmacology, 2010. **62**(9): p. 1189-1194.

52. Hao, J.; Li, S.K.; Kao, W.W.;Liu, C.Y., *Gene delivery to cornea.* Brain Res Bull, 2010. **81**(2-3): p. 256-61.
53. Blair-Parks, K.; Weston, B.C.;Dean, D.A., *High-level gene transfer to the cornea using electroporation.* J Gene Med, 2002. **4**(1): p. 92-100.
54. Souza, J.G.; Dias, K.; Pereira, T.A.; Bernardi, D.S.;Lopez, R.F., *Topical delivery of ocular therapeutics: carrier systems and physical methods.* J Pharm Pharmacol, 2014. **66**(4): p. 507-30.
55. Pescina, S.; Sonvico, F.; Santi, P.;Nicoli, S., *Therapeutics and carriers: the dual role of proteins in nanoparticles for ocular delivery.* Curr Top Med Chem, 2015. **15**(4): p. 369-85.
56. Marano, R.J.; Wimmer, N.; Kearns, P.S.; Thomas, B.G.; Toth, I.; Brankov, M.;Rakoczy, P.E., *Inhibition of in vitro VEGF expression and choroidal neovascularization by synthetic dendrimer peptide mediated delivery of a sense oligonucleotide.* Exp Eye Res, 2004. **79**(4): p. 525-35.
57. Saettone, M.F.;Salminen, L., *Ocular inserts for topical delivery.* Advanced Drug Delivery Reviews, 1995. **16**(1): p. 95-106.
58. Jiang, C.; Moore, M.J.; Zhang, X.; Klassen, H.; Langer, R.;Young, M., *Intravitreal injections of GDNF-loaded biodegradable microspheres are neuroprotective in a rat model of glaucoma.* Mol Vis, 2007. **13**: p. 1783-92.
59. Lambiase, A.; Coassin, M.; Tirassa, P.; Mantelli, F.;Aloe, L., *Nerve growth factor eye drops improve visual acuity and electrofunctional activity in age-related macular degeneration: a case report.* Ann Ist Super Sanita, 2009. **45**(4): p. 439-42.
60. Maurice, D.M.;Polgar, J., *Diffusion across the sclera.* Exp Eye Res, 1977. **25**(6): p. 577-82.
61. Olsen, T.W.; Edelhauser, H.F.; Lim, J.I.;Geroski, D.H., *Human scleral permeability. Effects of age, cryotherapy, transscleral diode laser, and surgical thinning.* Invest Ophthalmol Vis Sci, 1995. **36**(9): p. 1893-903.
62. Pescina, S.; Antopolsky, M.; Santi, P.; Nicoli, S.;Murtomäki, L., *Effect of iontophoresis on the in vitro trans-scleral transport of three single stranded oligonucleotides.* European Journal of Pharmaceutical Sciences, 2013. **49**(2): p. 142-147.
63. Pescina, S.; Padula, C.; Santi, P.;Nicoli, S., *Effect of formulation factors on the trans-scleral iontophoretic and post-iontophoretic transports of a 40 kDa dextran in vitro.* European Journal of Pharmaceutical Sciences, 2011. **42**(5): p. 503-508.

64. Prausnitz, M.R.;Noonan, J.S., *Permeability of cornea, sclera, and conjunctiva: a literature analysis for drug delivery to the eye.* J Pharm Sci, 1998. **87**(12): p. 1479-88.
65. Pescina, S.; Santi, P.; Ferrari, G.; Padula, C.; Cavallini, P.; Govoni, P.;Nicoli, S., *Ex vivo models to evaluate the role of ocular melanin in trans-scleral drug delivery.* European Journal of Pharmaceutical Sciences, 2012. **46**(5): p. 475-483.
66. Tratta, E.; Pescina, S.; Padula, C.; Santi, P.;Nicoli, S., *In vitro permeability of a model protein across ocular tissues and effect of iontophoresis on the transscleral delivery.* European Journal of Pharmaceutics and Biopharmaceutics, 2014. **88**(1): p. 116-122.
67. Cazares-Delgadillo, J.; Naik, A.; Ganem-Rondero, A.; Quintanar-Guerrero, D.;Kalia, Y.N., *Transdermal delivery of cytochrome C--A 12.4 kDa protein--across intact skin by constant-current iontophoresis.* Pharmaceutical Research, 2007. **24**(7): p. 1360-8.
68. Dubey, S.;Kalia, Y.N., *Understanding the poor iontophoretic transport of lysozyme across the skin: When high charge and high electrophoretic mobility are not enough.* Journal of Controlled Release, 2014. **183**(0): p. 35-42.
69. Grimaudo, M.A.; Tratta, E.; Pescina, S.; Padula, C.; Santi, P.;Nicoli, S., *Parameters affecting the transscleral delivery of two positively charged proteins of comparable size.* Int J Pharm, 2017. **521**(1-2): p. 214-221.
70. Wilkins, D.K.; Grimshaw, S.B.; Receveur, V.; Dobson, C.M.; Jones, J.A.;Smith, L.J., *Hydrodynamic Radii of Native and Denatured Proteins Measured by Pulse Field Gradient NMR Techniques.* Biochemistry, 1999. **38**(50): p. 16424-16431.
71. Selsted, M.E.;Martinez, R.J., *A simple and ultrasensitive enzymatic assay for the quantitative determination of lysozyme in the picogram range.* Analytical Biochemistry, 1980. **109**(1): p. 67-70.
72. Wetter, L.R.;Deutsch, H.F., *IMMUNOLOGICAL STUDIES ON EGG WHITE PROTEINS: IV. IMMUNOCHEMICAL AND PHYSICAL STUDIES OF LYSOZYME.* Journal of Biological Chemistry, 1951. **192**(1): p. 237-242.
73. Vincentelli, R.; Canaan, S.; Campanacci, V.; Valencia, C.; Maurin, D.; Frassinetti, F.; Scappucini-Calvo, L.; Bourne, Y.; Cambillau, C.;Bignon, C., *High-throughput automated refolding screening of inclusion bodies.* Protein Science : A Publication of the Protein Society, 2004. **13**(10): p. 2782-2792.
74. Potts, A.M., *The Reaction of Uveal Pigment in Vitro with Polycyclic Compounds.* Invest Ophthalmol, 1964. **3**: p. 405-16.

75. Davies, R.C.; Neuberger, A.;Wilson, B.M., *The dependence of lysozyme activity on pH and ionic strength.* Biochim Biophys Acta, 1969. **178**(2): p. 294-305.
76. Bharti, B., *Adsorption, Aggregation and Structure Formation in Systems of Charged Particles: From Colloidal to Supracolloidal Assembly*. 2014: Springer.
77. Pescina, S.; Govoni, P.; Antopolsky, M.; Murtomäki, L.; Padula, C.; Santi, P.;Nicoli, S., *Permeation of Proteins, Oligonucleotide and Dextrans Across Ocular Tissues: Experimental Studies and a Literature Update.* Journal of Pharmaceutical Sciences, 2015. **104**(7): p. 2190-2202.
78. Nicoli, S.; Ferrari, G.; Quarta, M.; Macaluso, C.; Govoni, P.; Dallatana, D.;Santi, P., *Porcine sclera as a model of human sclera for in vitro transport experiments: histology, SEM, and comparative permeability.* Molecular Vision, 2009. **15**: p. 259-266.
79. Hirvonen, J.;Guy, R.H., *Transdermal iontophoresis: modulation of electroosmosis by polypeptide.* J Control Release, 1998. **50**(1-3): p. 283-9.
80. Bosma, J.C.;Wesselingh, J.A., *Partitioning and diffusion of large molecules in fibrous structures.* J Chromatogr B Biomed Sci Appl, 2000. **743**(1-2): p. 169-80.
81. Cai, C.; Bakowsky, U.; Rytting, E.; Schaper, A.K.;Kissel, T., *Charged nanoparticles as protein delivery systems: a feasibility study using lysozyme as model protein.* Eur J Pharm Biopharm, 2008. **69**(1): p. 31-42.
82. Jeong, Y.; Park, S.S.; Sung, A.R.;Ha, C.-S., *Comparative Studies on Drug Delivery Behavior of Mesoporous Silicas.* Molecular Crystals and Liquid Crystals, 2014. **600**(1): p. 70-80.
83. Sober, H.A., *Handbook of biochemistry; Selected data for molecular biology. Editor: Herbert A. Sober; Advisory Board chairman: Robert A. Harte; compiler: Eva K. Sober, in collaboration with a large number of scientists*, ed. H.A. Sober and C. Chemical Rubber. 1970, Cleveland: Chemical Rubber Co.
84. Wang, J.;Hou, T., *Application of molecular dynamics simulations in molecular property prediction II: diffusion coefficient.* J Comput Chem, 2011. **32**(16): p. 3505-19.
85. Begoña Delgado-Charro, M.; Rodríguez-Bayón, A.M.;Guy, R.H., *Iontophoresis of nafarelin: Effects of current density and concentration on electrotransport in vitro.* Journal of Controlled Release, 1995. **35**(1): p. 35-40.
86. Hoogstraate, A.J.; Srinivasan, V.; Sims, S.M.;Higuchi, W.I., *Iontophoretic enhancement of peptides: behaviour of leuprolide versus model permeants.* Journal of Controlled Release, 1994. **31**(1): p. 41-47.

87. Marro, D.; Kalia, Y.N.; Delgado-Charro, M.B.;Guy, R.H., *Contributions of electromigration and electroosmosis to iontophoretic drug delivery.* Pharmaceutical Research, 2001. **18**(12): p. 1701-8.
88. Murtomäki, L.; Vainikka, T.; Pescina, S.;Nicoli, S., *Drug adsorption on bovine and porcine sclera studied with streaming potential.* Journal of Pharmaceutical Sciences, 2013. **102**(7): p. 2264-2272.
89. Vandamme, M.P.I.; Moss, J.M.; Murphy, W.H.;Preston, B.N., *Binding Properties of Glycosaminoglycans to Lysozyme-Effect of Salt and Molecular Weight.* Archives of Biochemistry and Biophysics, 1994. **310**(1): p. 16-24.
90. Moss, J.M.; Van Damme, M.P.; Murphy, W.H.;Preston, B.N., *Dependence of salt concentration on glycosaminoglycan-lysozyme interactions in cartilage.* Arch Biochem Biophys, 1997. **348**(1): p. 49-55.
91. Welsch, N.; Lu, Y.; Dzubiella, J.;Ballauff, M., *Adsorption of proteins to functional polymeric nanoparticles.* Polymer, 2013. **54**(12): p. 2835-2849.
92. Srikantha, N.; Mourad, F.; Suhling, K.; Elsaid, N.; Levitt, J.; Chung, P.H.; Somavarapu, S.;Jackson, T.L., *Influence of molecular shape, conformability, net surface charge, and tissue interaction on transscleral macromolecular diffusion.* Experimental Eye Research, 2012. **102**(0): p. 85-92.
93. Vilaseca, P.; Dawson, K.A.;Franzese, G., *Understanding and modulating the competitive surface-adsorption of proteins through coarse-grained molecular dynamics simulations.* Soft Matter, 2013. **9**(29): p. 6978-6985.
94. *Introduction to Colloid and Surface Chemistry, Fourth Edition, D. J. Shaw. Butter-worth/Heinemann, Oxford, 1992. pp. vii + 306. $27.95. (ISBN 0-7506-1182-0).* Journal of Dispersion Science and Technology, 1994. **15**(1): p. 119-119.
95. Cheruvu, N.P.S.; Amrite, A.C.;Kompella, U.B., *Effect of Eye Pigmentation on Transscleral Drug Delivery.* Investigative ophthalmology & visual science, 2008. **49**(1): p. 333-341.
96. Du, W.; Sun, S.; Xu, Y.; Li, J.; Zhao, C.; Lan, B.; Chen, H.;Cheng, L., *The Effect of Ocular Pigmentation on Transscleral Delivery of Triamcinolone Acetonide.* Journal of Ocular Pharmacology and Therapeutics, 2013. **29**(7): p. 633-638.
97. Mani, I.; Sharma, V.; Tamboli, I.;Raman, G., *Interaction of melanin with proteins--the importance of an acidic intramelanosomal pH.* Pigment Cell Res, 2001. **14**(3): p. 170-9.

98. Simon, J.D.; Hong, L.;Peles, D.N., *Insights into Melanosomes and Melanin from Some Interesting Spatial and Temporal Properties.* The Journal of Physical Chemistry B, 2008. **112**(42): p. 13201-13217.
99. Towns, J.K.;Regnier, F.E., *Capillary electrophoretic separations of proteins using nonionic surfactant coatings.* Anal Chem, 1991. **63**(11): p. 1126-32.
100. Mandal, A.; Bisht, R.; Rupenthal, I.D.;Mitra, A.K., *Polymeric micelles for ocular drug delivery: From structural frameworks to recent preclinical studies.* J Control Release, 2017. **248**: p. 96-116.
101. Torchilin, V.P., *Micellar nanocarriers: pharmaceutical perspectives.* Pharmaceutical Research, 2007. **24**(1): p. 1-16.
102. Gaucher, G.; Dufresne, M.H.; Sant, V.P.; Kang, N.; Maysinger, D.;Leroux, J.C., *Block copolymer micelles: preparation, characterization and application in drug delivery.* J Control Release, 2005. **109**(1-3): p. 169-88.
103. Malmsten, M., *Surfactants and Polymers in Drug Delivery*. 2002: Taylor & Francis.
104. Vaishya, R.D.; Khurana, V.; Patel, S.;Mitra, A.K., *Controlled ocular drug delivery with nanomicelles.* Wiley Interdisciplinary Reviews: Nanomedicine and Nanobiotechnology, 2014. **6**(5): p. 422-437.
105. Jiao, J., *Polyoxyethylated nonionic surfactants and their applications in topical ocular drug delivery.* Adv Drug Deliv Rev, 2008. **60**(15): p. 1663-73.
106. Torchilin, V.P., *Structure and design of polymeric surfactant-based drug delivery systems.* J Control Release, 2001. **73**(2-3): p. 137-72.
107. Rosen, M.J., *Surfactants and Interfacial Phenomena*. 2004: Wiley.
108. Owen, S.C.; Chan, D.P.Y.;Shoichet, M.S., *Polymeric micelle stability.* Nano Today, 2012. **7**(1): p. 53-65.
109. Kwon, G.S.;Okano, T., *Polymeric micelles as new drug carriers.* Advanced Drug Delivery Reviews, 1996. **21**(2): p. 107-116.
110. Pepiæ, I.; Lovriæ, J.;Filipoviæ-Grèiæ, J., *Polymeric micelles in ocular drug delivery: Rationale, strategies and challenges.* Chemical and Biochemical Engineering Quarterly, 2012. **26**(4): p. 365-377.
111. Alexandridis, P.;Yang, L., *SANS Investigation of Polyether Block Copolymer Micelle Structure in Mixed Solvents of Water and Formamide, Ethanol, or Glycerol.* Macromolecules, 2000. **33**(15): p. 5574-5587.
112. Harris, J.M.; Martin, N.E.;Modi, M., *Pegylation: a novel process for modifying pharmacokinetics.* Clin Pharmacokinet, 2001. **40**(7): p. 539-51.

113. Benahmed, A.; Ranger, M.;Leroux, J.C., *Novel polymeric micelles based on the amphiphilic diblock copolymer poly(N-vinyl-2-pyrrolidone)-block-poly(D,L-lactide).* Pharmaceutical Research, 2001. **18**(3): p. 323-8.
114. Xiong, X.B.; Falamarzian, A.; Garg, S.M.;Lavasanifar, A., *Engineering of amphiphilic block copolymers for polymeric micellar drug and gene delivery.* J Control Release, 2011. **155**(2): p. 248-61.
115. Patel, A.; Cholkar, K.; Agrahari, V.;Mitra, A.K., *Ocular drug delivery systems: An overview.* World J Pharmacol, 2013. **2**(2): p. 47-64.
116. Liang, H.; Brignole-Baudouin, F.; Rabinovich-Guilatt, L.; Mao, Z.; Riancho, L.; Faure, M.O.; Warnet, J.M.; Lambert, G.;Baudouin, C., *Reduction of quaternary ammonium-induced ocular surface toxicity by emulsions: an in vivo study in rabbits.* Mol Vis, 2008. **14**: p. 204-16.
117. Ali, M.; Horikawa, S.; Venkatesh, S.; Saha, J.; Hong, J.W.;Byrne, M.E., *Zero-order therapeutic release from imprinted hydrogel contact lenses within in vitro physiological ocular tear flow.* J Control Release, 2007. **124**(3): p. 154-62.
118. Rahman, M.Q.; Chuah, K.S.; Macdonald, E.C.; Trusler, J.P.;Ramaesh, K., *The effect of pH, dilution, and temperature on the viscosity of ocular lubricants--shift in rheological parameters and potential clinical significance.* Eye (Lond), 2012. **26**(12): p. 1579-84.
119. Prosperi-Porta, G.; Kedzior, S.; Muirhead, B.;Sheardown, H., *Phenylboronic-Acid-Based Polymeric Micelles for Mucoadhesive Anterior Segment Ocular Drug Delivery.* Biomacromolecules, 2016. **17**(4): p. 1449-57.
120. Du Toit, L.C.; Pillay, V.; Choonara, Y.E.; Govender, T.;Carmichael, T., *Ocular drug delivery - a look towards nanobioadhesives.* Expert Opin Drug Deliv, 2011. **8**(1): p. 71-94.
121. Alonso, M.J.;Sanchez, A., *The potential of chitosan in ocular drug delivery.* J Pharm Pharmacol, 2003. **55**(11): p. 1451-63.
122. de la Fuente, M.; Ravina, M.; Paolicelli, P.; Sanchez, A.; Seijo, B.;Alonso, M.J., *Chitosan-based nanostructures: a delivery platform for ocular therapeutics.* Adv Drug Deliv Rev, 2010. **62**(1): p. 100-17.
123. Pepic, I.; Hafner, A.; Lovric, J.; Pirkic, B.;Filipovic-Grcic, J., *A nonionic surfactant/chitosan micelle system in an innovative eye drop formulation.* J Pharm Sci, 2010. **99**(10): p. 4317-25.
124. Lin, H.R.;Chang, P.C., *Novel pluronic-chitosan micelle as an ocular delivery system.* J Biomed Mater Res B Appl Biomater, 2013. **101**(5): p. 689-99.

125. Hafner, A.; Lovric, J.; Romic, M.D.; Juretic, M.; Pepic, I.; Cetina-Cizmek, B.;Filipovic-Grcic, J., *Evaluation of cationic nanosystems with melatonin using an eye-related bioavailability prediction model.* Eur J Pharm Sci, 2015. **75**: p. 142-50.
126. Yang, J.; Yan, J.; Zhou, Z.;Amsden, B.G., *Dithiol-PEG-PDLLA micelles: preparation and evaluation as potential topical ocular delivery vehicle.* Biomacromolecules, 2014. **15**(4): p. 1346-54.
127. Di Prima, G.; Saladino, S.; Bongiovi, F.; Adamo, G.; Ghersi, G.; Pitarresi, G.;Giammona, G., *Novel inulin-based mucoadhesive micelles loaded with corticosteroids as potential transcorneal permeation enhancers.* Eur J Pharm Biopharm, 2017. **117**: p. 385-399.
128. Li, X.; Zhang, Z.; Li, J.; Sun, S.; Weng, Y.;Chen, H., *Diclofenac/biodegradable polymer micelles for ocular applications.* Nanoscale, 2012. **4**(15): p. 4667-73.
129. Gupta, A.K.; Madan, S.; Majumdar, D.K.;Maitra, A., *Ketorolac entrapped in polymeric micelles: preparation, characterisation and ocular anti-inflammatory studies.* Int J Pharm, 2000. **209**(1-2): p. 1-14.
130. Di Tommaso, C.; Bourges, J.L.; Valamanesh, F.; Trubitsyn, G.; Torriglia, A.; Jeanny, J.C.; Behar-Cohen, F.; Gurny, R.;Moller, M., *Novel micelle carriers for cyclosporin A topical ocular delivery: in vivo cornea penetration, ocular distribution and efficacy studies.* Eur J Pharm Biopharm, 2012. **81**(2): p. 257-64.
131. Civiale, C.; Licciardi, M.; Cavallaro, G.; Giammona, G.;Mazzone, M.G., *Polyhydroxyethylaspartamide-based micelles for ocular drug delivery.* Int J Pharm, 2009. **378**(1-2): p. 177-86.
132. Chetoni, P.; Panichi, L.; Burgalassi, S.; Benelli, U.;Saettone, M.F., *Pharmacokinetics and anti-inflammatory activity in rabbits of a novel indomethacin ophthalmic solution.* J Ocul Pharmacol Ther, 2000. **16**(4): p. 363-72.
133. Duan, Y.; Cai, X.; Du, H.;Zhai, G., *Novel in situ gel systems based on P123/TPGS mixed micelles and gellan gum for ophthalmic delivery of curcumin.* Colloids Surf B Biointerfaces, 2015. **128**: p. 322-30.
134. Jaiswal, M.; Kumar, M.;Pathak, K., *Zero order delivery of itraconazole via polymeric micelles incorporated in situ ocular gel for the management of fungal keratitis.* Colloids Surf B Biointerfaces, 2015. **130**: p. 23-30.
135. Cholkar, K.; Gilger, B.C.;Mitra, A.K., *Topical, Aqueous, Clear Cyclosporine Formulation Design for Anterior and Posterior Ocular Delivery.* Transl Vis Sci Technol, 2015. **4**(3): p. 1.

136. Cholkar, K.; Gunda, S.; Earla, R.; Pal, D.;Mitra, A.K., *Nanomicellar Topical Aqueous Drop Formulation of Rapamycin for Back-of-the-Eye Delivery.* AAPS PharmSciTech, 2015. **16**(3): p. 610-22.
137. Vaishya, R.D.; Gokulgandhi, M.; Patel, S.; Minocha, M.;Mitra, A.K., *Novel Dexamethasone-Loaded Nanomicelles for the Intermediate and Posterior Segment Uveitis.* AAPS PharmSciTech, 2014. **15**(5): p. 1238-1251.
138. Salama, A.H.;Shamma, R.N., *Tri/tetra-block co-polymeric nanocarriers as a potential ocular delivery system of lornoxicam: in-vitro characterization, and in-vivo estimation of corneal permeation.* Int J Pharm, 2015. **492**(1-2): p. 28-39.
139. Pepic, I.; Jalsenjak, N.;Jalsenjak, I., *Micellar solutions of triblock copolymer surfactants with pilocarpine.* Int J Pharm, 2004. **272**(1-2): p. 57-64.
140. Ribeiro, A.; Sosnik, A.; Chiappetta, D.A.; Veiga, F.; Concheiro, A.;Alvarez-Lorenzo, C., *Single and mixed poloxamine micelles as nanocarriers for solubilization and sustained release of ethoxzolamide for topical glaucoma therapy.* J R Soc Interface, 2012. **9**(74): p. 2059-69.
141. Ribeiro, A.; Sandez-Macho, I.; Casas, M.; Alvarez-Perez, S.; Alvarez-Lorenzo, C.;Concheiro, A., *Poloxamine micellar solubilization of alpha-tocopherol for topical ocular treatment.* Colloids Surf B Biointerfaces, 2013. **103**: p. 550-7.
142. Xin, J.; Tang, J.; Bu, M.; Sun, Y.; Wang, X.; Wu, L.;Liu, H., *A novel eye drop of alpha tocopherol to prevent ocular oxidant damage: improve the stability and ocular efficacy.* Drug Dev Ind Pharm, 2016. **42**(4): p. 525-34.
143. Alvarez-Rivera, F.; Fernandez-Villanueva, D.; Concheiro, A.;Alvarez-Lorenzo, C., *alpha-Lipoic Acid in Soluplus((R)) Polymeric Nanomicelles for Ocular Treatment of Diabetes-Associated Corneal Diseases.* J Pharm Sci, 2016. **105**(9): p. 2855-63.
144. Elsaid, N.; Somavarapu, S.;Jackson, T.L., *Cholesterol-poly(ethylene) glycol nanocarriers for the transscleral delivery of sirolimus.* Exp Eye Res, 2014. **121**: p. 121-9.
145. Tong, Y.C.; Chang, S.F.; Liu, C.Y.; Kao, W.W.; Huang, C.H.;Liaw, J., *Eye drop delivery of nano-polymeric micelle formulated genes with cornea-specific promoters.* J Gene Med, 2007. **9**(11): p. 956-66.
146. Liaw, J.; Chang, S.F.;Hsiao, F.C., *In vivo gene delivery into ocular tissues by eye drops of poly(ethylene oxide)-poly(propylene oxide)-poly(ethylene oxide) (PEO-PPO-PEO) polymeric micelles.* Gene Ther, 2001. **8**(13): p. 999-1004.
147. Guo, C.; Zhang, Y.; Yang, Z.; Li, M.; Li, F.; Cui, F.; Liu, T.; Shi, W.;Wu, X., *Nanomicelle formulation for topical delivery of cyclosporine A into the cornea: in*

vitro mechanism and in vivo permeation evaluation. Scientific Reports, 2015. **5**: p. 12968.

148. Luschmann, C.; Tessmar, J.; Schoeberl, S.; Strauss, O.; Luschmann, K.;Goepferich, A., *Self-assembling colloidal system for the ocular administration of cyclosporine A.* Cornea, 2014. **33**(1): p. 77-81.
149. Gayton, J.L., *Etiology, prevalence, and treatment of dry eye disease.* Clinical Ophthalmology (Auckland, N.Z.), 2009. **3**: p. 405-412.
150. Kunert, K.S.; Tisdale, A.S.; Stern, M.E.; Smith, J.A.;Gipson, I.K., *Analysis of topical cyclosporine treatment of patients with dry eye syndrome: effect on conjunctival lymphocytes.* Arch Ophthalmol, 2000. **118**(11): p. 1489-96.
151. Mondon, K.; Zeisser-Labouebe, M.; Gurny, R.;Moller, M., *Novel cyclosporin A formulations using MPEG-hexyl-substituted polylactide micelles: a suitability study.* Eur J Pharm Biopharm, 2011. **77**(1): p. 56-65.
152. el Tayar, N.; Mark, A.E.; Vallat, P.; Brunne, R.M.; Testa, B.;van Gunsteren, W.F., *Solvent-dependent conformation and hydrogen-bonding capacity of cyclosporin A: evidence from partition coefficients and molecular dynamics simulations.* J Med Chem, 1993. **36**(24): p. 3757-64.
153. Springsteen, G.;Wang, B., *A detailed examination of boronic acid–diol complexation.* Tetrahedron, 2002. **58**(26): p. 5291-5300.
154. Liu, S.; Jones, L.;Gu, F.X., *Development of mucoadhesive drug delivery system using phenylboronic acid functionalized poly(D,L-lactide)-b-dextran nanoparticles.* Macromol Biosci, 2012. **12**(12): p. 1622-6.
155. Donnenfeld, E.;Pflugfelder, S.C., *Topical ophthalmic cyclosporine: pharmacology and clinical uses.* Surv Ophthalmol, 2009. **54**(3): p. 321-38.
156. Halloran, P.F.; Kung, L.;Noujaim, J., *Calcineurin and the biological effect of cyclosporine and tacrolimus.* Transplant Proc, 1998. **30**(5): p. 2167-70.
157. Li, Y.; Johnson, N.; Capano, M.; Edwards, M.;Crompton, M., *Cyclophilin-D promotes the mitochondrial permeability transition but has opposite effects on apoptosis and necrosis.* Biochem J, 2004. **383**(Pt 1): p. 101-9.
158. Pflugfelder, S.C., *Antiinflammatory therapy for dry eye.* Am J Ophthalmol, 2004. **137**(2): p. 337-42.
159. Di Tommaso, C.; Behar-Cohen, F.; Gurny, R.;Moller, M., *Colloidal systems for the delivery of cyclosporin A to the anterior segment of the eye.* Ann Pharm Fr, 2011. **69**(2): p. 116-23.

160. Lallemand, F.; Schmitt, M.; Bourges, J.L.; Gurny, R.; Benita, S.;Garrigue, J.S., *Cyclosporine A delivery to the eye: A comprehensive review of academic and industrial efforts.* Eur J Pharm Biopharm, 2017. **117**: p. 14-28.
161. Lallemand, F.; Daull, P.; Benita, S.; Buggage, R.;Garrigue, J.S., *Successfully improving ocular drug delivery using the cationic nanoemulsion, novasorb.* J Drug Deliv, 2012. **2012**: p. 604204.
162. Agarwal, P.;Rupenthal, I.D., *Modern approaches to the ocular delivery of cyclosporine A.* Drug Discov Today, 2016. **21**(6): p. 977-88.
163. Rubin, M.;Rao, S.N., *Efficacy of topical cyclosporin 0.05% in the treatment of posterior blepharitis.* J Ocul Pharmacol Ther, 2006. **22**(1): p. 47-53.
164. Schechter, B.A.; Katz, R.S.;Friedman, L.S., *Efficacy of topical cyclosporine for the treatment of ocular rosacea.* Adv Ther, 2009. **26**(6): p. 651-9.
165. Spadavecchia, L.; Fanelli, P.; Tesse, R.; Brunetti, L.; Cardinale, F.; Bellizzi, M.; Rizzo, G.; Procoli, U.; Bellizzi, G.;Armenio, L., *Efficacy of 1.25% and 1% topical cyclosporine in the treatment of severe vernal keratoconjunctivitis in childhood.* Pediatr Allergy Immunol, 2006. **17**(7): p. 527-32.
166. Akpek, E.K.; Dart, J.K.; Watson, S.; Christen, W.; Dursun, D.; Yoo, S.; O'Brien, T.P.; Schein, O.D.;Gottsch, J.D., *A randomized trial of topical cyclosporin 0.05% in topical steroid-resistant atopic keratoconjunctivitis.* Ophthalmology, 2004. **111**(3): p. 476-82.
167. Price, M.O.;Price, F.W., Jr., *Efficacy of topical cyclosporine 0.05% for prevention of cornea transplant rejection episodes.* Ophthalmology, 2006. **113**(10): p. 1785-90.
168. Lallemand, F.; Felt-Baeyens, O.; Besseghir, K.; Behar-Cohen, F.;Gurny, R., *Cyclosporine A delivery to the eye: a pharmaceutical challenge.* Eur J Pharm Biopharm, 2003. **56**(3): p. 307-18.
169. Ames, P.;Galor, A., *Cyclosporine ophthalmic emulsions for the treatment of dry eye: a review of the clinical evidence.* Clinical investigation, 2015. **5**(3): p. 267-285.
170. Liang, H.; Baudouin, C.; Daull, P.; Garrigue, J.-S.;Brignole-Baudouin, F., *Ocular safety of cationic emulsion of cyclosporine in an in vitro corneal wound-healing model and an acute in vivo rabbit model.* Molecular Vision, 2012. **18**: p. 2195-2204.
171. Sandri, G.; Bonferoni, M.C.; Gokce, E.H.; Ferrari, F.; Rossi, S.; Patrini, M.;Caramella, C., *Chitosan-associated SLN: in vitro and ex vivo characterization of cyclosporine A loaded ophthalmic systems.* J Microencapsul, 2010. **27**(8): p. 735-46.

172. Basaran, E.; Demirel, M.; Sirmagul, B.;Yazan, Y., *Cyclosporine-A incorporated cationic solid lipid nanoparticles for ocular delivery.* J Microencapsul, 2010. **27**(1): p. 37-47.
173. Shen, J.; Wang, Y.; Ping, Q.; Xiao, Y.;Huang, X., *Mucoadhesive effect of thiolated PEG stearate and its modified NLC for ocular drug delivery.* J Control Release, 2009. **137**(3): p. 217-23.
174. Liu, S.; Dozois, M.D.; Chang, C.N.; Ahmad, A.; Ng, D.L.; Hileeto, D.; Liang, H.; Reyad, M.M.; Boyd, S.; Jones, L.W.;Gu, F.X., *Prolonged Ocular Retention of Mucoadhesive Nanoparticle Eye Drop Formulation Enables Treatment of Eye Diseases Using Significantly Reduced Dosage.* Mol Pharm, 2016. **13**(9): p. 2897-905.
175. Basaran, E.; Yenilmez, E.; Berkman, M.S.; Buyukkoroglu, G.;Yazan, Y., *Chitosan nanoparticles for ocular delivery of cyclosporine A.* J Microencapsul, 2014. **31**(1): p. 49-57.
176. Liu, S.; Chang, C.N.; Verma, M.S.; Hileeto, D.; Muntz, A.; Stahl, U.; Woods, J.; Jones, L.W.;Gu, F.X., *Phenylboronic acid modified mucoadhesive nanoparticle drug carriers facilitate weekly treatment of experimentallyinduced dry eye syndrome.* Nano Research, 2015. **8**(2): p. 621-635.
177. Karn, P.R.; Cho, W.; Park, H.J.; Park, J.S.;Hwang, S.J., *Characterization and stability studies of a novel liposomal cyclosporin A prepared using the supercritical fluid method: comparison with the modified conventional Bangham method.* Int J Nanomedicine, 2013. **8**: p. 365-77.
178. Luschmann, C.; Tessmar, J.; Schoeberl, S.; Strauss, O.; Framme, C.; Luschmann, K.;Goepferich, A., *Developing an in situ nanosuspension: a novel approach towards the efficient administration of poorly soluble drugs at the anterior eye.* Eur J Pharm Sci, 2013. **50**(3-4): p. 385-92.
179. Bonferoni, M.C.; Sandri, G.; Dellera, E.; Rossi, S.; Ferrari, F.; Zambito, Y.;Caramella, C., *Palmitoyl Glycol Chitosan Micelles for Corneal Delivery of Cyclosporine.* J Biomed Nanotechnol, 2016. **12**(1): p. 231-40.
180. Cambon, A.; Brea, J.; Loza, M.I.; Alvarez-Lorenzo, C.; Concheiro, A.; Barbosa, S.; Taboada, P.;Mosquera, V., *Cytocompatibility and P-glycoprotein inhibition of block copolymers: structure-activity relationship.* Mol Pharm, 2013. **10**(8): p. 3232-41.
181. Batrakova, E.V.; Li, S.; Li, Y.; Alakhov, V.Y.;Kabanov, A.V., *Effect of pluronic P85 on ATPase activity of drug efflux transporters.* Pharmaceutical Research, 2004. **21**(12): p. 2226-33.

182. Collnot, E.M.; Baldes, C.; Wempe, M.F.; Hyatt, J.; Navarro, L.; Edgar, K.J.; Schaefer, U.F.;Lehr, C.M., *Influence of vitamin E TPGS poly(ethylene glycol) chain length on apical efflux transporters in Caco-2 cell monolayers.* J Control Release, 2006. **111**(1-2): p. 35-40.
183. Collnot, E.M.; Baldes, C.; Wempe, M.F.; Kappl, R.; Huttermann, J.; Hyatt, J.A.; Edgar, K.J.; Schaefer, U.F.;Lehr, C.M., *Mechanism of inhibition of P-glycoprotein mediated efflux by vitamin E TPGS: influence on ATPase activity and membrane fluidity.* Mol Pharm, 2007. **4**(3): p. 465-74.
184. Bakshi, M.S.;Sachar, S., *Influence of temperature on the mixed micelles of Pluronic F127 and P103 with dimethylene-bis-(dodecyldimethylammonium bromide).* J Colloid Interface Sci, 2006. **296**(1): p. 309-15.
185. Sancho, C.M.; Herrero Vanrell, R.;Negro, S., *Determination of Vitamin E Acid Succinate in Biodegradable Microspheres by Reversed-Phase High-Performance Liquid Chromatography.* Journal of Chromatographic Science, 2004. **42**(1): p. 43-48.
186. Balls, M.; Botham, P.A.; Bruner, L.H.;Spielmann, H., *The EC/HO international validation study on alternatives to the draize eye irritation test.* Toxicol In Vitro, 1995. **9**(6): p. 871-929.
187. Zhang, Z.; Tan, S.;Feng, S.S., *Vitamin E TPGS as a molecular biomaterial for drug delivery.* Biomaterials, 2012. **33**(19): p. 4889-906.
188. Sinko, P.J., *Martin's Physical Pharmacy and Pharmaceutical Sciences: Physical Chemical and Biopharmaceutical Principles in the Pharmaceutical Sciences*. 2006: Lippincott Williams & Wilkins.
189. Franken, L.E.; Boekema, E.J.;Stuart, M.C.A., *Transmission Electron Microscopy as a Tool for the Characterization of Soft Materials: Application and Interpretation.* Adv Sci (Weinh), 2017. **4**(5): p. 1600476.
190. Pandit, J.C.; Nagyova, B.; Bron, A.J.;Tiffany, J.M., *Physical properties of stimulated and unstimulated tears.* Exp Eye Res, 1999. **68**(2): p. 247-53.
191. Duvvuri, S.; Majumdar, S.;Mitra, A.K., *Role of metabolism in ocular drug delivery.* Curr Drug Metab, 2004. **5**(6): p. 507-15.
192. Nakano, M.; Lockhart, C.M.; Kelly, E.J.;Rettie, A.E., *Ocular cytochrome P450s and transporters: roles in disease and endobiotic and xenobiotic disposition.* Drug Metab Rev, 2014. **46**(3): p. 247-60.
193. Seen, S.;Tong, L., *Dry eye disease and oxidative stress.* Acta Ophthalmol, 2017.

194. Yadav, U.C.; Kalariya, N.M.;Ramana, K.V., *Emerging role of antioxidants in the protection of uveitis complications.* Curr Med Chem, 2011. **18**(6): p. 931-42.
195. Grover, A.K.;Samson, S.E., *Antioxidants and vision health: facts and fiction.* Mol Cell Biochem, 2014. **388**(1-2): p. 173-83.
196. Lawrenson, J.G.;Grzybowski, A., *Controversies in the Use of Nutritional Supplements in Ophthalmology.* Curr Pharm Des, 2015. **21**(32): p. 4667-72.
197. Ostacolo, C.; Marra, F.; Laneri, S.; Sacchi, A.; Nicoli, S.; Padula, C.;Santi, P., *Alpha-tocopherol pro-vitamins: synthesis, hydrolysis and accumulation in rabbit ear skin.* J Control Release, 2004. **99**(3): p. 403-13.
198. Marra, F.; Ostacolo, C.; Laneri, S.; Bernardi, A.; Sacchi, A.; Padula, C.; Nicoli, S.;Santi, P., *Synthesis, hydrolysis, and skin retention of amino acid esters of alpha-tocopherol.* J Pharm Sci, 2009. **98**(7): p. 2364-76.
199. *Cyclosporin - allergan. Ciclosporin - allergan, cyclosporin ophthalmic emulsion, cyclosporine - Allergan, Restasis.* Drugs R D, 2003. **4**(2): p. 126-7.
200. M.A. Fathalla, Z.; Vangala, A.; Longman, M.; Khaled, K.A.; Hussein, A.K.; El-Garhy, O.H.;Alany, R.G., *Poloxamer-based thermoresponsive ketorolac tromethamine in situ gel preparations: Design, characterisation, toxicity and transcorneal permeation studies.* European Journal of Pharmaceutics and Biopharmaceutics, 2017. **114**: p. 119-134.
201. Caruso, C.; Ostacolo, C.; Epstein, R.L.; Barbaro, G.; Troisi, S.;Capobianco, D., *Transepithelial Corneal Cross-Linking With Vitamin E-Enhanced Riboflavin Solution and Abbreviated, Low-Dose UV-A: 24-Month Clinical Outcomes.* Cornea, 2016. **35**(2): p. 145-150.
202. Pescina, S.; Govoni, P.; Potenza, A.; Padula, C.; Santi, P.;Nicoli, S., *Development of a Convenient ex vivo Model for the Study of the Transcorneal Permeation of Drugs: Histological and Permeability Evaluation.* Journal of Pharmaceutical Sciences, 2015. **104**(1): p. 63-71.
203. Debbasch, C.; Brignole, F.; Pisella, P.J.; Warnet, J.M.; Rat, P.;Baudouin, C., *Quaternary ammoniums and other preservatives' contribution in oxidative stress and apoptosis on Chang conjunctival cells.* Invest Ophthalmol Vis Sci, 2001. **42**(3): p. 642-52.
204. Leonardi, A.; Van Setten, G.; Amrane, M.; Ismail, D.; Garrigue, J.S.; Figueiredo, F.C.;Baudouin, C., *Efficacy and safety of 0.1% cyclosporine A cationic emulsion in the treatment of severe dry eye disease: a multicenter randomized trial.* Eur J Ophthalmol, 2016. **26**(4): p. 287-96.

205. Mandal, A.; Cholkar, K.; Khurana, V.; Shah, A.; Agrahari, V.; Bisht, R.; Pal, D.;Mitra, A.K., *Topical Formulation of Self-Assembled Antiviral Prodrug Nanomicelles for Targeted Retinal Delivery.* Mol Pharm, 2017. **14**(6): p. 2056-2069.
206. Li, J.; Li, Z.; Zhou, T.; Zhang, J.; Xia, H.; Li, H.; He, J.; He, S.;Wang, L., *Positively charged micelles based on a triblock copolymer demonstrate enhanced corneal penetration.* International Journal of Nanomedicine, 2015. **10**: p. 6027-6037.
207. Gipson, I.K.; Spurr-Michaud, S.; Argueso, P.; Tisdale, A.; Ng, T.F.;Russo, C.L., *Mucin gene expression in immortalized human corneal-limbal and conjunctival epithelial cell lines.* Invest Ophthalmol Vis Sci, 2003. **44**(6): p. 2496-506.
208. Komai, Y.;Ushiki, T., *The three-dimensional organization of collagen fibrils in the human cornea and sclera.* Invest Ophthalmol Vis Sci, 1991. **32**(8): p. 2244-58.
209. Pijanka, J.K.; Coudrillier, B.; Ziegler, K.; Sorensen, T.; Meek, K.M.; Nguyen, T.D.; Quigley, H.A.;Boote, C., *Quantitative Mapping of Collagen Fiber Orientation in Non-glaucoma and Glaucoma Posterior Human Sclerae.* Investigative ophthalmology & visual science, 2012. **53**(9): p. 5258-5270.
210. Hellberg, M.R.; Ke, T.L.; Haggard, K.; Klimko, P.G.; Dean, T.R.;Graff, G., *The hydrolysis of the prostaglandin analog prodrug bimatoprost to 17-phenyl-trinor PGF2alpha by human and rabbit ocular tissue.* J Ocul Pharmacol Ther, 2003. **19**(2): p. 97-103.
211. Foroutan, S.M.;Watson, D.G., *The in vitro evaluation of polyethylene glycol esters of hydrocortisone 21-succinate as ocular prodrugs.* Int J Pharm, 1999. **182**(1): p. 79-92.
212. Kirchhof, S.; Goepferich, A.M.;Brandl, F.P., *Hydrogels in ophthalmic applications.* Eur J Pharm Biopharm, 2015. **95**(Pt B): p. 227-38.
213. Karki, S.; Kim, H.; Na, S.-J.; Shin, D.; Jo, K.;Lee, J., *Thin films as an emerging platform for drug delivery.* Asian Journal of Pharmaceutical Sciences, 2016. **11**(5): p. 559-574.
214. Fathi, M.; Barar, J.; Aghanejad, A.;Omidi, Y., *Hydrogels for ocular drug delivery and tissue engineering.* BioImpacts : BI, 2015. **5**(4): p. 159-164.
215. Kumari, A.; Sharma, P.K.; Garg, V.K.;Garg, G., *Ocular inserts - Advancement in therapy of eye diseases.* J Adv Pharm Technol Res, 2010. **1**(3): p. 291-6.
216. Calles, J.A.; Tartara, L.I.; Lopez-Garcia, A.; Diebold, Y.; Palma, S.D.;Valles, E.M., *Novel bioadhesive hyaluronan-itaconic acid crosslinked films for ocular therapy.* Int J Pharm, 2013. **455**(1-2): p. 48-56.

217. Foureaux, G.; Franca, J.R.; Nogueira, J.C.; Fulgencio Gde, O.; Ribeiro, T.G.; Castilho, R.O.; Yoshida, M.I.; Fuscaldi, L.L.; Fernandes, S.O.; Cardoso, V.N.; Cronemberger, S.; Faraco, A.A.;Ferreira, A.J., *Ocular Inserts for Sustained Release of the Angiotensin-Converting Enzyme 2 Activator, Diminazene Aceturate, to Treat Glaucoma in Rats.* PLoS One, 2015. **10**(7): p. e0133149.
218. Jafariazar, Z.; Jamalinia, N.; Ghorbani-Bidkorbeh, F.;Mortazavi, S.A., *Design and Evaluation of Ocular Controlled Delivery System for Diclofenac Sodium.* Iran J Pharm Res, 2015. **14**(Suppl): p. 23-31.
219. Prabhu, P.; Dubey, A.; Parth, V.;Ghate, V., *Investigation of hydrogel membranes containing combination of gentamicin and dexamethasone for ocular delivery.* Int J Pharm Investig, 2015. **5**(4): p. 214-25.
220. Deshpande, P.B.; Dandagi, P.; Udupa, N.; Gopal, S.V.; Jain, S.S.;Vasanth, S.G., *Controlled release polymeric ocular delivery of acyclovir.* Pharm Dev Technol, 2010. **15**(4): p. 369-78.
221. Everaert, A.; Broeckx, G.; Fransen, E.; Ludwig, A.; Kiekens, F.;Weyenberg, W., *Evaluation of a newly developed HPMC ophthalmic insert with sustained release properties as a carrier for thermolabile therapeutics.* Int J Pharm, 2015. **481**(1-2): p. 37-46.
222. Hermans, K.; Van den Plas, D.; Kerimova, S.; Carleer, R.; Adriaensens, P.; Weyenberg, W.;Ludwig, A., *Development and characterization of mucoadhesive chitosan films for ophthalmic delivery of cyclosporine A.* Int J Pharm, 2014. **472**(1-2): p. 10-9.
223. Koelwel, C.; Rothschenk, S.; Fuchs-Koelwel, B.; Gabler, B.; Lohmann, C.;Gopferich, A., *Alginate inserts loaded with epidermal growth factor for the treatment of keratoconjunctivitis sicca.* Pharm Dev Technol, 2008. **13**(3): p. 221-31.
224. Guter, M.;Breunig, M., *Hyaluronan as a promising excipient for ocular drug delivery.* Eur J Pharm Biopharm, 2017. **113**: p. 34-49.
225. Saettone, M.F.; Monti, D.; Torracca, M.T.;Chetoni, P., *Mucoadhesive ophthalmic vehicles: evaluation of polymeric low-viscosity formulations.* J Ocul Pharmacol, 1994. **10**(1): p. 83-92.
226. Loftsson, T.; Jarho, P.; Masson, M.;Jarvinen, T., *Cyclodextrins in drug delivery.* Expert Opin Drug Deliv, 2005. **2**(2): p. 335-51.
227. Johannsdottir, S.; Kristinsson, J.K.; Fulop, Z.; Asgrimsdottir, G.; Stefansson, E.;Loftsson, T., *Formulations and toxicologic in vivo studies of aqueous cyclosporin*

A eye drops with cyclodextrin nanoparticles. Int J Pharm, 2017. **529**(1-2): p. 486-490.

228. Concheiro, A.;Alvarez-Lorenzo, C., *Chemically cross-linked and grafted cyclodextrin hydrogels: from nanostructures to drug-eluting medical devices.* Adv Drug Deliv Rev, 2013. **65**(9): p. 1188-203.
229. Nava-Ortiz, C.A.; Burillo, G.; Concheiro, A.; Bucio, E.; Matthijs, N.; Nelis, H.; Coenye, T.;Alvarez-Lorenzo, C., *Cyclodextrin-functionalized biomaterials loaded with miconazole prevent Candida albicans biofilm formation in vitro.* Acta Biomater, 2010. **6**(4): p. 1398-404.
230. Tan, A.S.;Berridge, M.V., *Superoxide produced by activated neutrophils efficiently reduces the tetrazolium salt, WST-1 to produce a soluble formazan: a simple colorimetric assay for measuring respiratory burst activation and for screening anti-inflammatory agents.* J Immunol Methods, 2000. **238**(1-2): p. 59-68.
231. Steiling, W.; Bracher, M.; Courtellemont, P.;de Silva, O., *The HET-CAM, a Useful In Vitro Assay for Assessing the Eye Irritation Properties of Cosmetic Formulations and Ingredients.* Toxicol In Vitro, 1999. **13**(2): p. 375-84.
232. Tomihata, K.;Ikada, Y., *Preparation of cross-linked hyaluronic acid films of low water content.* Biomaterials, 1997. **18**(3): p. 189-195.
233. Blanco-Fernandez, B.; Rial-Hermida, M.I.; Alvarez-Lorenzo, C.;Concheiro, A., *Edible chitosan/acetylated monoglyceride films for prolonged release of vitamin E and antioxidant activity.* Journal of Applied Polymer Science, 2013. **129**(2): p. 626-635.